

ABSTRACT

Title of Thesis: EXTENSIVE STUDY OF WALL-VENT
COMPARTMENT FIRE BEHAVIORS UNDER
LIMITED VENTILATION

Degree candidate: Yunyong Utiskul

Degree and year: Master of Science, 2003

Thesis Directed by: Professor James G. Quintiere
Department of Fire Protection Engineering

The objective of this study was to investigate the behavior of liquid pool fires under limited ventilation in wall-vented compartment. Fifty-four small-scale experiments were conducted to measure characteristics of heptane fires: burning rate, oxygen concentration, gas temperature, and heat flux to the fuel and enclosure surface, in a cubic compartment of sides 40 cm. Experimental results were presented and based on a ventilation parameter, representing ratio of air flow to fuel flow. Limited ventilation regime was examined to study the effect of extinction and influence of oxygen. Interesting low-ventilation fire phenomena oscillatory and ghosting flames, burning at the air inlet were observed. Oxygen and temperature at extinction and steady oscillation from experiment were in good agreement to the extinction theory. Experimental results were compared with a mathematical model.

EXTENSIVE STUDY OF WALL-VENT COMPARTMENT FIRE BEHAVIOR
UNDER LIMITED VENTILATION

By

Yunyong Utiskul

Thesis submitted to the Faculty of the Graduate School of the
University of Maryland, College Park in partial fulfillment
of the requirements for the degree of
Master of Science
2003

Advisory Committee:

Professor James G. Quintiere, Chair
Professor James A. Milke
Professor Andre Marshall

ACKNOWLEDGMENTS

I would like to thank Dr. James G. Quintiere, my advisor, for helping me through this process with his great knowledge, kindness, and patience. Also I would like to give my appreciation to the thesis committee members, Dr. James Milke and Dr. Andre Marshall, as well as the Department of Fire Protection Engineering.

I would like to thank Dr. Tomohiro Naruse for designing and building this well instrumented compartment and Kaoru Wakatsuki for his suggestions and help on this project.

I would like to thank the following friends and colleagues, Boonmee for being a great tutor of my Fire Dynamics class, Xin and Jonathan for reviewing my work, Joe for sharing his helpful instrumentation knowledge and introducing Solidworks®, a very useful program, and Korn for helping, encouraging, and cooking delicious Thai food.

I would like to thank my family for their support and understanding.

TABLE OF CONTENTS

<u>List of Tables</u>	v
<u>List of Figures.....</u>	vi
<u>Nomenclatures.....</u>	ix
<u>1. Introduction.....</u>	1
<u>2. Experiment.....</u>	2
<u>2.1 Description of Experiment.....</u>	2
<u>2.2 Experiment Measurement and Apparatus.....</u>	3
<u>2.2.1 Temperature</u>	4
<u>2.2.2 Gas Mole Fraction</u>	4
<u>2.2.3 Fuel Mass Loss Rate</u>	6
<u>2.2.4 Heat Flux</u>	7
<u>2.2.5 Differential Pressure</u>	8
<u>2.2.6 Data Acquisition System</u>	8
<u>2.2.7 Miscellaneous</u>	10
<u>2.3 Experimental Procedure.....</u>	10
<u>2.3.1 Test Preparation</u>	10
<u>2.3.2 Test Procedure</u>	12
<u>3. Experimental Results and Observations.....</u>	14
<u>3.1 General Observations.....</u>	14
<u>3.1.1 Category 1: Extinction Due to Filling</u>	14
<u>3.1.2 Category 2: Extinction</u>	17
<u>3.1.3 Category 3: Burning at Vent</u>	20
<u>3.1.4 Category 4: Steady Burning</u>	22
<u>3.2 Explanation of Oscillation Fire Phenomena.....</u>	25
<u>3.3 Free Burning Results.....</u>	29
<u>4. Discussion and Analysis.....</u>	31
<u>4.1 Ventilation and Compartment Fire Behavior.....</u>	31
<u>4.1.1 Burning Rate</u>	38
<u>4.1.2 Gas Temperature</u>	41
<u>4.1.3 Oxygen and Carbon Monoxide Concentration</u>	42
<u>4.1.4 Heat Flux</u>	44
<u>4.2 Extinction Theory and Experimental Results.....</u>	46
<u>4.3 Dynamic Behavior: Experiment and Theory.....</u>	49
<u>4.4 Flame Heat Flux.....</u>	57
<u>4.4.1 Flame Emissivity</u>	57
<u>4.4.2 Total Flame Heat Flux within Compartment</u>	58
<u>4.4.3 Heat Loss through Water and Pan</u>	60

<u>5. Conclusion.....</u>	62
<u>Appendix A: Data Correction.....</u>	63
<u>Appendix B: Gas Temperature and Heat Flux Results.....</u>	66
<u>Appendix C: Detail Drawing.....</u>	69
<u>Appendix D: Experimental and Predicted Results.....</u>	70
<u>Reference.....</u>	125

LIST OF TABLES

<u>Table 3.1</u>	<u>Experimental Condition and Compartment Fire Behavior Summary.....</u>	<u>15</u>
<u>Table 3.2</u>	<u>Average Burning Rate and Heat Flux to the Fuel Surface from</u>	<u>29</u>
	<u>Free Burning</u>	
<u>Table 4.1</u>	<u>Criteria for selecting experimental results.....</u>	<u>37</u>
<u>Table 4.2</u>	<u>Flame Emissivity and Absorption Coefficient.....</u>	<u>58</u>

LIST OF FIGURES

<u>Figure 2.1 Isometric global view of compartment setup.....</u>	<u>2</u>
<u>Figure 2.2 Isometric sections showing experimental apparatus configuration.....</u>	<u>3</u>
<u>Figure 2.3 Gas analyzers for top (left) and bottom (right) gas tube.....</u>	<u>5</u>
<u>Figure 2.4 Load cell (left), Section detail view of Stand to load cell and pan (right)..</u>	<u>6</u>
<u>Figure 2.5 Heating system of supplied water to HF1.....</u>	<u>7</u>
<u>Figure 2.6 Pressure transducer (left) and electric manometer (right).....</u>	<u>8</u>
<u>Figure 2.7 Control and display panel of data acquisition program.....</u>	<u>9</u>
<u>Figure 2.8 Front panel locked by C-clamp.....</u>	<u>13</u>
<u>Figure 3.1 Extinction Due To Filling, $D_F = 9.5 \text{ cm}$, $A_0 = 4 \text{ cm}^2$, Case: 95-1×2.....</u>	<u>16</u>
<u>Figure 3.2 Extinction, $D_F = 9.5 \text{ cm}$, $A_0 = 12 \text{ cm}^2$, Case: 95-1×6.....</u>	<u>18</u>
<u>Figure 3.3 Extinction, $D_F = 9.5 \text{ cm}$, $A_0 = 24 \text{ cm}^2$, Case: 95-1×12.....</u>	<u>19</u>
<u>Figure 3.4 Vent Steady Burning, $D_F = 19.0 \text{ cm}$, $A_0 = 24 \text{ cm}^2$, Case: 190-1×40.....</u>	<u>20</u>
<u>Figure 3.5 Burning at Vent, $D_F = 19.0 \text{ cm}$, $A_0 = 60 \text{ cm}^2$, Case: 190-3×10.....</u>	<u>21</u>
<u>Figure 3.6 Oscillation in Steady Burning, $D_F = 9.5 \text{ cm}$, $A_0 = 60 \text{ cm}^2$, Case: 95-3×10.....</u>	<u>23</u>
<u>Figure 3.7 Steady Burning, $D_F = 9.5 \text{ cm}$, $A_0 = 240 \text{ cm}^2$, Case: 95-3×40.....</u>	<u>24</u>
<u>Figure 3.8 Differential pressure zoomed view from 9.5 cm panwith 21 cm^2 vent area</u>	<u>25</u>
<u>Figure 3.9 Oscillating Combustion, $D_F = 9.5 \text{ cm}$, $A_0 = 24 \text{ cm}^2$, Case: 95-1×12, Captured at 15 frame/second</u>	<u>26</u>
<u>Figure 3.10 Oscillating Combustion, $D_F = 19.0 \text{ cm}$, $A_0 = 60 \text{ cm}^2$, Case: 190-3×10, Captured at 15 frame/second</u>	<u>26</u>
<u>Figure 3.11 Ghosting Flame, $D_F = 9.5 \text{ cm}$, $A_0 = 24 \text{ cm}^2$, Case: 95-1×12,.....1:05 min, Captured at 15 frame/second</u>	<u>27</u>

<u>Figure 3.12 Ghosting Flame, $D_F = 9.5 \text{ cm}$, $A_0 = 24 \text{ cm}^2$, Case: 95-1×12, 1:17 min, Captured at 15 frame/second</u>	28
<u>Figure 3.13 Oscillatory Jet Flame at Vent, $D_F = 19.0 \text{ cm}$, $A_0 = 60 \text{ cm}^2$, Case: 190-3×10, Captured at 15 frame/second</u>	28
<u>Figure 3.14 Free Burning Rates</u>	30
<u>Figure 3.15 Heat Fluxes to Fuel Surface from Free Burning</u>	30
<u>Figure 4.1 Quasi-steady wall-vent compartment</u>	31
<u>Figure 4.2 Example for data selecting</u>	37
<u>Figure 4.3 Burning rate regimes</u>	38
<u>Figure 4.4 Gas Temperature versus ventilation parameter</u>	42
<u>Figure 4.5 Oxygen concentrations versus ventilation parameter</u>	43
<u>Figure 4.6 Carbon Monoxide concentrations versus ventilation parameter</u>	44
<u>Figure 4.7 Heat flux measured at the center of fuel pan versus ventilation parameter</u>	45
<u>Figure 4.8 Heat of vaporization in compartment versus ventilation parameter</u>	46
<u>Figure 4.9 Floor-level oxygen and temperature at extinction or steady burning</u>	49
<u>Figure 4.10 Experimental Results and Model Prediction in Regime 1</u>	52
<u>Figure 4.11 Experimental Results and Model Prediction in Regime 2</u>	53
<u>Figure 4.12 Experimental Results and Model Prediction in Regime 4 where oscillating combustion can be predicted by the model without oxygen adjustment</u>	54
<u>Figure 4.13 Experimental Results and Model Prediction in Regime 4 where oscillating combustion can be predicted by the model with oxygen adjustment</u>	55
<u>Figure 4.14 Burning rate from experiment and model</u>	56
<u>Figure 4.15 Oxygen concentration from experiment and model</u>	56

<u>Figure 4.16 Measured Heat Flux (HF1) and Total Flame Heat Flux, DF = 9.5 cm,...</u>	<u>60</u>
<u>A0 = 24 cm², Regime 2: O = Oscillation and G = Ghosting Flame</u>	
<u>Figure 4.17 Measured Heat Flux (HF1) and Total Flame Heat Flux, DF = 9.5 cm,...</u>	<u>60</u>
<u>A0 = 42 cm², Regime 4: O = Oscillation</u>	
<u>Figure 4.18 Total heat loss through pan and water.....</u>	<u>61</u>
<u>Figure A1 Force balance at water seal cup.....</u>	<u>63</u>
<u>Figure B1 Gas Temperature from center thermocouple tree (TC17-TC19).....</u>	<u>66</u>
<u>versus ventilation parameter</u>	
<u>Figure B2 Gas Temperature from back thermocouple tree (TC13-TC16).....</u>	<u>66</u>
<u>versus ventilation parameter</u>	
<u>Figure B3 Heat flux to floor (HF2) versus ventilation parameter.....</u>	<u>67</u>
<u>Figure B4 Heat flux to back wall (HF3) versus ventilation parameter.....</u>	<u>67</u>
<u>Figure B5 Heat flux to ceiling (HF4) versus ventilation parameter.....</u>	<u>68</u>
<u>Figure C1 Section View showing experimental apparatus.....</u>	<u>69</u>

NOMENCLATURE

A_0	Total Vent Area
A_F	Fuel Pan Area
A_s	Inside Compartment Surface Area
c_p	Specific Heat
C_d	Flow Coefficient
D_F	Fuel Pan Diameter
h	Convective Heat Transfer Coefficient
Δh_{air}	Heat of Combustion per unit mass of Air
Δh_c	Heat of Combustion per unit mass of Fuel
H	Compartment Height
H_n	Neutral Plane Height
k	Absorption Coefficient
L_m	Mean Beam Length
L	Latent Heat of Gasification
\dot{m}_i	Mass Inflow Rate
\dot{m}_F	Fuel Mass Loss Rate or Burning Rate
\dot{m}_o	Mass Outflow Rate
\dot{m}''_F	Burning Rate per Unit Area
$\dot{m}''_{F,\infty}$	Free Burning Rate per Unit Area
P	Pressure inside Enclosure
P_∞	Pressure outside Enclosure
$\dot{q}''_{e,r}$	External Radiant Heat Flux from Compartment and Hot Gases
\dot{q}''_f	Flame Heat Flux
\dot{Q}	Heat Release Rate
T	Temperature
T_f	Flame Temperature
T_∞	Ambient Temperature
v_i	Inflow Velocity
v_o	Outflow Velocity
Y_{ox}	Oxygen Mass Fraction in Compartment
$Y_{ox,\infty}$	Oxygen Mass Fraction of Air

1. Introduction

In order to predict the growth and evaluate the risk of fire within a room, it is important to understand the behavior and dynamics of fire controlled by ventilation. Large effects of ventilation on fire characteristics such as burning rate and compartment temperature have been found in previous studies [1,2]. Work done by Takeda and Akita [3] has revealed an interesting phenomenon called oscillatory combustion which usually occurred in ventilated control fire and had a possibility to occur in compartment steady burning as well. This behavior was also found by Tewarson [4] and Kim et al.[5]. Details of fire behavior stages in small-scale compartment have been provided by previous studies which focused on low ventilation. The wall-vent case done by Ringwelski [1] has shown this oscillation behavior occurring in some range of vent size; although in ceiling-vent case, done by Wakatsuki [2], has revealed this phenomenon only in a large opening case. The attempt to create a theoretical model to predict fires in wall-vent compartment has been made by Rangwala [6].

This study is essentially the continuing experimental work on low ventilation wall-vent compartment, with more instrumentation, and larger range of ventilation and fire size in order to investigate more details of fire behavior under low-ventilation.

2. Experiment

2.1 Description of the Experiment

The small-scale compartment was made of 1 inch thick M-Type Kaowool® Board and prepared to be able to perform experiments on several vent geometries and compartment depths. The global size is 40 cm × 40 cm × 120 cm. In this study, the location of back wall (in side the compartment) was located to make a perfect 40 cm cube box compartment. However, for further study, compartment depths can be varied by adjusting the back wall location. Steel angles were used to build structural frames which supported the floor, wall and ceiling boards. Figure 2.1 shows the isometric global view of the compartment as well as locations of the load cell and pressure transducers.

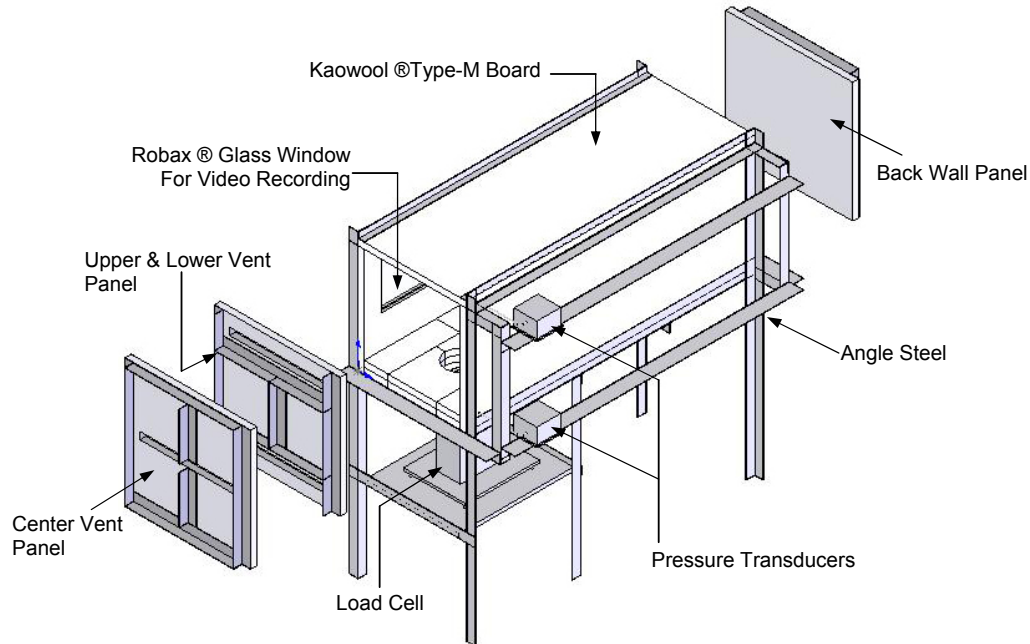


Figure 2.1 Isometric global view of compartment setup

The total area of top and bottom vents was varied from 2 to 240 cm². The liquid fuel used in this experiment was Heptane (C₇H₁₆) and was burned in four different modified Pyrex® glass pans of 6.5, 9.5, 12.0, and 19.0 cm diameter respectively.

2.2 Experimental Measurements and Apparatus

In this experiment, temperature, gas mole fraction, differential pressure, fuel mass loss rate or burning rate, and heat flux were measured. The apparatus configuration and location were presented in Figure 2.2; a detail drawing was illustrated in Appendix C. It should be noted that the fuel pan was set to be at the center of the compartment, and the fuel surface was at the same level of the floor.

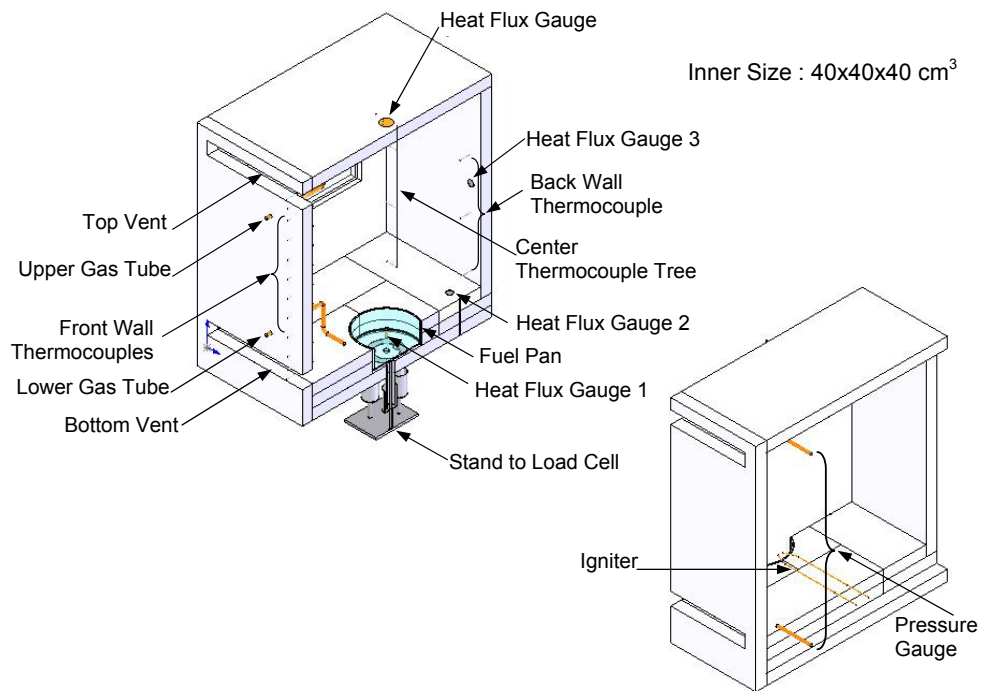


Figure 2.2 Isometric sections showing experimental apparatus configuration

2.2.1 Temperature

Type K thermocouple wires were used to measure gas and compartment surface temperature. As illustrated in Figure 2.2 and Appendix C, two thermocouples (TC1, TC12) were adjusted to be at center of top and bottom vents; ten thermocouples (TC2 to TC11) were installed into front wall, apart from the ceiling and floor at 1.5 cm, and at 4 cm from one another. Back wall thermocouples (TC13 to TC16) were located at 2 cm from the ceiling and floor, and 12 cm from one another. Three thermocouples (TC17 to TC19) were bundled up at the center of the compartment and from the ceiling were at 2, 14, and 26 cm, respectively. Also there were three thermocouples measuring the temperature at the surface next to the heat flux transducers located on floor, back wall, and ceiling.

2.2.2 Gas Mole Fraction

In this experiment, oxygen, carbon dioxide and carbon monoxide concentrations from sampling gas stations were measured. Two copper tubes were installed at 2 cm from the ceiling and floor and at 10 cm away from the vents to collect samples gas from the upper and lower portion of the compartment. The sampled gas would pass along a plastic tube through the cold trap, soot filter, moisture absorption and carbon dioxide absorption (for oxygen analyzer), then finally reached the gas analyzers.

It has been known that water vapor as well as carbon dioxide affects the accuracy of oxygen analyzers. To solve this problem, a $50 \times 30 \times 30$ cm ice box was used as a cold trap to condense water vapor in the sampling gas. Drierite®, a product made of anhydrous calcium sulfate to absorb moisture from gas, was used as a supplement to the cold trap. In addition, Ascarite®, a chemical agent made of sodium hydroxide coated

non-fibrous silicate, was used to trap carbon dioxide from sampling gas. Both Drierite® and Ascarite® were filled in polypropylene tubes in which the sampling gas passed through before it reached the gas analyzers.

Soot filters, type-304 Fisher Scientific, with Advantest glass sheet filter (934-AH) were used to remove soot from the sampling gas for both upper and lower gas analyzer systems. The filter sheet was replaced after completing four tests. Note that for the lower gas analyzers, which needed a vacuum pump, the soot filter was installed before the pump.

Oxygen concentration of lower gas sampling was measured by a Servomex Oxygen Analyzer Model 540A. Two Horiba PIR-2000 gas analyzers were used to measure carbon dioxide and carbon monoxide from lower sampling gas. An electric-powered vacuum pump, KNF UN0106, was needed to deliver sampling gas for these three analyzers; the flow rate was set to 60 ml/min and bypass flow rate 1.0 l/min. As for upper gas sampling, SIEMENS OXYMAT 6 was used to measure oxygen concentration, and SIEMENS ULTRAMAT 23 measured carbon dioxide and carbon monoxide concentration. The flow rate was at 1.0 l/min. Figure 2.3 shows all the gas analyzers used in this experiment.

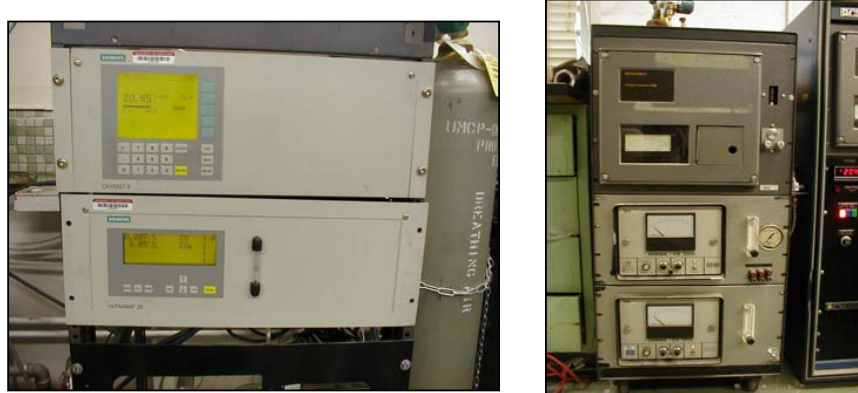


Figure 2.3 Gas analyzers for top (left) and bottom (right) gas tube.

2.2.3 Fuel Mass loss rate

The fuel mass loss rate or burning rate for each test was measured by using a load cell, Automatic Timing and Controls Model 6005D-050E01, shown in Figure 2.4. The stand to load cell which supported the Pyrex® fuel pan was made of a steel plate and an aluminum tube shown in Figure 2.4. The measurement span is 250 g with 2.0 kg load capacity and the output voltage signal from 0 to 1 volt. Since gas leakage through the load cell shaft opening could affect the vent flows, especially in a small-scale experiment, water seal cups were installed at all three legs of the load cell stand. The schematic is shown in Figure 2.4. The space between the fuel pan and surrounding floor board was approximately 2 mm to allow the pan to move freely.

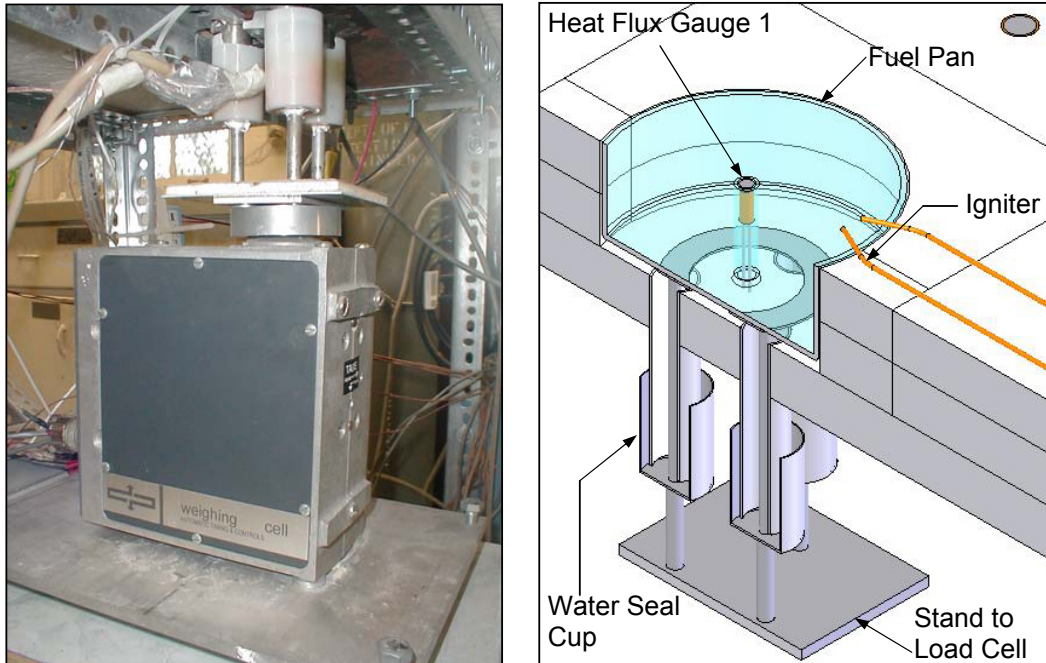


Figure 2.4 Load cell (left), Section detail view of Stand to load cell and pan (right)

2.2.4 Heat Flux

Three heat flux transducers (HF2 to HF4), Model 40-15-4-36-20-21124 MEDTHERM Corporation, were used to measure heat flux on the inside surface of the compartment, and installed at the floor, back wall, and ceiling as shown in Figure. Also one $\frac{1}{4}$ inch diameter heat flux transducer (HF1), Model 16-15SB-18-21033 MEDTHERM Corporation, was used to measure heat flux at fuel surface. In order to do so, every Pyrex® glass dish used as our fuel pan was modified to have a glass tube to allow placing the heat flux transducer, HF1, at the center of the pan. Cooling water supplied to the three heat flux transducers, HF2 to HF4, had flow rate approximately 11 ml/s, and 7 ml/s for HF1. However, to prevent condensation of water on the HF1 surface inside the flame sheet, before flowing through heat flux transducer, water supplied was heated and maintained at a temperature of approximately 65 °C by a custom made electric heater controlled by a transformer. See Figure 2.5.

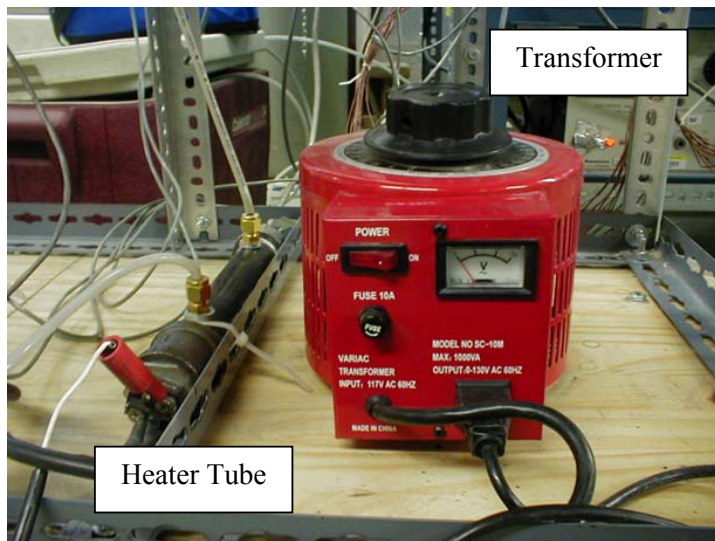


Figure 2.5 Heating system of supplied water to HF1

2.2.5 Differential Pressure

To observe the gas flow characteristic coming in and out of the compartment, measurements of the differential pressure between inside and outside of the compartment were needed. Therefore two differential pressure transducers, type-540A Datametrics Co.,Ltd., were set up on the top and bottom of the side wall and connected to the compartment by copper tubes. These pressure transducers sent the signal to an electric manometer made by Datametrics Co.,Ltd. which transferred a voltage signal acquired by data acquisition system. The multiplied range of the transducer was set to 1 on the electric manometer. The output ranged from 0 to 10 volts which corresponded to 0 to 133 Pa. See Figure 2.6.

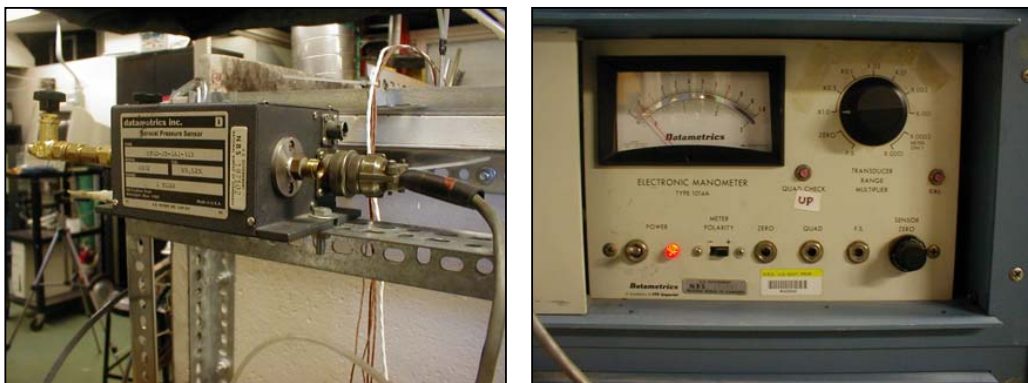


Figure 2.6 Pressure transducer (left) and electric manometer (right)

2.2.6 Data Acquisition System

All the data were taking using data acquisition system from National Instruments. PCI-MIO-16-E-4 DAQ Card, which was installed to 1.0 GHz Pentium III 128 MB memory Dell-PC, was connected to an SCXI-1100 chassis where two SCXI-1300 terminal block modules with 32 analog channels were installed to convert signals from

the sensors with high accuracy. To reduce the noise that thermocouples and other transducers inevitably pick up when we were taking data, the negative input of a floating thermocouple was connected to the chassis ground within terminal block SCXI-1300 and then reference to the building ground.

LabVIEW version 5.1 was used to acquire, display and save data from the data acquisition system. A custom program obtained from Wakatsuki [2] was modified to suit with this experiment. Figure 2.7 shows the program display panel. Data were basically taken at 1 Hz with 100 samples to average and 6,000 scan rate. However there were some tests that had been done by taking data at every 0.2 sec. in order to capture the frequency of oscillating combustion.

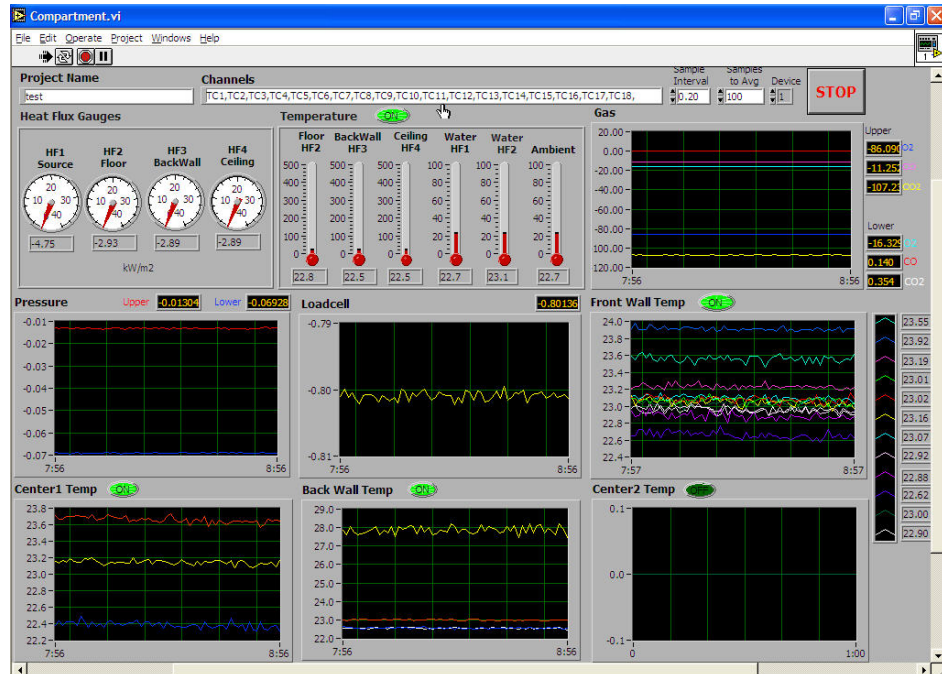


Figure 2.7 Control and display panel of data acquisition program

2.2.7 Miscellaneous

On the left wall of the compartment, $22 \times 27 \text{ cm}^2$ transparent glass windows were installed to make the observation of the compartment fire behavior and video shooting possible. With its extreme thermal shock resistance and very low thermal expansion properties, the 5 mm thick Robax® Transparent Glass-Ceramic was used for this purpose and designed for both cube and long depth compartment.

Especially for the small-scale experimental study, it is very important to keep the compartment completely sealed. To do so, all the leaks occurring from equipments that penetrated to the box such as thermocouple wires or any gaps from adjusting vent sizes were sealed by either LCI intumescent firestop sealant (LCI300) or RESBOND™ 907GF adhesive sealant which was more rigid and permanent.

In addition, it was necessary to have remote ignition of the Heptane liquid fuel, for vent size was very small in some cases. Therefore an electric spark igniter set up above fuel surface about 1 cm was equipped to initiate the combustion.

2.3 Experimental Procedure

All tests were strictly conducted according to the same preparation steps and test running procedures to make data from all cases consistent and comparable.

2.3.1 Test Preparation

Vent size: Small pieces of Kaowool® board were cut to meet desired shapes and assembled to the front wall panel to adjust the vent sizes. All connections and gaps were sealed with LCI intumescent sealant.

Gas Analyzer: In this process, it was important to check and adjust the gas flow rate shown by flow meters on both gas analyzers to stay in the right level, i.e. 1.0 l/min.

All chemical agents, Drierite® and Ascarite® were checked to see if they were needed to change. For instance, Drierite® would turn from blue to pink when it was saturated which would not trap any more moisture; Ascarite® would clog up and block the gas to flow to the tube which was indicated by the decrease of gas flow rate. In addition, the glass sheet filters normally were also changed after three or four tests had been performed, and every day new ice was used in gas cold trap (ice box) and mixed with some salt to make the water freezing point below 0 °C.

Thermocouples: Location and noise were of concern for the thermocouples. Since we were using flexible wire thermocouples which might easily have moved during the experiment, before each test the thermocouple beads were assured to be located at the right position as in the design drawing. Noise was occasionally picked up by thermocouples (also by other transducers) due to the connector from transducers or the ground reference was not properly connected to the systems. Hence before starting the actual test, it was necessary to pre-run the data acquisition program to see if there were any unusual signals.

Load Cell: As mentioned before, the load cell has a measurement range up to 250 g with 2.0 kg load capacity, and output signal from 0 to 1 volt. While in this experiment, the range of load applied to the cell was approximately from 200 to 1400 g. Therefore some preload as well as tare adjustment were applied to allow the output staying in working range (0 to 1 volt). In this process, fuel pan was placed on the stand and carefully adjusted to the position where the pan did not touch the floor and the heat flux transducer (HF1). Ten-gram standard weight was used to calibrate and check if the voltage output was correct, ~ 0.035 Volt per 10 g. In case the output was not stable or did

not come back to original point when the weight was removed, the fuel pan location had to be readjusted so that it did not touch the floor or the heat flux transducer, and moved freely.

Differential Pressure Transducers: Before conducting the test, a zero adjustment was performed to the pressure transducers. This process was done by using a bypass line to connect the pressure detection side to reference side so that the electric manometer give a 0 volt output [2].

Heat Flux Transducers: It was very important to have water flowing through all heat flux transducers for cooling purpose before running the test. However the water flown to HF1, the heat flux gauge at the fuel surface, had to be heated to 65 °C by adjusting the transformer.

Video: Every test in this experiment was video taped through the side wall window. A thin film of soap was applied to the cleaned glass by rubbing all around until we could see through the glass clearly. The purpose for this thin film was to prevent soot blocking when we shot the video.

2.3.2 Test Procedures

1. To prevent fuel from boiling at the bottom of the pan, water was firstly poured into the fuel pan until it reached about 4/5 of pan height, then followed by Heptane liquid fuel.
2. The front wall, which had the adjusted vents, was assembled to the compartment and locked tightly by c-clamps shown in Figure 2.8. Final seal for any leaks and gaps were made if there was one.

3. At this point, we were ready to run the test. The data acquisition program, LabVIEW, was set to run at time 0, then shooting video started after about 5 seconds, and the fuel was ignited by turning on the electric spark at 10 seconds. There were some cases that occasionally did not match each step exactly at the time described above. For the case of the biggest fire (19.0 cm diameter), if ignition was delayed, there was a chance to have an explosion due to the relatively large amount of fuel vapor evaporated from the big pan in the sealed compartment. Also with a small vent size, i.e. $1 \times 2 \text{ cm}^2$, a pressure pulse the water seal cups was experienced. As a result of that, it is recommended that the time to start ignition after closing the front wall should as short as possible to prevent accidents and damage.

4. The test would be ended basically the extinction occurred or when we ran out of the fuel; however, the data was recorded until all the gas concentration came back to their original levels, or in some cases, at least for 1 minute after extinction in order to cover the travel time of the gas to reach the analyzers.

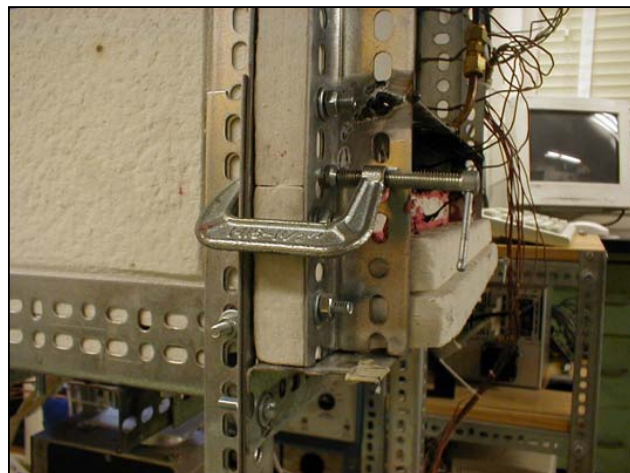


Figure 2.8 Front panel locked by C-clamp

3. Experimental Results and Observations

In this section, experimental results are categorized based on compartment fire behavior observed. Chosen examples of data plots from the tests which represent each category are illustrated along with fire behavior pictures captured from real-time videos. For the complete set of experimental results, the reader is directed towards the Appendix D. In addition, a closer look for some interesting compartment fire behavior with some explanations is also presented in this chapter.

3.1 General Observations

As mentioned above that the experimental results are grouped according to fire behavior, but indeed extinction criteria is also considered as an important factor to determine preliminarily how and when the ventilation size affects the enclosure fire. Extinction, which in this study means the fire is gone and some fuel is left in the pan, is observed in Category 1 and 2, while in Category 3 and 4 the fire is out because of exhausted fuel. The observation summary of all cases that were tested is presented in Table 3.1.

3.1.1 Category 1: Extinction Due to Filling

This group is the case where the ventilation factor is small, in other words, vent size is very small compared to fuel pan area. As the fire starts, it continues burning for a while and then becomes extinguished because the compartment is filled and the air supply is not sufficient due to the very small vents. Moreover, in this case the air inflow from the lower vent does not appear to blow the fire so much, as vent size is small; hence, the vent wind effect is not felt by the fire. There is no oscillating combustion observed in this case, but ghosting flames may occur just before extinction. It shall be noted that for

the small fire size case, i.e. 6.5 cm diameter, which falls in to this group criteria, the fire behaves as a tall steady laminar flame all the time before it goes to extinction. The selected experimental data shown in Figure 3.1 is from the test where the 9.5 cm pool fire was burned and the total vent area was 4 cm² (2-1×2 cm vents). At the Initial Stage, the fuel was just ignited and burned with an unsteady puffing character. At the same time, the fire generated combustion products push gas out from the compartment through both the top and bottom as seen in differential pressure chart show positive values. Then the fire became a stable vertical plume with a constant burning rate and there was no effect from the wind on the flame shape.

Vent		Fuel Pan			
Size (cm×cm)	A ₀ (cm ²)	6.5 cm A _F = 33.2 cm ²	9.5 cm A _F = 70.9 cm ²	12.0 cm A _F = 113.1 cm ²	19.0 cm A _F = 283.6 cm ²
1×1	2	B, C1	E, C1	G, E, C1	E, C1
1×2	4	O, E, C2	E, C1		
1×3	6	O, G, E, C2	O, G, E, C2	G, E, C1	G, E, C1
1×4	8	O, G, E, C2	O, G, E, C2		
1×5	10	O, B, C4		G, E, C2	O, G, E, C2
1×6	12	O, B, C4	O, G, E, C2		
1×9	18	O, B, C4	O, G, E, C2	O, G, E, C2	O, E, C2
1×12	24	O, B, C4	O, G, E, C2		
1×15	30		O, E, C2	O, E, C2	
1×21	42		O, B, C4	O, B, C4	
1×30	60		O, B, C4	O, B, C4	
1×40	80		B, C4	O, B, C4	O, B, C3
3×1	9	O, G, E, C2	O, G, E, C2		
3×2	12	O, G, E, C2			
3×3	18	O, B, C4	O, G, E, C2		
3×4	24		O, G, E, C2		
3×5	30		O, G, E, C2		O, E, C2
3×7	42	B, C4	O, B, C4		O, E, C2
3×10	60		O, B, C4		O, B, V, C3
3×15	90	B, C4	B, C4		O, B, V, C3
3×20	120		B, C4		
3×30	180	B, C4	B, C4		
3×40	240	B, C4	B, C4		O, B, V, C3

Note: A₀ = Total area of top and bottom vent E = Extinction
A_F = Area of fuel pan B = Burn-out
O = Oscillating Combustion V = Burning at Lower Vent
G = Ghosting Flame C1 to C4 = Category 1 to 4

Table 3.1 Experimental Condition and Compartment Fire Behavior Summary

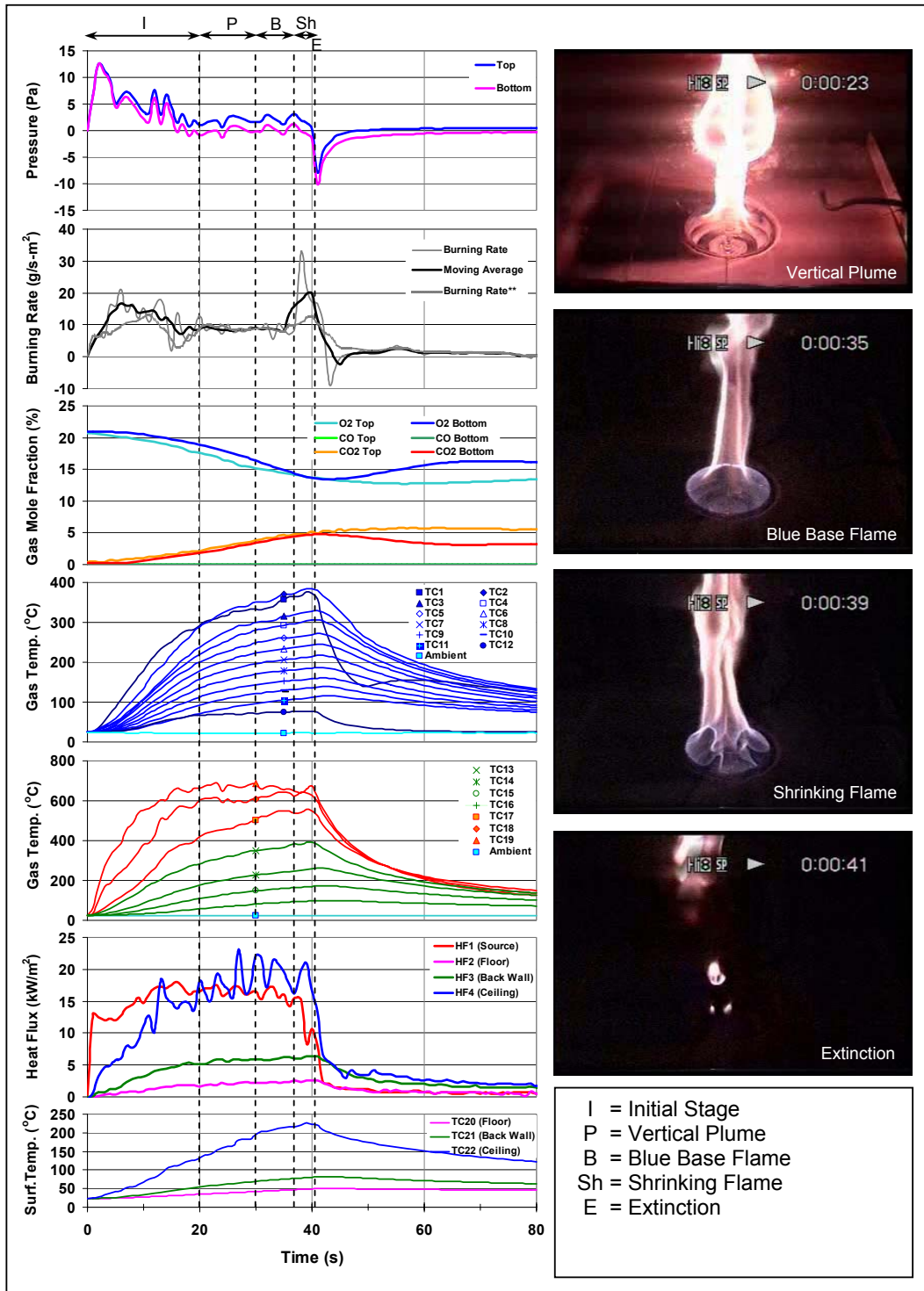


Figure 3.1 Extinction Due To Filling, $D_F = 9.5 \text{ cm}$, $A_0 = 4 \text{ cm}^2$, Case: 95-1×2

As time went on, the oxygen concentration dropped because the fire was consuming the oxygen and the compartment was being filled by product gases and air entered in. The flame became blue and thinner and then shrunk and finally extinguished a detached flame without oscillation could be observed as well for some cases near extinction. This process essentially indicated the insufficiency of oxygen due to filling of the nearly closed compartment. It should be noted that differential pressure chart in Figure 3.1 shows a quite high value compared to other cases at the fire initiation and extinction stage, i.e. 12 Pa and 10 Pa, respectively. This peak pressure amplitude happens for small vents. It also leads to an error in the burning rate obtained from load cell. A correction of the mass loss rate due to this pressure effect can be found in Appendix A. The corrected burning rate is denoted by (**).

3.1.2 Category 2: Extinction

In this category, extinction takes place as in Category 1, but the difference is that the larger ventilation in Category 2 allows air from outside to come in and sustain the fire. Extinction still occurs and is preceded by either oscillations or ghosting flames. More details in these two phenomena are discussed in section 3.2. Two selected tests for this category, 9.5 cm pan with 6 cm^2 ($2-1 \times 6 \text{ cm}$ vents), 9.5 cm pan with 12 cm^2 ($2-1 \times 12 \text{ cm}$ vents), are presented in Figure 3.2 and Figure 3.3 respectively. It can be seen that the fire, in both cases, was blown backward after an initial steady vertical plume. Then oscillating combustion occurred, followed by a ghosting flame, and finally extinction took place. This process shows the effect of low ventilation, as well as air entrainment through lower vent, on the compartment fire.

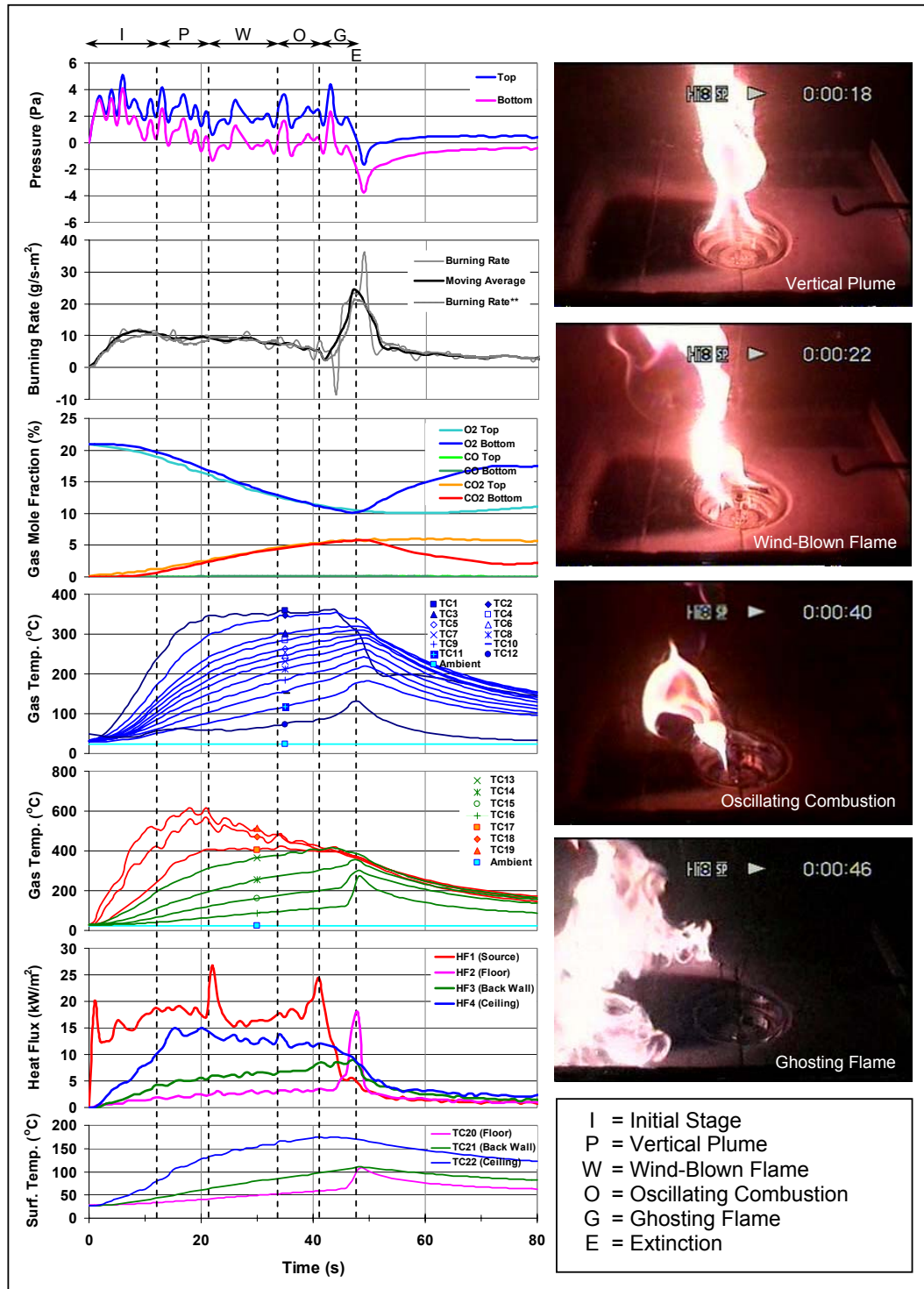


Figure 3.2 Extinction, $D_F = 9.5 \text{ cm}$, $A_0 = 12 \text{ cm}^2$, Case: 95-1×6

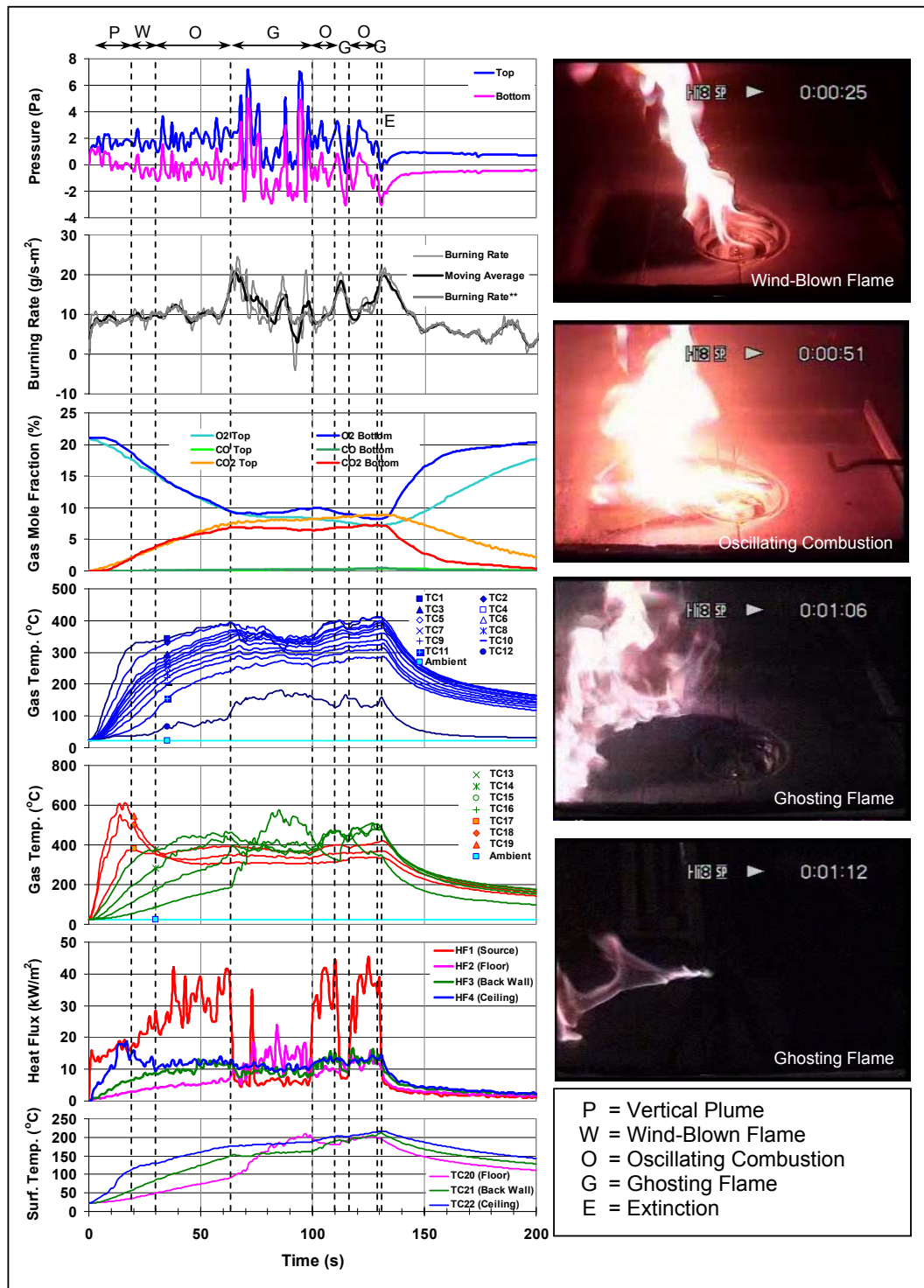


Figure 3.3 Extinction, $D_F = 9.5 \text{ cm}$, $A_0 = 24 \text{ cm}^2$, Case: 95-1×12

3.1.3 Category 3: Burning at Vent

An interesting phenomenon, burning at the lower vent, is observed in burning a relatively large pool fire in wall-vent compartment. Indeed, it occurs in all cases where the 19.0 cm diameter fire is burning with the vent size between 60 to 240 cm². The vent fire can exhibit both oscillatory and steady burning behavior depending on vent size and geometry, and continues burning until the fuel in the pan is exhausted. Figure 3.4 shows a steady linear-flame burning from 19.0 cm pan test with 80 cm²(2-1×40), and Figure 3.5 shows a selected test with experimental results, 19.0 cm with 60 cm² (2-3×10 cm), where vent oscillatory burning occurs.

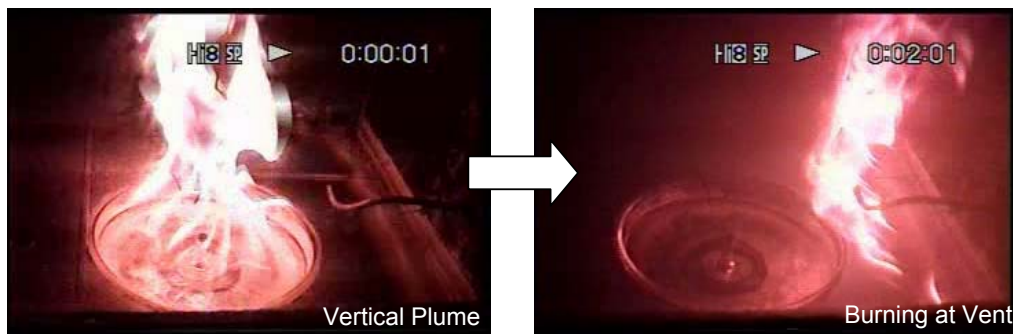


Figure 3.4 Vent Steady Burning, $D_F = 19.0$ cm, $A_0 = 24$ cm², Case: 190-1×40

This is the traditional ventilation-limited fire in that the oxygen is nearly zero in the upper layer. This indicates that all of the incoming oxygen is burned. There is so much excess fuel that it burns where oxygen fire enters.

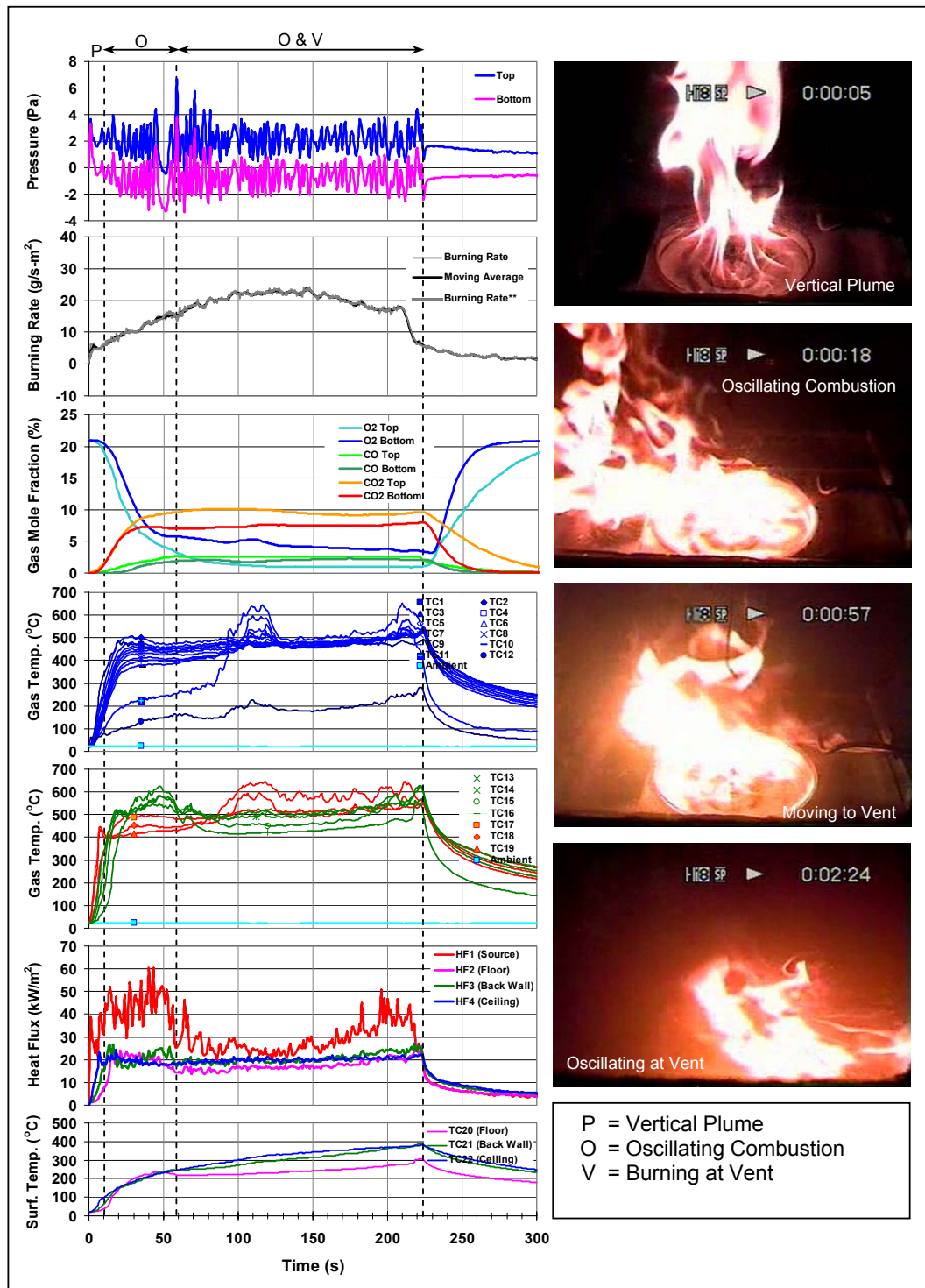


Figure 3.5 Burning at Vent, $D_F = 19.0$ cm, $A_0 = 60$ cm², Case: 190-3×10

3.1.4 Category 4: Steady Burning

In this category, steady burning can be presented in two forms, steady oscillation and normal quasi-steady burning [7]. The oscillating combustion in this category is different from the one in category 2 in that the fire can continue burning while maintaining the oscillations until the fuel is exhausted as shown in Figure 3.6. As for the case where the vent size is very large, normal quasi-steady burning with bi-directional flow is observed in all sizes of pan fires except in the largest one, 19.0 cm diameter. Figure 3.7 shows the example of this case.

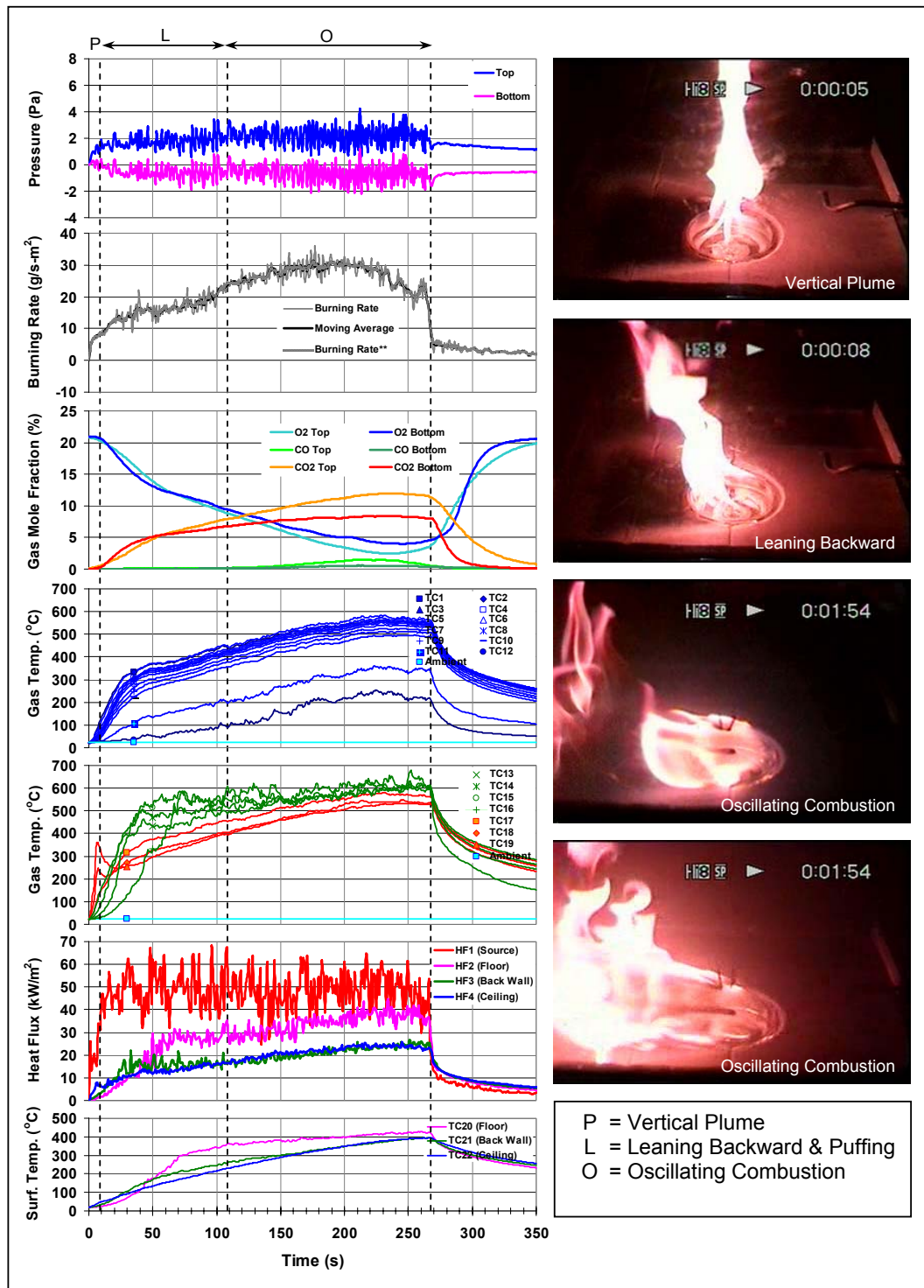


Figure 3.6 Oscillation in Steady Burning, $D_F = 9.5 \text{ cm}$, $A_0 = 60 \text{ cm}^2$, Case: 95-3×10

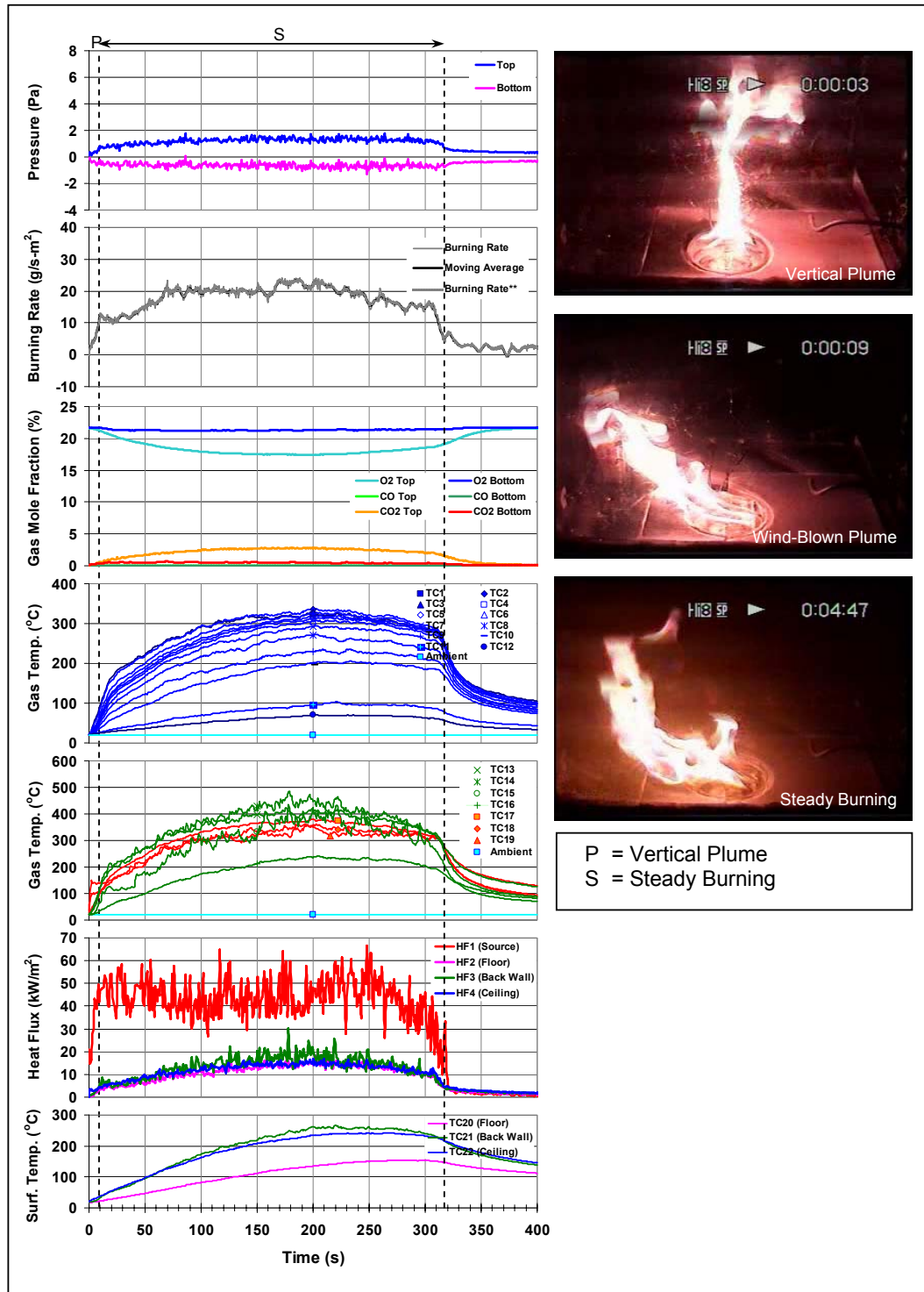


Figure 3.7 Steady Burning, $D_F = 9.5 \text{ cm}$, $A_0 = 240 \text{ cm}^2$, Case: 95-3×40

3.2 Explanation of Oscillation Fire Phenomena

In this study, **oscillating combustion** can be defined as a phenomenon of fire that goes on and off repeatedly above the fuel surface at some frequency under low-ventilation circumstance within an enclosure. The oscillation normally can be seen in a region of, so called, intermediate vent sizes [1,6] which lies between very small and large vents where extinction and steady burning (exhausted fuel) take place, correspondingly. Generally, the oscillation frequency is in the order of 1 Hz, yet this may vary for some cases due to different fire and vent sizes. The zoomed view of differential pressure plotted from the 9.5 cm pan with 21 cm^2 vent area case, where data are taken at every 0.2 sec., is presented in Figure 3.8 to show the oscillation frequency. Indeed, this phenomenon could be considered as a transition between extinction and steady burning, because it has been observed in both cases, i.e. occurring before the fire extinguishes or continues as oscillatory burning until the fuel exhausts.

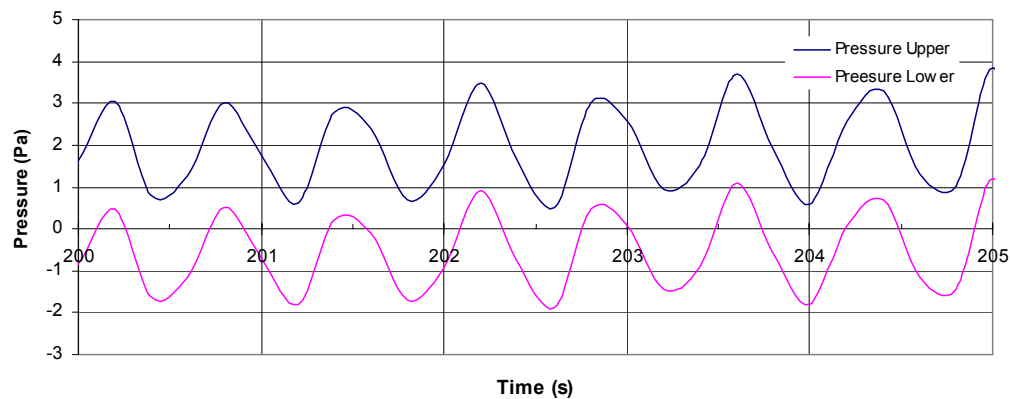


Figure 3.8 Differential pressure zoomed view from 9.5 cm pan with 21 cm^2 vent area

The oscillating combustion process can keep going on until the fuel is exhausted, or it is possible to see extinction can occur during this process. This depends on the size

of the ventilation. If the vent is small, extinction occurs, while oscillatory steady burning can be expected for the larger vent. Figure 3.9 and Figure 3.10 show oscillating behavior of two fire sizes, 9.5 cm and 19.0 cm.

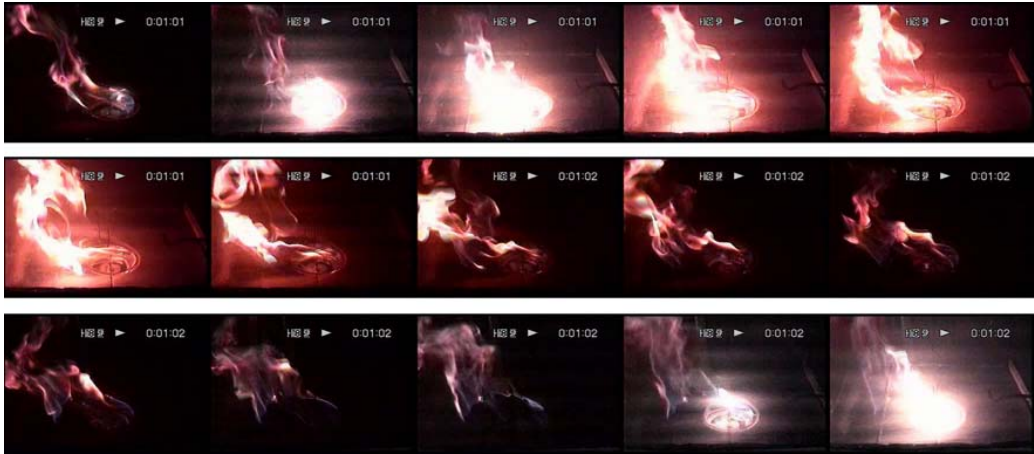


Figure 3.9 Oscillating Combustion, $D_F = 9.5 \text{ cm}$, $A_0 = 24 \text{ cm}^2$, Case: 95-1×12,

Captured at 15 frame/second



Figure 3.10 Oscillating Combustion, $D_F = 19.0 \text{ cm}$, $A_0 = 60 \text{ cm}^2$, Case: 190-3×10,

Captured at 15 frame/second

Another interesting oscillation fire phenomena is **ghosting flames** or a flame that detaches from the fuel surface and floats around the compartment with same oscillatory

behavior. This ghosting phenomena also oscillates with the same manner as described previously in oscillating combustion over fuel surface, but the difference is that ghosting flame will float around to find a favorable location to maintain the reaction. One can see this ghosting flame as an indication of the end of the oscillating combustion period, and it usually happens before extinction. Figure 3.11 and Figure 3.12 illustrate ghosting flame. Also previously in Figure 3.3, it is interesting to see the fire switches between an oscillation and ghosting flames for several periods, while in most cases oscillation usually happens before ghosting then extinction occurs.

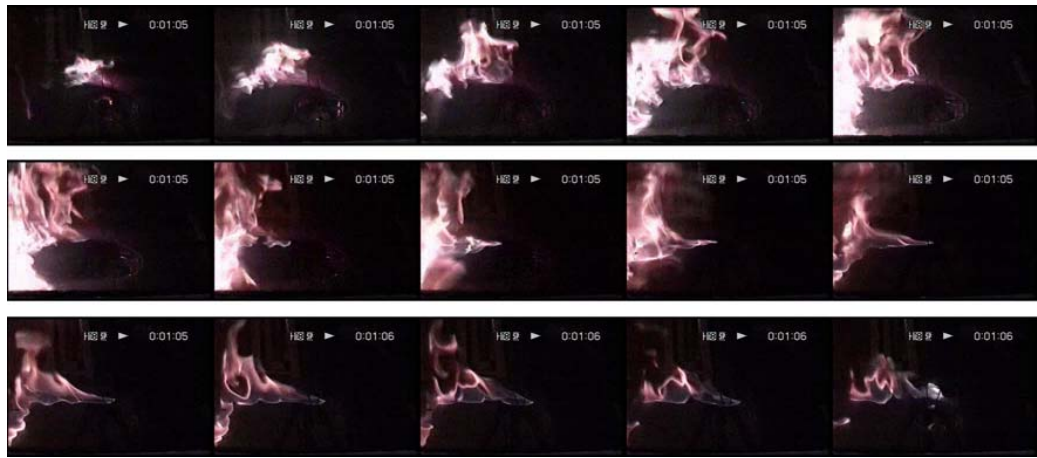


Figure 3.11 Ghosting Flame, $D_F = 9.5 \text{ cm}$, $A_0 = 24 \text{ cm}^2$, Case: 95-1×12,
1:05 min, Captured at 15 frame/second

In addition, as previously mentioned in the last section, oscillating combustion involves burning at vent, which was only observed for the in large pan cases (19.0 cm diameter). The process of oscillation in these cases happens much faster than in smaller pan cases. Also the frequency of oscillation is increasing (from 1 Hz to 2 Hz) while the flame is moving to the lower vent, and exhibits the jet flame from lower vent as shown in

Figure 3.13. This vent burning essentially indicates the complete ventilated controlled fire in the compartment; since the oxygen is all consumed.

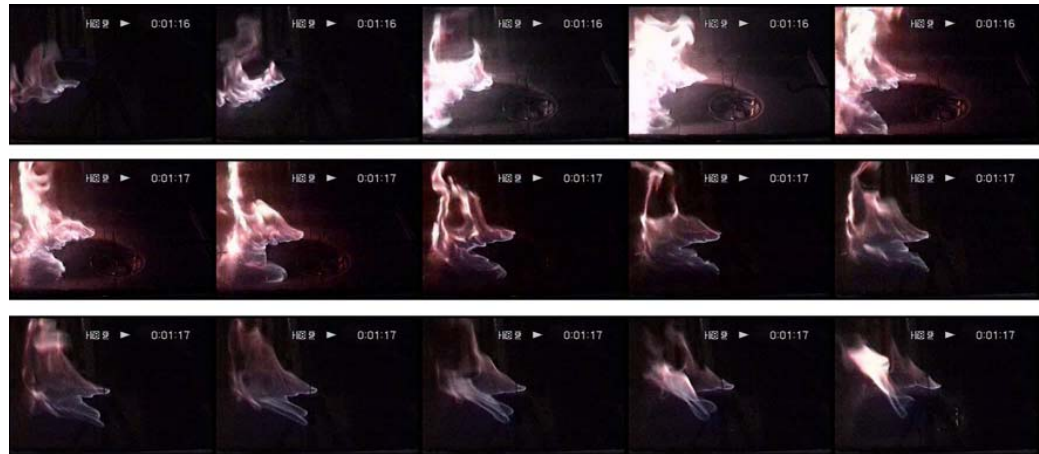


Figure 3.12 Ghosting Flame, $D_F = 9.5 \text{ cm}$, $A_0 = 24 \text{ cm}^2$, Case: 95-1×12,
1:17 min, Captured at 15 frame/second



Figure 3.13 Oscillatory Jet flame at Vent, $D_F = 19.0 \text{ cm}$, $A_0 = 60 \text{ cm}^2$, Case: 190-3×10,
Captured at 15 frame/second

3.3 Free Burning Result

The burning rate and heat flux to the fuel surface of free burning, out side of the compartment, were examined for each pan size in order to use as reference value. Although it shall be noted that in this experiment, the fuel pan location was adjusted to have the fuel surface stayed at the same level as the floor. Therefore in the free burning tests, some pieces of Kawool board were put next to the pans in order to have the same pan-floor orientation as in the compartment, which is that fuel surface and floor were at the same level. As a result of this arrangement, the free burning rate results we obtained in this study were higher than the ones from Wakatsuki [2] and Ringwelski [1]. This could be due to the difference of air entrainment flow which leads to different heat transfer coefficient. Summary of results are shown below in Table 3.2 and Figure 3.14 and Figure 3.15.

Fuel Pan Diameter	Average Burning Rate ($\text{g}/\text{m}^2\text{s}$)	Average Heat Flux (kW/m^2)
6.5 cm	12.87	19.34
9.5 cm	11.11	19.82
12.0 cm	11.81	22.74
19.0 cm	12.85	27.24

Table 3.2 Average Burning Rate and Heat Flux to the Fuel Surface from Free Burning

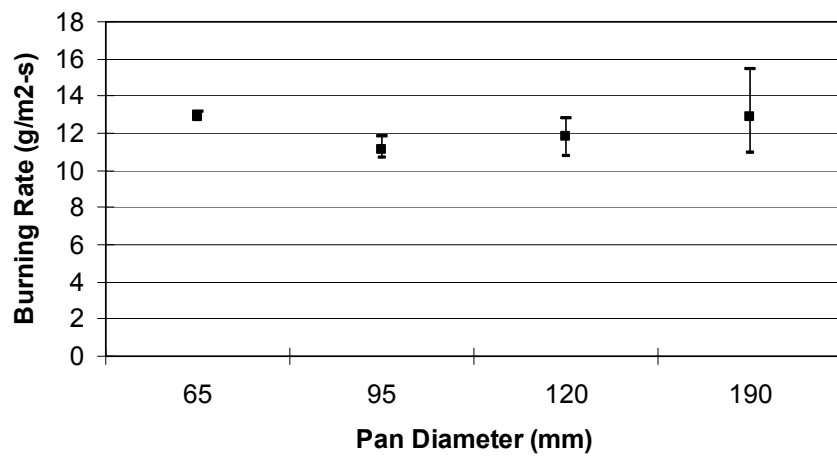


Figure 3.14 Free Burning Rates

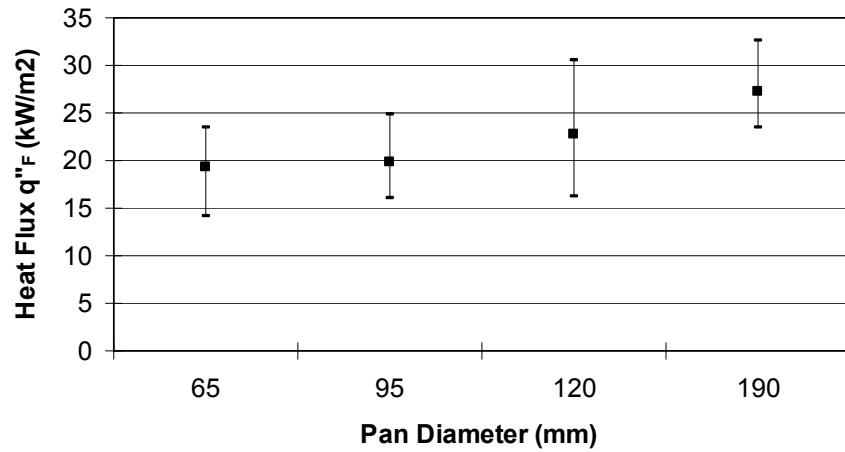


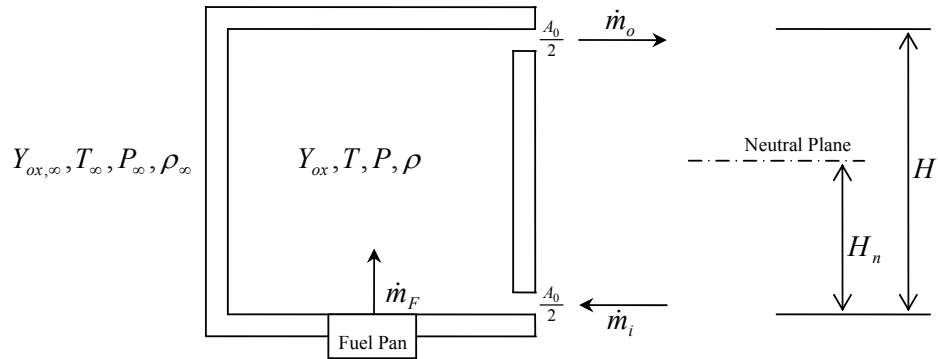
Figure 3.15 Heat Fluxes to Fuel Surface from Free Burning

4. Discussion and Analysis

Following up the experimental data in Chapter 3, discussion and analysis on results are presented here in this chapter. The significant independent variables that control the behavior of fire in wall-vent compartment are determined. A summary of all experimental results are present in terms of such variables, and discussed. A comparison of theory and measurement is also presented.

4.1 Ventilation and Compartment Fire Behaviors

In order to present the experimental results and categorize the fire behavior examined in this study, independent governing parameters shall be determined. The governing parameters are determined by examining quasi-steady burning conditions. These then are used to explain the dynamic burning conditions.



$$A_0 = \text{Total vent area}$$

Figure 4.1 Quasi-steady wall-vent compartment

Conservation of Mass

$$\dot{m}_F + \dot{m}_i = \dot{m}_o \quad (4.1)$$

Conservation of Energy

$$\dot{m}_o c_p T - \dot{m}_i c_p T_\infty - \dot{m}_F c_p T = \dot{Q} - h A_s (T - T_\infty) \quad (4.2)$$

Conservation of Species

$$\dot{m}_o Y_{ox} - \dot{m}_i Y_{ox,\infty} = -\frac{\dot{Q}}{\Delta h_{air} / Y_{ox,\infty}} \quad (4.3)$$

Heat Release Rate

$$\dot{Q} = \dot{m}_F \Delta h_c \quad \text{for } \Phi < 1 \quad (4.4a)$$

$$\dot{Q} = \dot{m}_i \Delta h_{air} \quad \text{for } \Phi > 1 \quad (4.4b)$$

where $\Phi = \frac{\dot{m}_F / \dot{m}_i Y_{ox,\infty}}{r}$ and r is stoich. fuel/oxygen

Consider the bottom vent.

From Bernoulli equation,

$$\frac{v_i^2}{2} + \frac{P}{\rho_\infty} = \frac{P_\infty}{\rho_\infty}, \text{ and } P - P_\infty = H_n(\rho - \rho_\infty)g.$$

Then

$$v_i = \sqrt{\frac{2H_n(\rho_\infty - \rho)g}{\rho_\infty}} = \sqrt{\frac{2H_n(T - T_\infty)g}{T}}.$$

As for top vent,

$$\frac{v_o^2}{2} + \frac{P_\infty}{\rho} = \frac{P}{\rho}, \text{ and } P - P_\infty = (H - H_n)(\rho_\infty - \rho)g$$

yields

$$v_o = \sqrt{\frac{2(H - H_n)(\rho_\infty - \rho)g}{\rho}} = \sqrt{\frac{2(H - H_n)(T - T_\infty)g}{T_\infty}}.$$

Then from

$$\dot{m} = C_d A \rho v ; \text{ where } C_d \text{ is flow coefficient,}$$

we have

$$\dot{m}_i = 0.5 C_d A_0 \rho_\infty \sqrt{\frac{2H_n(T - T_\infty)g}{T}} \quad (4.5)$$

$$\dot{m}_o = 0.5 C_d A_0 \rho \sqrt{\frac{2(H - H_n)(T - T_\infty)g}{T_\infty}}. \quad (4.6)$$

Substitute Eq (4.5) and (4.6) into Eq (4.1) we have

$$0.5 C_d A_0 \rho \sqrt{\frac{2(H - H_n)(T - T_\infty)g}{T_\infty}} = 0.5 C_d A_0 \rho_\infty \sqrt{\frac{2H_n(T - T_\infty)g}{T}} + \dot{m}_F. \quad (4.7)$$

Dividing Eq (4.7) with \dot{m}_i yields

$$\frac{0.5 C_d A_0 \rho \sqrt{\frac{2(H - H_n)(T - T_\infty)g}{T_\infty}}}{1 + \mu} = 0.5 C_d A_0 \rho_\infty \sqrt{\frac{2H_n(T - T_\infty)g}{T}}$$

$$\text{where } \mu = \frac{\dot{m}_F}{\dot{m}_i},$$

$$\frac{\sqrt{(H - H_n)\left(\frac{T}{T_\infty} - 1\right)}}{1 + \mu} = \frac{T}{T_\infty} \sqrt{H_n\left(1 - \frac{T_\infty}{T}\right)}$$

$$\frac{\sqrt{(H - H_n)\left(\frac{T}{T_\infty} - 1\right)}}{1 + \mu} = \sqrt{H_n \frac{T}{T_\infty} \left(\frac{T}{T_\infty} - 1\right)}$$

$$\frac{(H - H_n)}{(1 + \mu)^2} = H_n \frac{T}{T_\infty}$$

$$\frac{H}{H_n} = \frac{T}{T_\infty} (1 + \mu)^2 + 1 \quad (4.8)$$

Substituting Eq (4.8) into Eq (4.5) and (4.6) yields

$$\dot{m}_i = \frac{0.5C_d A_0 \sqrt{H} \rho_\infty \sqrt{g} \sqrt{2 \left(1 - \frac{T_\infty}{T}\right)}}{\left(1 + (1 + \mu)^2 \frac{T}{T_\infty}\right)^{1/2}} \quad (4.9)$$

$$\dot{m}_o = \frac{0.5C_d A_0 \sqrt{H} \rho \sqrt{g} (1 + \mu) \sqrt{2 \left(\frac{T}{T_\infty} - 1\right) \frac{T}{T_\infty}}}{\left(1 + (1 + \mu)^2 \frac{T}{T_\infty}\right)^{1/2}}. \quad (4.10)$$

For small \dot{m}_F , $\mu \rightarrow 0$.

Then from (4.9) and (4.10)

$$\dot{m}_i = 0.5C_d A_0 \sqrt{H} \rho_\infty \sqrt{g} \sqrt{2} \begin{pmatrix} 1 - \frac{T_\infty}{T} \\ 1 + \frac{T}{T_\infty} \end{pmatrix}^{1/2} \quad (4.11)$$

$$\dot{m}_o = 0.5C_d A_0 \sqrt{H} \rho \sqrt{g} \sqrt{2} \begin{pmatrix} \left(\frac{T}{T_\infty} - 1\right) \\ \left(\frac{T}{T_\infty} + 1\right) \end{pmatrix} \begin{pmatrix} \frac{T}{T_\infty} \\ \frac{T}{T_\infty} \end{pmatrix}^{1/2}$$

$$\dot{m}_o = 0.5C_d A_0 \sqrt{H} \rho \left(\frac{T}{T_\infty}\right) \sqrt{g} \sqrt{2} \begin{pmatrix} 1 - \frac{T_\infty}{T} \\ 1 + \frac{T}{T_\infty} \end{pmatrix}^{1/2}$$

$$\dot{m}_o = 0.5C_d A_0 \sqrt{H} \rho_\infty \sqrt{g} \sqrt{2} \begin{pmatrix} 1 - \frac{T_\infty}{T} \\ 1 + \frac{T}{T_\infty} \end{pmatrix}^{1/2}. \quad (4.12)$$

From Eq (4.2), the term $\dot{m}_F c_p T$ is relatively small [8] and $\dot{m}_o \approx \dot{m}_i$, therefore the Conservation of Energy becomes

$$\dot{m}_o c_p (T - T_\infty) = \dot{Q} - h A_s (T - T_\infty). \quad (4.13)$$

Substituting \dot{m}_o into Eq (4.13) and divided by $A_F \dot{m}_{F,\infty}'' c_p T_\infty$ to make \dot{Q} dimensionless yield

$$\frac{\dot{Q}}{A_F \dot{m}_{F,\infty}'' c_p T_\infty} = \frac{A_0 \sqrt{H} \rho_\infty \sqrt{g}}{A_F \dot{m}_{F,\infty}''} 0.5 C_d \sqrt{2} \left(\frac{T}{T_\infty} - 1 \right) \left(\frac{1 - \frac{T_\infty}{T}}{1 + \frac{T}{T_\infty}} \right)^{1/2} + \frac{h A_s}{A_F \dot{m}_{F,\infty}'' c_p} \left(\frac{T}{T_\infty} - 1 \right) \quad (4.14)$$

Now from Conservation of Species with $\dot{m}_o \approx \dot{m}_i$, we have

$$\dot{m}_i \left(\frac{Y_{ox}}{Y_{ox,\infty}} - 1 \right) \Delta h_{air} = -\dot{Q} \quad (4.15)$$

Substituting \dot{m}_i by Eq (4.11) and making \dot{Q} dimensionless by $A_F \dot{m}_{F,\infty}'' c_p T_\infty$ yields

$$\frac{\dot{Q}}{A_F \dot{m}_{F,\infty}'' c_p T_\infty} = \frac{A_0 \sqrt{H} \rho_\infty \sqrt{g}}{A_F \dot{m}_{F,\infty}''} \left(\frac{0.5 C_d \sqrt{2}}{c_p T_\infty} \right) \left(\frac{1 - \frac{T_\infty}{T}}{1 + \frac{T}{T_\infty}} \right)^{1/2} \left(1 - \frac{Y_{ox}}{Y_{ox,\infty}} \right) \Delta h_{air}. \quad (4.16)$$

Also from Eq (4.4a)

$$\frac{\dot{Q}}{A_F \dot{m}_{F,\infty}'' c_p T_\infty} = \frac{\dot{m}_F}{A_F \dot{m}_{F,\infty}''} \left(\frac{\Delta h_c}{c_p T_\infty} \right), \quad (4.17)$$

where \dot{m}_F can be presented from the compartment burning rate model [6] as

$$\dot{m}_F = \dot{m}_{F,\infty} \left(\frac{Y_{ox}}{Y_{ox,air}} \right) + \frac{F A_F \sigma (T_g^4 - T_\infty^4)}{L} \quad (4.18)$$

Now from Eq (4.14), (4.16), (4.17) and (4.18), we can conclude that

$$\begin{aligned} T &= f\left(\frac{A_0 \sqrt{H} \rho_\infty \sqrt{g}}{A_F \dot{m}_{F,\infty}''}, \frac{A_s h}{A_F \dot{m}_{F,\infty}''}\right), \\ Y_{ox} &= f\left(\frac{A_0 \sqrt{H} \rho_\infty \sqrt{g}}{A_F \dot{m}_{F,\infty}''}, T\right), \\ \frac{\dot{m}_F}{A_F} &= f(Y_{ox}, T). \end{aligned} \quad (4.19)$$

Therefore,

$$\left. \begin{array}{c} T \\ Y_{ox} \\ \frac{\dot{m}_F}{A_F} \end{array} \right\} = f\left(\frac{A_0 \sqrt{H} \rho_\infty \sqrt{g}}{A_F \dot{m}_{F,\infty}''}, \frac{A_s h}{A_F \dot{m}_{F,\infty}''}\right). \quad (4.20)$$

We shall see that the significant independent variables that govern the burning rate or more precise fuel mass loss rate, is the ratio of air flow to fuel flow, and the ratio of compartment surface area to fuel area as in the right side of Eq (4.20) respectively. In this study, we shall examine fire behavior principally in terms of only one variable which is the air flow to the fuel flow, $\left(\frac{A_0 \sqrt{H} \rho_\infty \sqrt{g}}{A_F \dot{m}_{F,\infty}''}\right)$. This will be used to represent the experimental data results and the regimes of fire behavior described previously in Chapter 3. In our case, the free-burning mass loss rate for each fuel pan size is not very different, hence only $\left(\frac{A_0 \sqrt{H} \rho_\infty \sqrt{g}}{A_F}\right)$ will be used. This is in compliance with Bullen and Thomas [9]. In this study it will be called the ***ventilation parameter***.

Since the results examined in this study are transient for the most part, it is important to evaluate the summary result from each case with consistency. The data was carefully picked based on the same criteria presented in Table 4.1.

Criteria	Extinction	Steady or Burned out
Burning Rate	Average value before extinction	Average at peak
O ₂ Conc.	At extinction	Minimum
Gas Temperature	At extinction	Maximum
Heat Flux	Consistent with burning rate	Consistent with burning rate
CO and CO ₂ Conc.	At extinction	Maximum

Table 4.1 Criteria for selecting experimental results

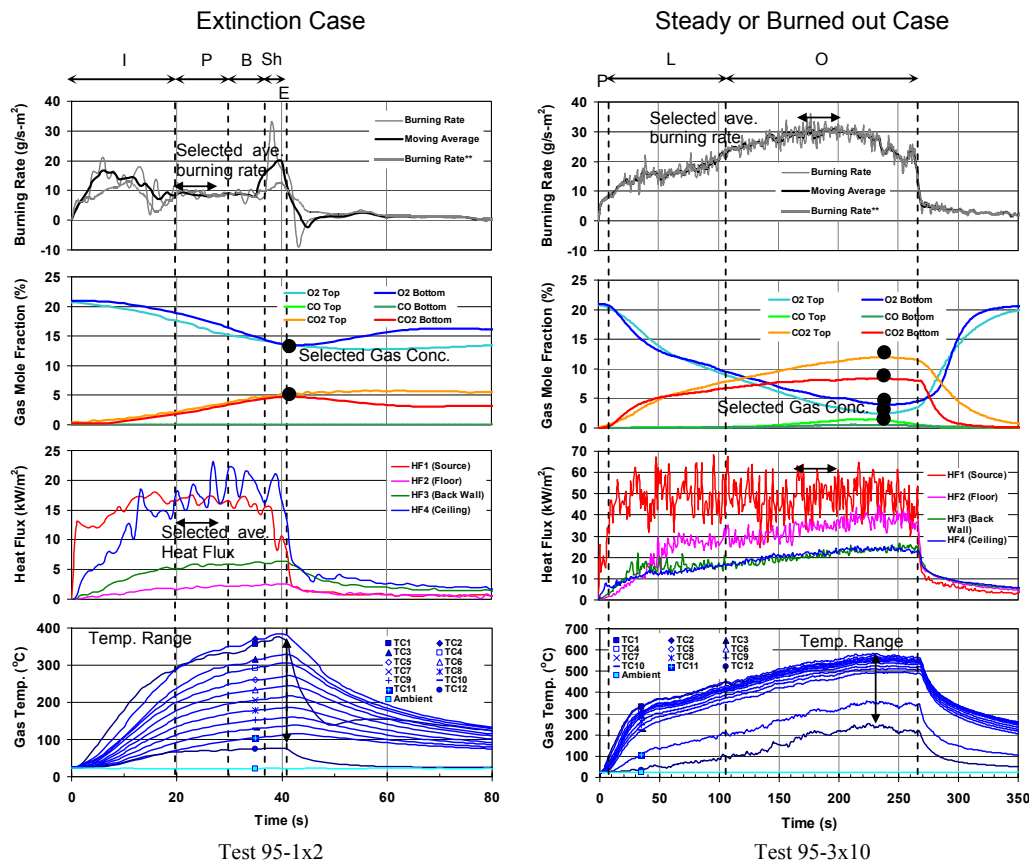


Figure 4.2 Example for data selecting

4.1.1 Burning rate

The burning rate per unit area is plotted as a function of the ventilation parameter for each pan diameter. This is shown in Figure 4.3 where regime 1 to 4 refers to fire categories. Essentially this plot represents the dimensionless dependence of burning rate, since $\dot{m}_{F,\infty}''$ is approximately constant at 12.28 g/m²s. Burning rate data from Ringwelski [1] are also included in this plot. The dark border around the plot represents observed extinction, while borderless means the fuel was exhausted or burned out. The numbers in the legend represent fuel pan diameter in mm.

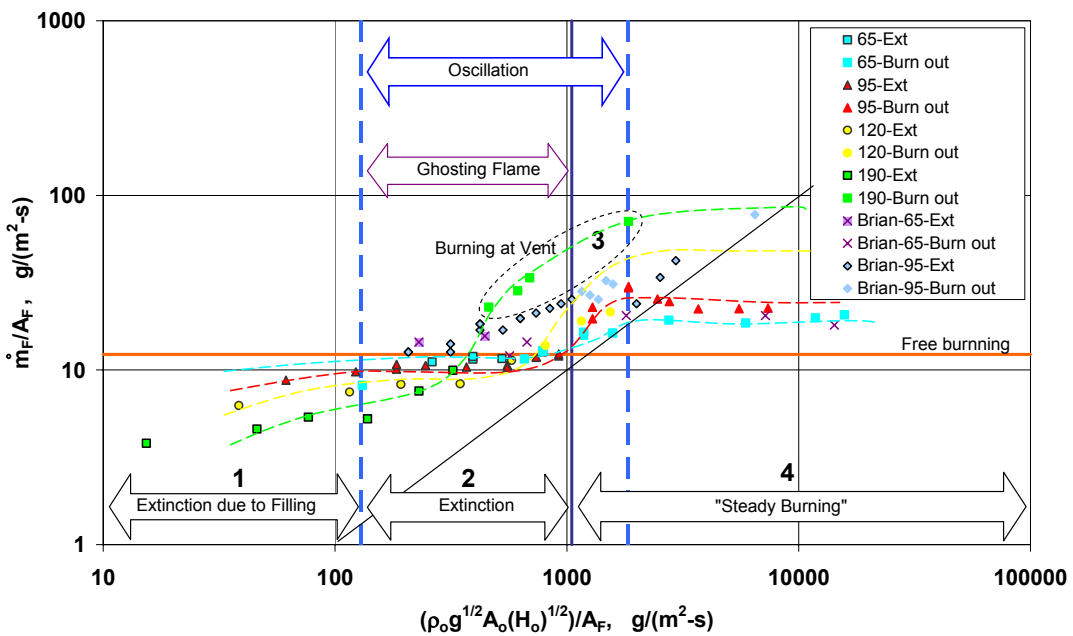


Figure 4.3 Burning rate regimes

The burning rate from each test was carefully picked based on the same criteria. For cases where extinction occurred, a burning rate at the point where initial stage of burning had passed was selected, and as for the fuel exhausted cases, the maximum steady point was picked.

From the plot we can see that the fire behavior regimes lie from extinction to steady burning with increasing ventilation parameter. Burning at the vent occurred only for the 19.0 cm diameter pan and starts at the ventilation parameter $\sim 460 \text{ g}/(\text{m}^2\cdot\text{s})$. The dash curves show the predicted trend of burning rate per unit area for each pan size. Furthermore, the stoichiometric line, assuming bi-directional steady flow, is added to the plot in Figure 4.3. This dark line shows that the regimes 1 to 3 would be in the fuel-rich stage.

It is interesting to see that in the steady burning regime, the higher burning rate increases with pan diameter, while in extinction regime, the burning rate decrease with pan diameter. In addition, the burning rate in the beginning of regime 2 tends to get the value close to $10 \text{ g}/\text{m}^2\text{s}$ slightly less than the free burning value. Then it suddenly jumps to a much higher value when in regime 4. This can be explained by burning rate model, Eq (4.18) [2] previously described, and the behavior of the fire scenario observed. In the regime 1, where the ventilation parameter is very small, extinction occurs due to the exhausted oxygen consumed by combustion and the filling of hot gases. This regime can be thought of as an almost sealed compartment in which the larger the fire, the faster the oxygen is consumed. Therefore, the lower burning rate per unit area is a result of low oxygen fraction. As for the regime 4, the burning behavior is more affected by the external heat radiating from the compartment by the upper hot gases rather than by ventilation. More precisely, the behavior is more governed by the independent variable, $A_s h / A_F \dot{m}_{F,\infty}''$, rather than ventilation parameter. Hence the burning rates for larger pans are higher than the smaller pan, and all of them are higher than burning rate in absence of enclosure.

Considering now the regime 2 where oscillation and ghosting flame phenomena occur, the burning rates again are controlled by ventilation. Also the blowing of air through bottom vent has been observed to influence ghosting and oscillation combustion. The burning rate characteristic in this regime can be explained according to how oscillation and the ghosting fire occur as described before in Chapter 3. In the beginning or at the left side of the regime, most of the data stay below, yet close to the free-burning line. This indicates the effect of low ventilation with the presence of oscillation, followed by a ghosting flame which detaches away from the pan and continues oscillating. This behavior does not increase the burning rate so much, as the flame does not heat the fuel for a long time before it detaches away as a ghosting flame, and extinction finally occurs. Whereas in the beginning of the regime 4, in which oscillation still persists until fuel exhausts, the burning rate increases with time until it reaches some “steady stage”. It should be noted that the burning rate results from the case where the fuel is exhausted is much higher than that of the oscillating fire in regime 2. In addition, the oscillating flame exhibits more heat flux to fuel than the vertical plume since the flame gets closer to the fuel surface due to wind effects. As a result, the increase of burning rate value in this transition region between regime 2 and 4 can be observed.

As for the regime 3, the largest pan performs an interesting phenomenon that the fuel only burns at the lower vent where air enters and there is no flame appears on the pan. This behavior shows the fuel-rich stage where the flame burns all the entering air. In this case the highly jump of the burning rate occurs due to thermal feedback.

4.1.2 Gas Temperature

Gas temperatures are plotted against the ventilation parameters the same way as in burning rate and shown in Figure 4.4. Each plot represents an average temperature from the maximum and then consistent minimum temperature which are taken from each test. These temperatures are from the front wall thermocouple data (only from TC 2 to TC 11) which does not include top and bottom vent flow temperatures (TC 1 and TC 12).

As illustrated in the plot, the larger fire has the higher average temperature, while in regime 1 the average temperature is not very high and tends to go down when the ventilation parameter reach regime 2. As entering in the region of ghosting behavior, the temperature does not appear to increase very much which implies that the thermocouple cannot response fast enough to capture the fluctuation of ghosting and weak oscillating behavior. Then the temperatures start increasing in larger ventilation parameter where the stronger ghosting is observed, then peak temperatures are seen in the steady oscillation region, between regime 2 and 4. As entering the steady burning regime, now the temperature tends to go down. It should be noted that the range between maximum and minimum value is different from test to test; although, it can be said that the temperature ratio from top to bottom can vary from 1.5 to 2, approximately. Furthermore, additional temperature data from the center and back thermocouples are presented in the same manner as in Figure 4.4 and located in Appendix B.

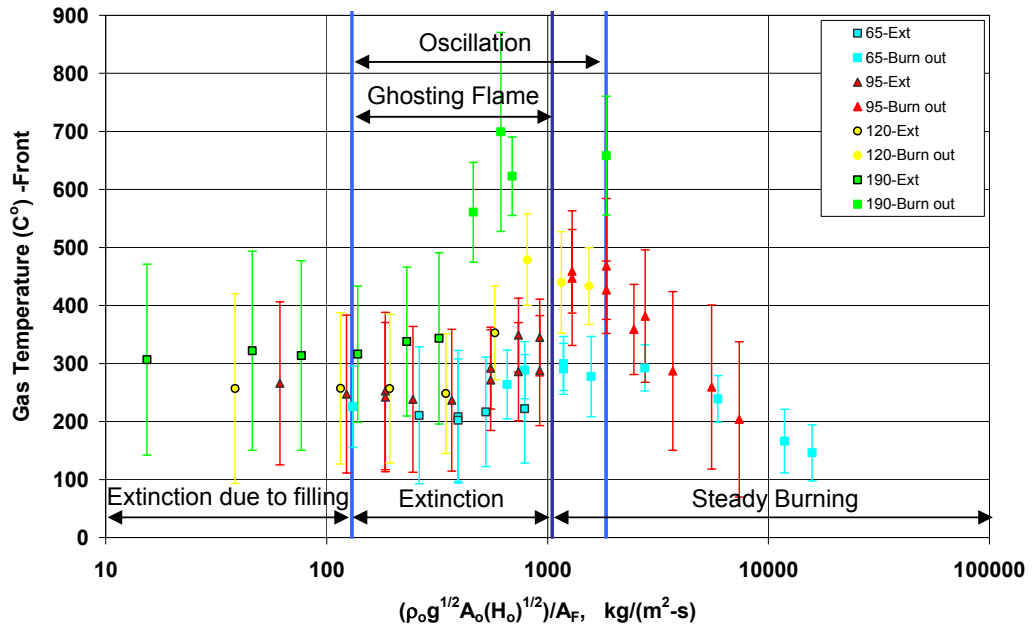


Figure 4.4 Gas Temperature versus ventilation parameter

4.1.3 Oxygen and Carbon Monoxide Concentration

Oxygen mole fraction is plotted as a function of ventilation parameter in Figure 4.5, it includes data taken from bottom and top portion of the compartment. The symbol represents the lower oxygen concentration near the fuel pan, while the dash extended line indicates the oxygen concentration in upper layer. For cases where extinction occurs, the oxygen mole fraction results presented here are taken just before extinction. As for the steady burning cases, the selected point is the first lowest concentration recorded at bottom of the compartment. The data from the top portion of the compartment is always consistent to time corresponding to the lower compartment. From Figure 4.5 it can be seen that the oxygen concentrations near the fuel pan for the extinction cases are in range of 8 to 13 percent. The plot tends to decrease as the ventilation parameter approaches to

the boundary of extinction. Then at about 1000 g/m²s the oxygen increases in the steady burning regime.

It is interesting to note that for some extinction cases, the upper compartment concentration is higher than the lower concentrations; whereas in the fuel burn-out cases, this behavior reverses. The latter behavior is more expected. We believe the former is due to the mixing and oscillatory effects at low ventilation.

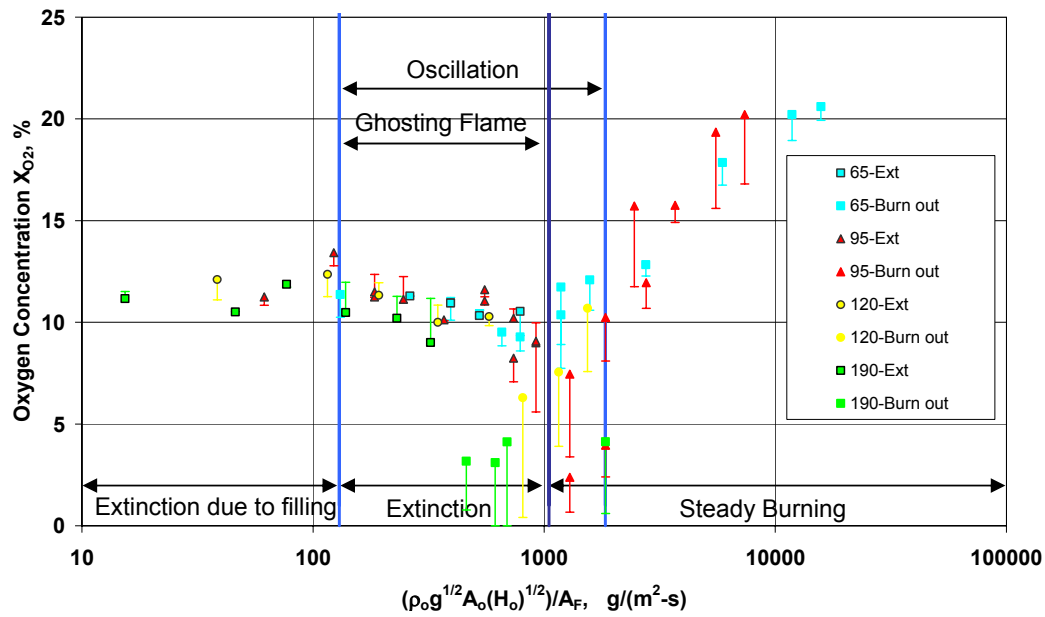


Figure 4.5 Oxygen concentrations versus ventilation parameter

The maximum carbon monoxide concentration is plotted against the ventilation parameter in Figure 4.6. The symbol represents the lower carbon monoxide concentration near the fuel pan, while the dash extended line indicates the carbon monoxide concentration in upper layer. High value of carbon monoxide concentration is observed in oscillation region.

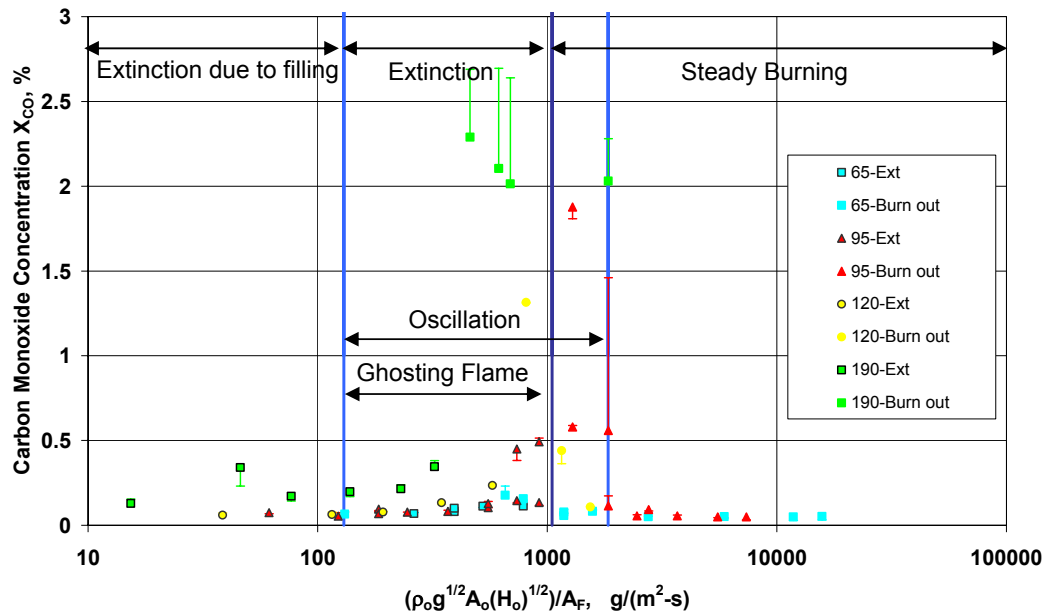


Figure 4.6 Carbon Monoxide Concentration versus ventilation parameter

4.1.4 Heat Flux

The heat flux that has been measured in this experiment is also presented here with respect to the ventilation parameter. The heat flux reported was selected at the same time consistent with the reported burning rate. The heat flux measured at the center of the pan (HF1), shown in Figure 4.7, reveals the effect of flame heating on the burning rate. In comparison with burning rate in Figure 4.3 and considering the 9.5 pan result, we see that the heat flux increase sharply at the ventilation parameter $\sim 550 \text{ g/m}^2\text{s}$. Then in the region of steady oscillation, the burning rate increases consistent with the heat flux measured. We think in the “steady” oscillation regime at larger ventilation, the burning rate increases due to an increase in the heat transfer coefficient. Additional plots of heat flux measured at the floor, wall and ceiling can be found in Appendix B. Those plots are illustrated in the same manner as in Figure 4.5, and also show the geometry and character of the flame depending upon whether it leans backward or stays straight up.

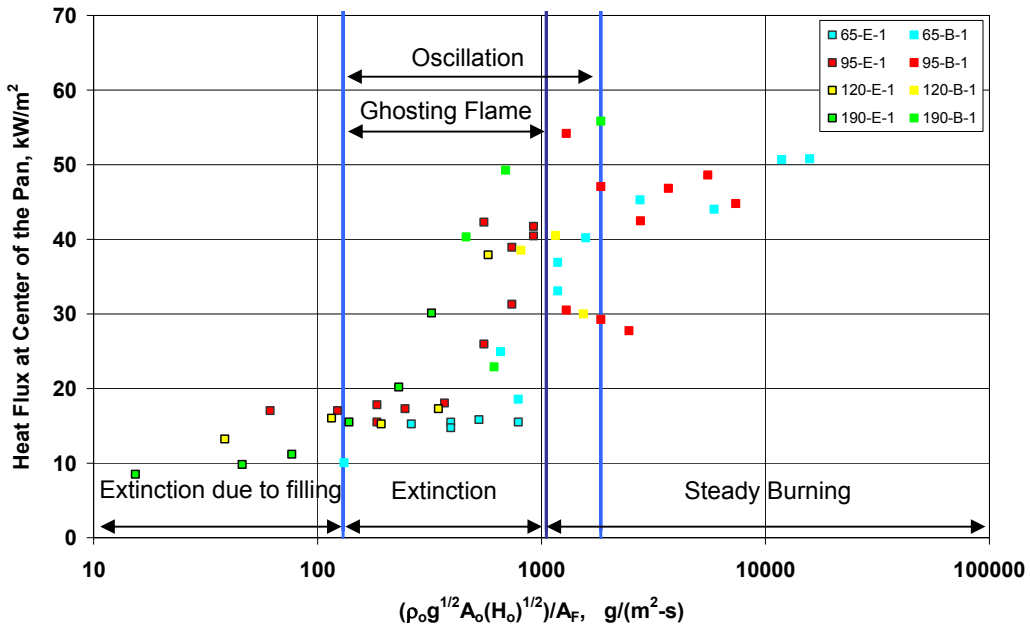


Figure 4.7 Heat flux measured at the center of fuel pan versus ventilation parameter

To investigate more detail on how flame heat flux and burning rate correlate, their ratio is plotted against the ventilation parameter in Figure 4.8. This ratio represents the “effective” heat of gasification. It is higher than the thermodynamic value because it does not discount heat loss to the fuel pan.

From Figure 4.8 it can be seen that in the regime 1 and 4 where no oscillation observed the heat of vaporization is about 2 kJ/g, while in the oscillation region the range is from 1 to 4 kJ/g. The thermodynamic value is 0.48 kJ/g.

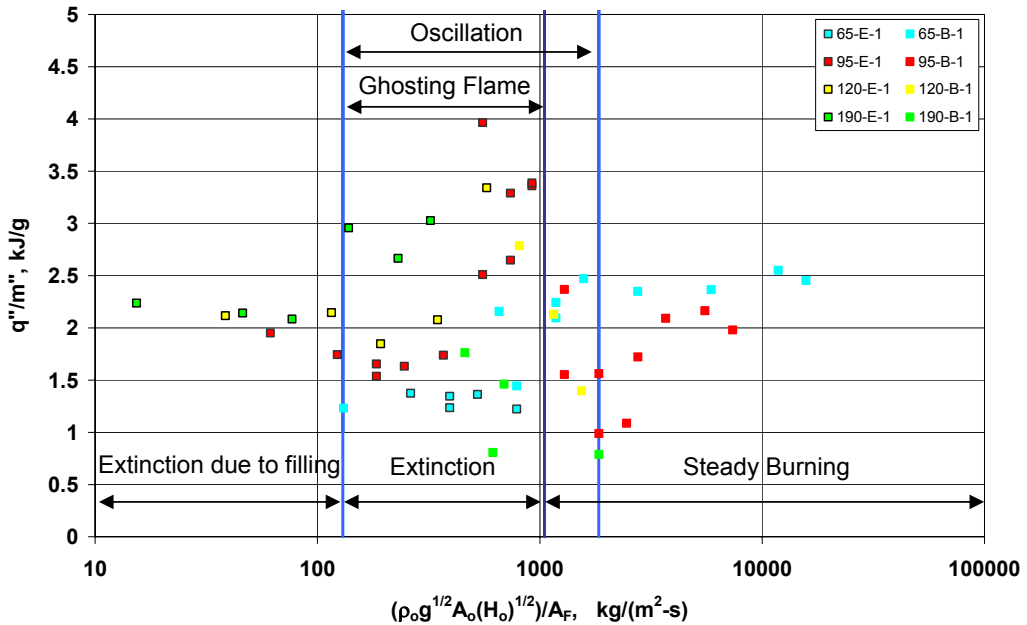


Figure 4.8 Heat of vaporization in compartment versus ventilation parameter

4.2 Extinction Theory and Experimental Results

It has been shown that extinction of the fire depends on the local temperature, oxygen concentration and heat flux to the fuel [6,8]. The relationship between oxygen concentration and temperature at extinction is presented below; however, for more detail in developing this analysis, the reader should refer to previous work done by Rangwala[6] and Quintiere[8].

The burning rate per unit area, for small B-number [8], is given in terms of ambient oxygen mass fraction, temperature, and heat flux components as

$$\dot{m}_F L = \frac{h_c}{c_p} \left[Y_{ox,\infty} \frac{\Delta h_c}{r} - c_p (T_v - T_\infty) \right] + \varepsilon_f \sigma T_f^4 + \dot{q}_{e,r}'' - \sigma (T_v^4 - T_\infty^4) \quad (4.21)$$

where

$\frac{h_c}{c_p} \left[Y_{ox,\infty} \frac{\Delta h_c}{r} - c_p (T_v - T_\infty) \right]$ is the convective flame heat flux term

$\varepsilon_f \sigma T_f^4$ is the radiative heat flux from flame to surface, where $\varepsilon_f = (1 - e^{-kL_m})$ and

k is an absorption coefficient that depends on soot concentration, and L_m is the mean beam length. However, this radiation term can be neglected at extinction.

$\dot{q}_{e,r}''$ is external radiant heat flux from compartment and hot gases.

$\sigma(T_v^4 - T_\infty^4)$ is heat loss from fuel surface to surroundings.

L is the heat of gasification.

The flame temperature is given as

$$c_p (T_f - T_\infty) = \frac{\Delta h_c - L + c_p (T_v - T_\infty) + \frac{\dot{q}_{e,r}'' - \sigma(T_v^4 - T_\infty^4)}{\dot{m}_F''}}{1 + \left(\frac{r}{Y_{ox,\infty}} \right)} \quad (4.22)$$

Substituting for the burning rate, in Eq (4.21) and (4.22), yields a correlation of oxygen, temperature, and external heat flux for a given flame temperature.

$$\frac{h_c}{c_p} \left[Y_{ox,\infty} \Delta h_c / r - c_p (T_v - T_\infty) \right] \left\{ \frac{1}{[\Delta h_c + c_p (T_v - T_\infty)] - \left[1 + \left(\frac{r}{Y_{ox,\infty}} \right) \right] c_p (T_f - T_\infty)} - \frac{1}{L} \right\} = \frac{\dot{q}_{e,r}'' - \sigma(T_v^4 - T_\infty^4)}{L} \quad (4.23)$$

In the compartment case, the external radiant heat flux is presented in terms of the measured upper smoke layer temperature. However, we shall examine our extinction behavior in terms of $Y_{ox,\infty}$ as measured in the lower compartment near the flame, and the

corresponding temperature (T_∞) at that point. By examining our temperature profiles we estimate that the upper layer temperature is about 1.6 (in K) higher than the lower larger value. Hence the net surface flux and enthalpy terms change as follows

$$\begin{aligned}\dot{q}_{e,r}'' &= \sigma(T_{upper}^4 - T_\infty^4) = \sigma((1.6T_{lower})^4 - T_\infty^4) \\ c_p(T_v - T_\infty) &= c_p(T_v - T_{lower})\end{aligned}\quad (4.24)$$

Based on Eq (4.23) and (4.24), the oxygen concentration at extinction is plotted against the temperature in Figure 4.9 with $T_f = 1300^\circ\text{C}$, $r = 3.18$, $c_p = 1.2 \text{ J/g-K}$, $T_v = 98^\circ\text{C}$, $\Delta h_c = 41.2 \text{ kJ/g}$, and $L = 0.318 \text{ kJ/g}$ assuming bulk boiling.

Experimental results are plotted in Figure 4.9. Oxygen concentration at the lower portion of the compartment and temperature from thermocouple TC11, located at 1.5 cm above the floor, at a consistent time is presented in Figure 4.9. The data points are distinguished as dark-solid-border (extinction), no-border (burn out until fuel exhaustion). As in Figure 4.5, the end point of the line connected to the symbol indicates the oxygen concentration at the top portion of the compartment.

It can be seen from Figure 4.9 that the experimental result and extinction theory based on a critical flame temperature at extinction of 1300°C are in good agreement. The data points which represent steady oscillation (burn-out with oscillatory behavior) are represented by \times . Oscillation behavior is a form of extinction in which the flame begins to be suppressed due to reduced oxygen concentration. This is followed by a rekindling when airflow is induced again into the compartment. [9] In addition, the plot also indicates that the oxygen at extinction decreases when the compartment is heated.

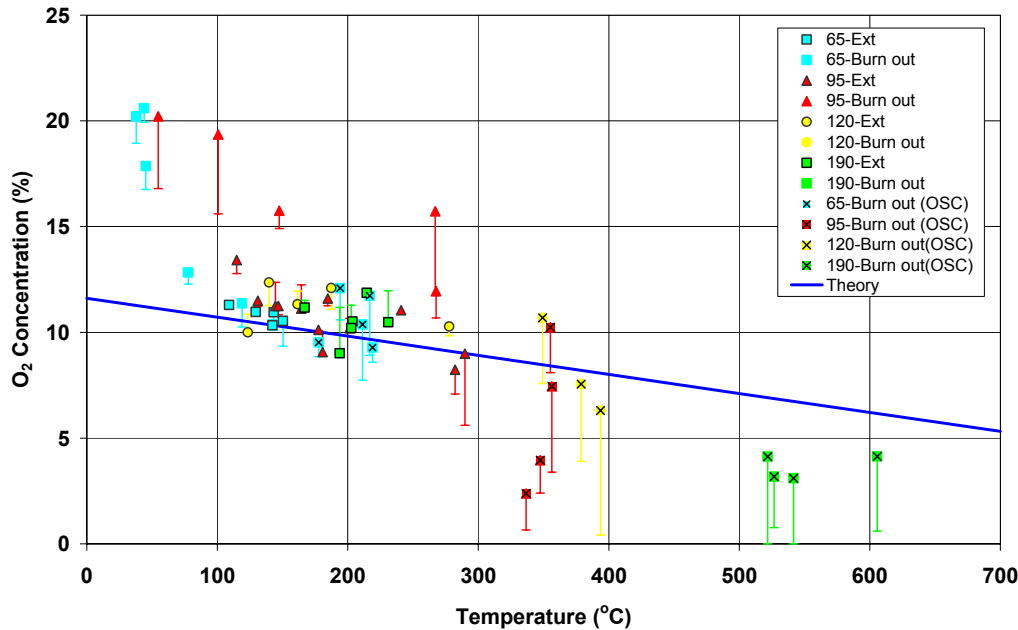


Figure 4.9 Floor-level oxygen and temperature at extinction or at steady burning

4.3 Dynamic Behavior: Experiment and Theory

A mathematical model created by Rangwala [6] was run to predict the mass loss rate, differential pressure, oxygen mole fraction and temperature in order to compare with the experimental results. In this study, only a brief description of the model is presented. For complete details and explanation on how this model was derived, the reader is directed to the cited reference [6].

The burning rate model is given as presented before in Eq (4.18)

$$\dot{m}_F = \dot{m}_{F,\infty} \left(\frac{Y_{ox}}{Y_{ox,air}} \right) + \frac{FA_F \sigma (T_g^4 - T_\infty^4)}{L} \quad (4.25)$$

This model is actually a simplified form of Eq (4.21) in order to explicitly relate the burning rate in the enclosure to the experimental free burning rates with the effect of

oxygen concentration and the external heat flux. The critical burning rate at extinction can be determined by using the oxygen and temperature based on Eq (4.23), where extinction would occur. A criteria of a sustained flame is established based on a critical burning rate.

Energy Release Criteria is given as follow:

$$\begin{aligned}
 Y_{ox} \geq Y_{ox,crit}, \dot{m}_F'' \geq \dot{m}_{F,crit} &\Rightarrow \dot{Q} = \dot{m}_F'' \Delta h_c A_F \\
 Y_{ox} = 0 \quad \left\{ \begin{array}{ll} \dot{m}_F'' \geq \dot{m}_{F,crit} & \Rightarrow \dot{Q} = \dot{m}_{ox,in} \Delta h_{ox}; \text{ Ventilation limited burning} \\ \dot{m}_F'' < \dot{m}_{F,crit} & \Rightarrow \dot{Q} = 0; \text{ Extinction} \end{array} \right. \\
 Y_{ox} < Y_{ox,crit}, \dot{m}_F'' < \dot{m}_{F,crit} &\Rightarrow \dot{Q} = 0; \text{ Extinction}
 \end{aligned} \tag{4.26}$$

This is similar to Eq (4.4) where the energy released is based on equivalence ratio. The mass flow rates through the top and bottom vent are determined based on differential pressure in accordance with Bernoulli's equation and a flow coefficient.

$$\begin{aligned}
 \dot{m}_b &= \eta(\Delta P_b) C_d A_o \sqrt{2\rho|\Delta P_b|} - \eta(-\Delta P_b) C_d A_o \sqrt{2\rho|\Delta P_b|} \\
 \dot{m}_t &= \eta(\Delta P_t) C_d A_o \sqrt{2\rho|\Delta P_t|} - \eta(-\Delta P_t) C_d A_o \sqrt{2\rho|\Delta P_t|}
 \end{aligned} \tag{4.27}$$

Finally conservation equations are presented below.

Conservation of Mass

$$\rho_\infty T_\infty V \frac{d(1/T)}{dt} + \dot{m}_t + \dot{m}_b - \dot{m}_F = 0 \tag{4.28}$$

Conservation of Energy

$$\left(\frac{V}{\gamma - 1} \right) \frac{dP}{dt} + \dot{m}_t c_p [\eta(\Delta P_t) T + \eta(-\Delta P_t) T_\infty] + \dot{m}_b c_p [\eta(\Delta P_b) T + \eta(-\Delta P_b) T_\infty] - \dot{m}_F c_p T_F = \dot{Q} - hA (T - T_\infty) \tag{4.29}$$

Conservation of Species

$$\rho_\infty T_\infty V \frac{d(Y_{ox}/T)}{dt} + [\eta(\Delta P_b)Y_{ox} + \eta(-\Delta P_b)(0.233)]\dot{m}_b + [\eta(\Delta P_t)Y_{ox} - \eta(-\Delta P_t)(0.233)]\dot{m}_t = -\dot{Q}/\Delta h_{ox}$$

(4.30)

Using Mathematica® to solve these equations, the theoretical prediction is computed and compared to the experimental results for every case. Selected examples are shown below, while the complete set on every test is presented in the Appendix section. The experimental results are annotated to indicate the flame behavior as follows: I = Initial Stage, P = Vertical Plume, B = Blue Base Flame, Sh = Shrinking Flame, W = Wind-Blown Flame, L = Leaning Backward and Puffing Flame, O = Oscillating Flame, G = Ghosting Flame, E = Extinction. All annotations were similar to those used before in Chapter 3.

Figure 4.10 shows an example of experimental results and the model predictions for Regime 1, extinction due to filling. Extinction occurs at an oxygen concentration of 13 % which is slightly higher than the predicted value. However, the burning rates are in good agreement. Furthermore, the time to extinction between the prediction and experiment is not so different, about 5 sec. Overall, the predicted values from the uniform property model are in rough agreement with the measurement.

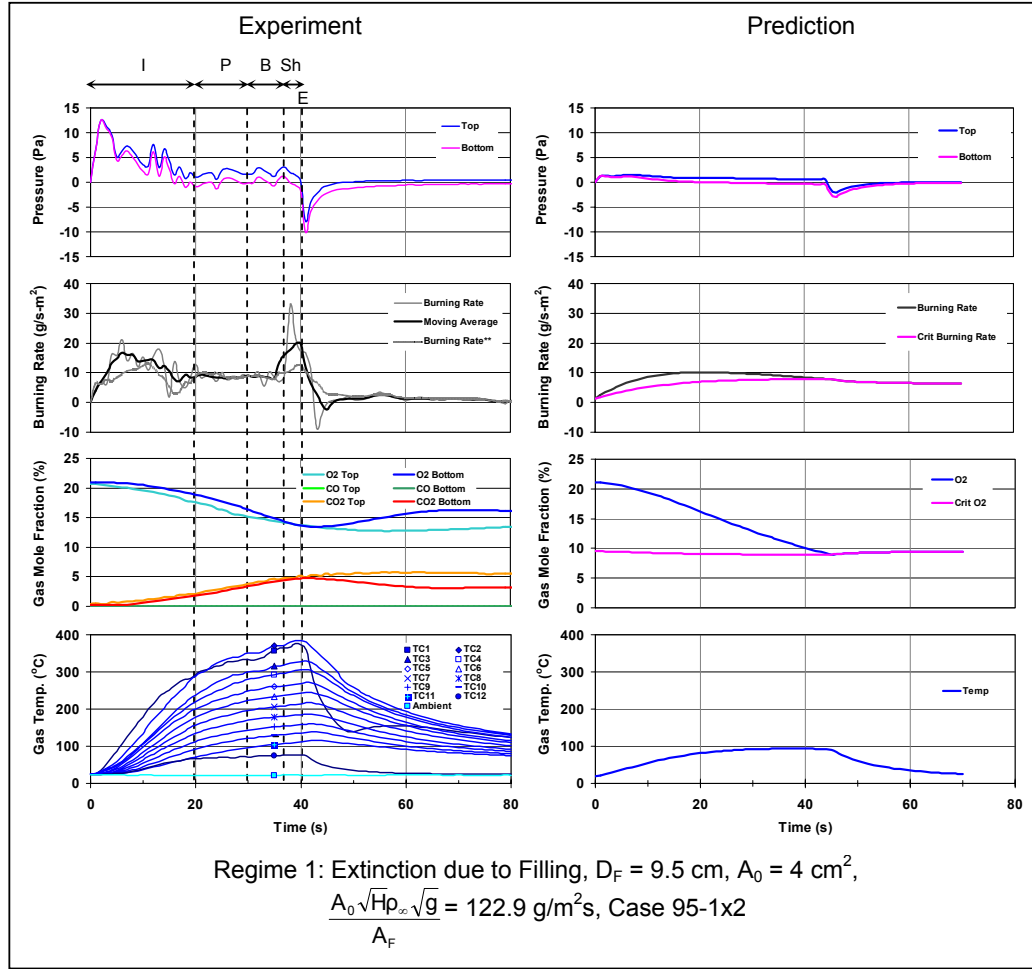


Figure 4.10 Experimental Results and Model Prediction in Regime 1

Now in Figure 4.11 an example from Regime 2 (oscillation and ghosting flame) is presented. The model is not able to demonstrate the oscillation behavior. Nevertheless, the burning rate and extinction time from the model are in good agreement with the experimental result. The point where the burning rate reaches its critical value is about equal to the time for extinction in this case, 48 sec. It should be noted that in this region, the geometry of the flame changes from a vertical plume, to a wind-blown flame, to a

leaning flame close to fuel surface, and finally a detached flame (ghosting) that moves away from the pan.

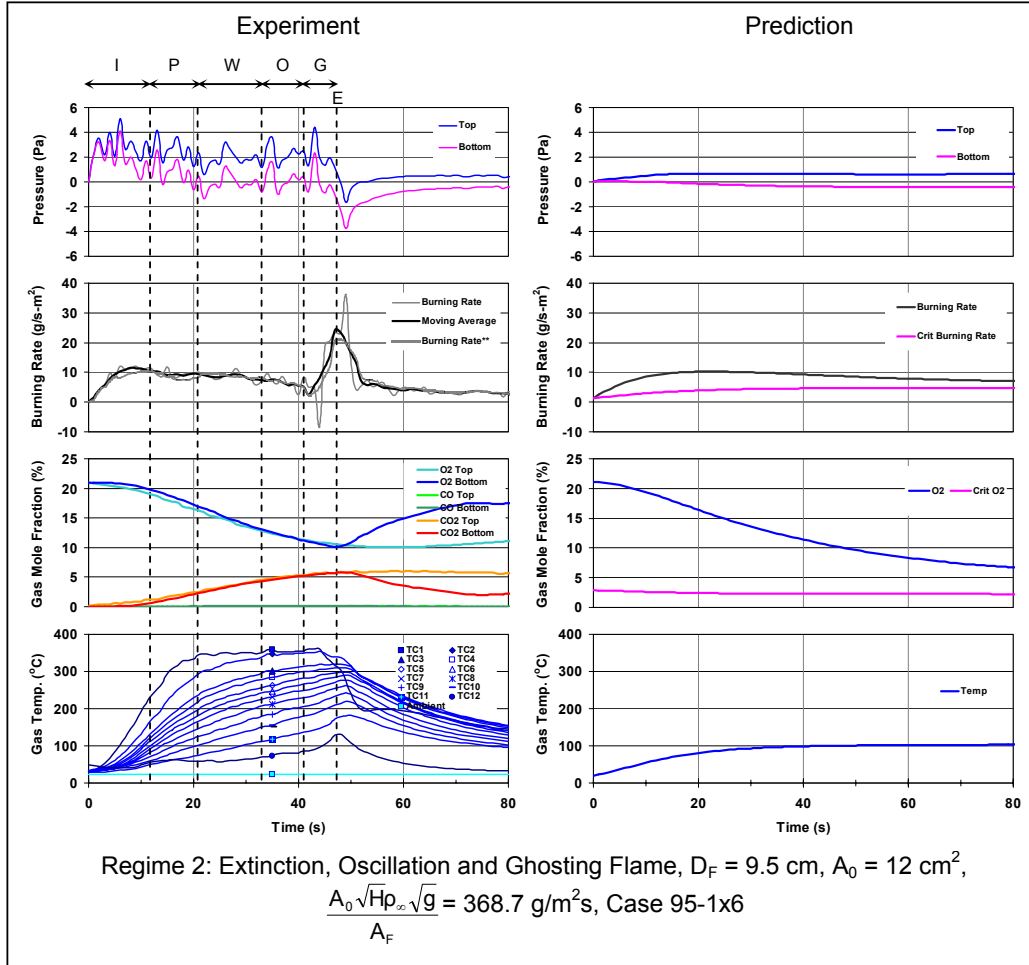


Figure 4.11 Experimental Results and Model Prediction in Regime 2

Figure 4.12 and Figure 4.13 show the steady oscillation case, where the flame keeps oscillating until the fuel is exhausted. As for the case in Figure 4.10, the model is able to simulate the oscillatory behavior as seen in differential pressure plot. However, in Figure 4.12, oscillation cannot be achieved by the model. But with an adjustment about

0.5 in the critical oxygen value according to Rangwala[6], the model now can exhibit oscillation shown by light line. Note that the difference between these two cases is the ventilation size. The case shown in Figure 4.10 has the larger vent size. Hence, the model is able to simulate oscillation for a large vent, while the adjustment of critical oxygen is needed for the smaller ventilation.

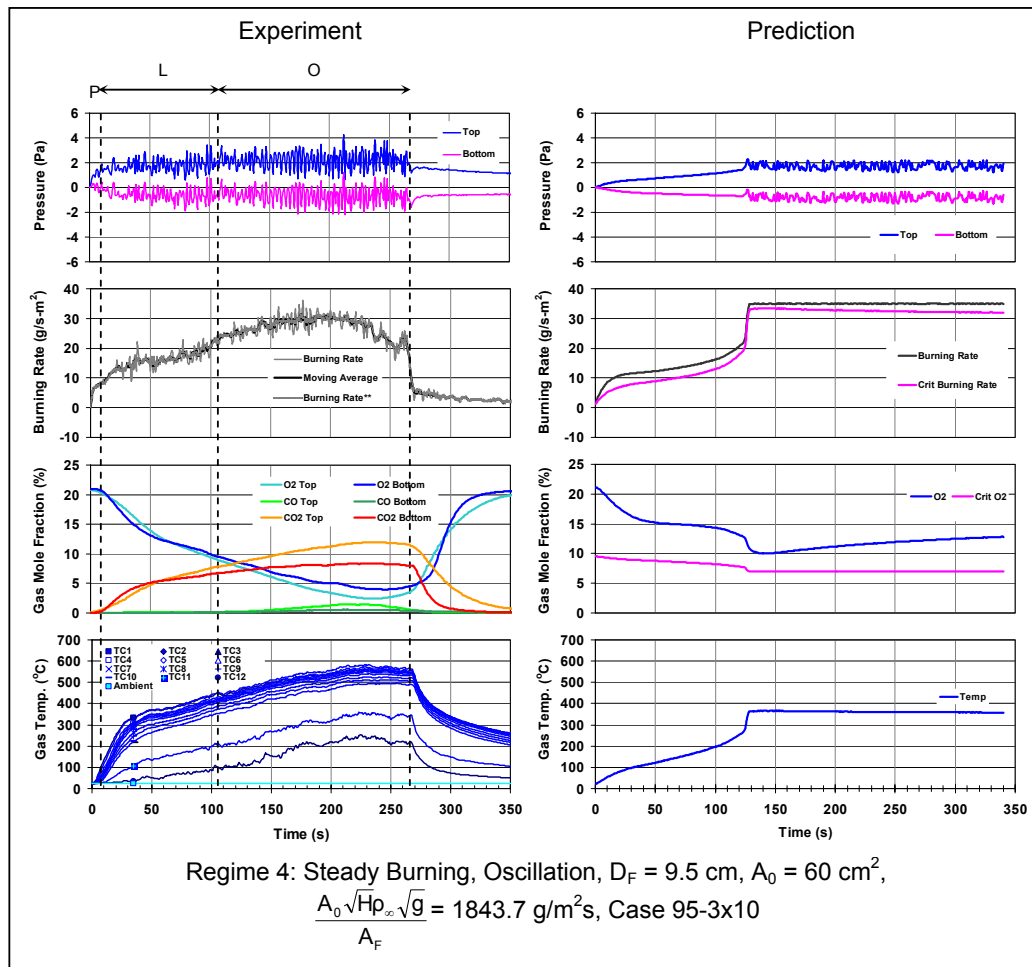


Figure 4.12 Experimental Results and Model Prediction in Regime 4 where oscillating combustion can be predicted by the model without oxygen adjustment

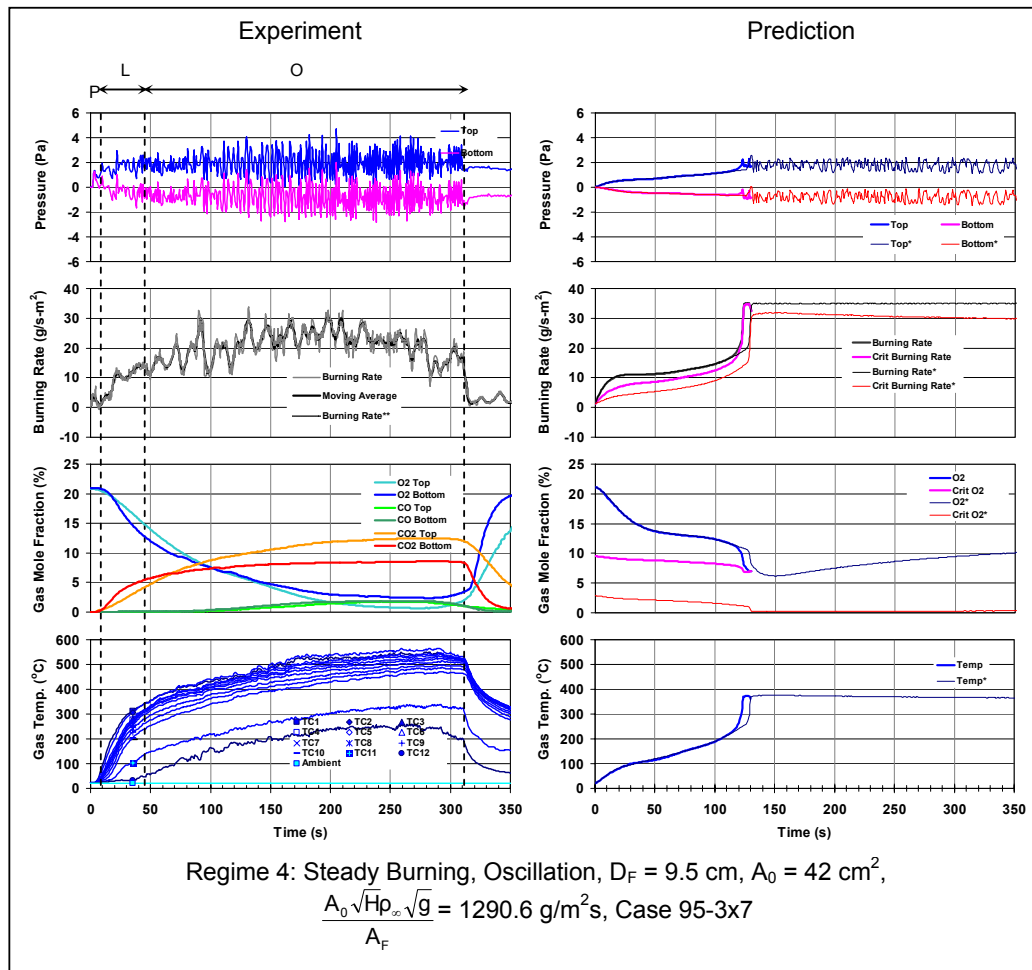


Figure 4.13 Experimental Results and Model Prediction in Regime 4 where oscillating combustion can be predicted by the model with oxygen adjustment

Predicted maximum burning rates and minimum oxygen concentration taken from model are plotted in Figure 4.14 and Figure 4.15 against the ventilation parameter, respectively. Solid lines represent the prediction. The model gives good agreement for the burning rate and oxygen concentrations in terms of trend, but only rough agreement in actual value.

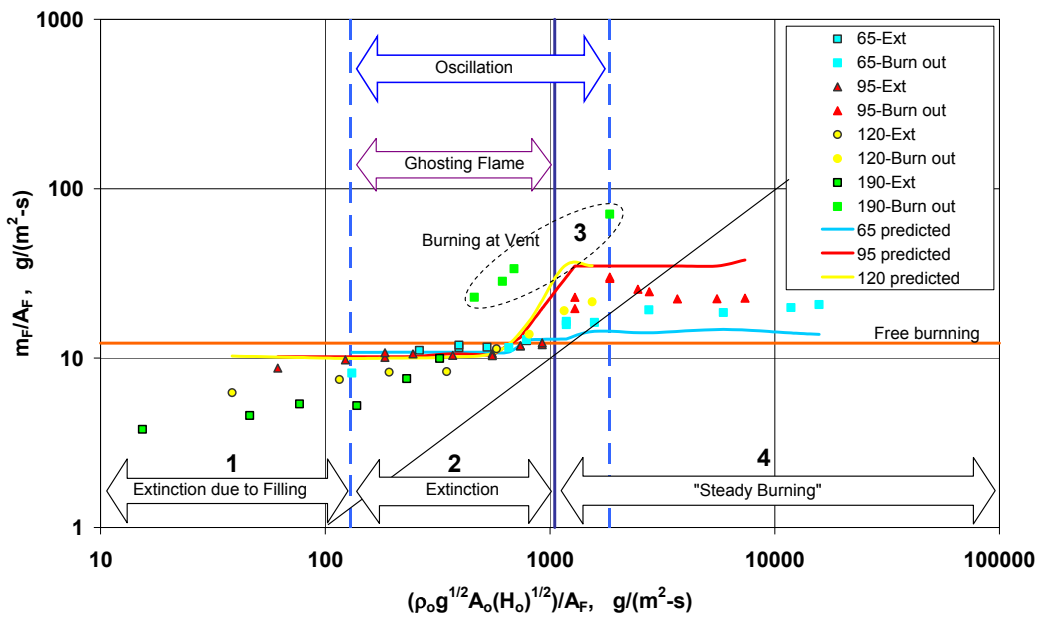


Figure 4.14 Burning rate from experiment and model

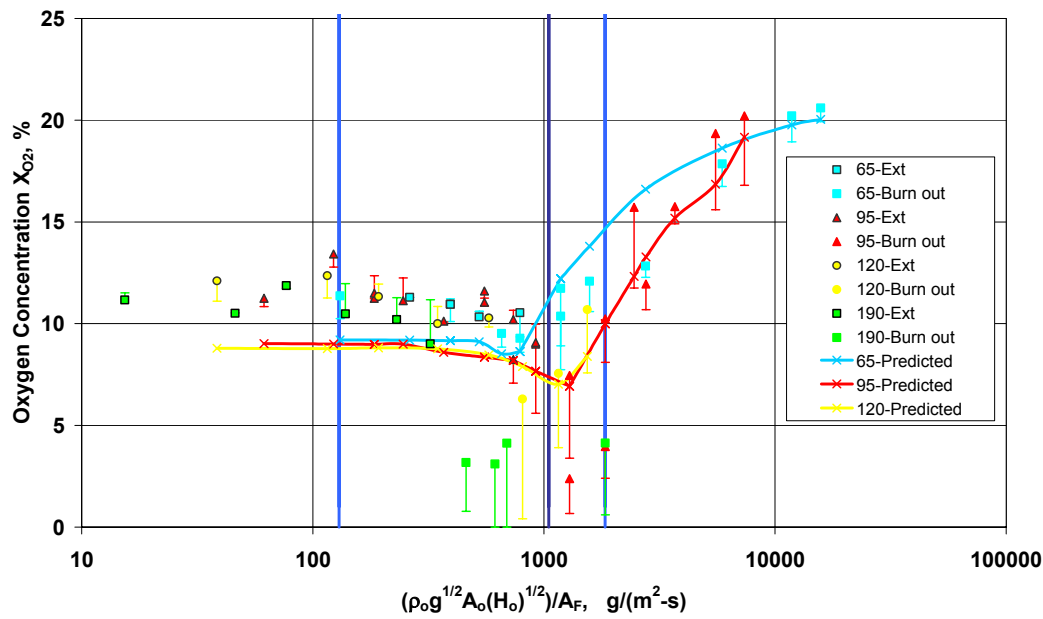


Figure 4.15 Oxygen concentrations from experiment and model

4.4 Flame Heat Flux

Since the burning rate of a pool fire depends on net heat flux added to fuel, it is important to investigate the influence of each heat flux component in order to understand how the compartment phenomena influence the burning rate. By using the data from heat flux meter (HF1) measured at the center of fuel pan, some analysis can be done as follows:

4.4.1 Flame Emissivity

For a free burning, the heat flux measured from the flame is given as

$$\begin{aligned}\dot{q}_{m,\infty}'' &= \dot{q}_f'' = \dot{q}_{f,c}'' + \dot{q}_{f,r}'' \\ \dot{q}_{m,\infty}'' &= h_c(T_f - T_s) + \varepsilon_f \sigma(T_f^4 - T_{sur}^4) \\ \varepsilon_f &= (1 - e^{-kL_m})\end{aligned}\quad (4.31)$$

where $\dot{q}_{m,\infty}''$ is free burning heat flux measured by heat flux meter (HF1)

\dot{q}_f'' is total heat flux from flame

h_c is convective heat transfer coefficient

T_f is flame temperature

T_s is fuel surface temperature $\sim T_v = 98^\circ\text{C}$

T_{sur} is heat flux meter surface $\sim 65^\circ\text{C}$

k is a absorption coefficient depends on soot concentration

L_m is mean beam length.

By estimating $h_c \sim 20 \text{ kW/m}^2\text{K}$, and $T_f \sim 800^\circ\text{C}$, the flame emissivity can be determined as shown in Table 4.2. Now by measuring flame height (L_f) and estimating

the mean beam length based on flame height as ninety percent of pan diameter, $L_m/D = 0.90$ (circular cylinder of semi-infinite height radiating to element at center of base)[17], the absorption coefficient also can be calculated and presented in Table 4.2.

It can be seen that the emissivity of the flame ranges from 0.07 to 0.18 approximately which suggests that the flame is very transparent [18], therefore most of the external radiation from compartment would be able to reach the fuel surface in case of vertical plume burning.

Pan Dia, D (cm)	Flame Height, L_f (m)	\dot{q}_f'' (kW/m ²)	ε_f	L_f/D	L_m/D	L_m (m)	k (m ⁻¹)
6.5	24	19.34	0.071	3.69	0.90	0.059	1.263
9.5	30	19.82	0.078	3.15	0.90	0.086	0.946
12.0	45	22.74	0.117	3.75	0.90	0.108	1.151
19.0	68	27.65	0.183	3.58	0.90	0.171	1.181

Table 4.2 Flame Emissivity and Absorption Coefficient

4.4.2 Total Flame Heat Flux within Compartment

Now let us consider in the enclosure pool fire burning. The heat flux measured at the center of the pan becomes

$$\dot{q}_m'' = \dot{q}_f'' + \dot{q}_e'' \quad (4.32)$$

\dot{q}_m'' is heat flux measured at the center of the pan in compartment,

\dot{q}_e'' is external heat flux due to hot gas layer or heat from compartment given as ,

$$\dot{q}_e'' = F(1 - \varepsilon_f)\sigma(T_g^4 - T_s^4)$$

F is the view factor.

Then

$$\dot{q}_m'' = \dot{q}_f'' + F(1 - \varepsilon_f)\sigma(T_g^4 - T_s^4) \quad (4.33)$$

According to flame emissivity that is calculated previously for free burning case, most of the external heat flux has a high possibility to penetrate through the flame and reach the fuel surface. Therefore it is reasonable to assume that the flame blocking term, $F(1 - \varepsilon_f)$, equals to one. Here the view factor is taken as 1. Hence, Eq (4.33) becomes

$$\dot{q}_f'' = \dot{q}_m'' - \sigma(T_g^4 - T_s^4) \quad (4.34)$$

By substituting heat flux measured and gas temperature from experimental results, the flame heat flux that accounts for both convection and radiation within compartment can be estimated. For a boundary layer wind-blown flame, \dot{q}_m'' will be different than the vertical plume value given here.

Considering Figure 4.16, the case where oscillation and ghosting flames occurred, \dot{q}_f'' is calculated based on the average hot gas temperature, TC6, and heat flux measured at the center of the pan as in Eq (4.33). It shows that the effect of external heat flux increases with time as the gas temperature increases. The difference between heat flux measured, \dot{q}_m'' , and flame heat flux, \dot{q}_f'' , is approximately 7 kW/m^2 . When ghosting flames occur, \dot{q}_f'' becomes nearly zero as the flame detaches away from fuel surface. Now when the flame comes back and oscillates above the fuel surface, the flame heat flux increases, then now both flame and external heat flux affect the burning rate.

As for steady oscillation case shown in Figure 4.17, it is seen that from 50 s to 270 s the flame heat flux is quite stable $\sim 35 \text{ kW/m}^2$, while the measured heat flux tends to increase approximately from 40 to 50 kW/m^2 . This agrees with the fact that external heat will increase with the temperature of enclosure.

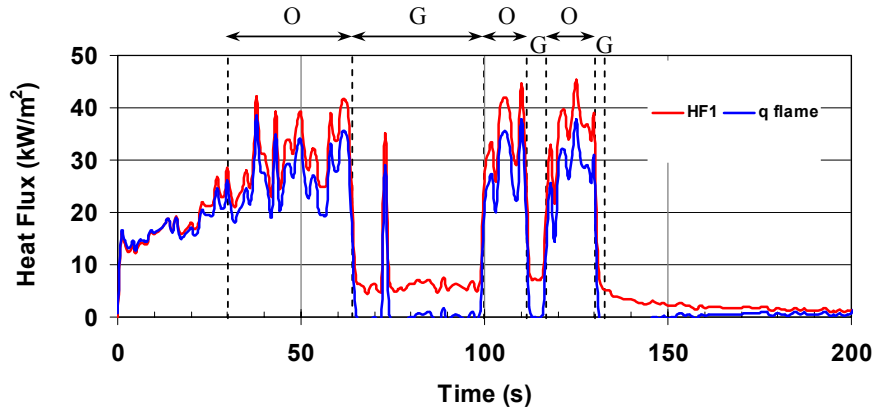


Figure 4.16 Measured Heat Flux (HF1) and Total Flame Heat Flux, $D_F = 9.5 \text{ cm}$,
 $A_0 = 24 \text{ cm}^2$, Regime 2: O = Oscillation and G = Ghosting Flame

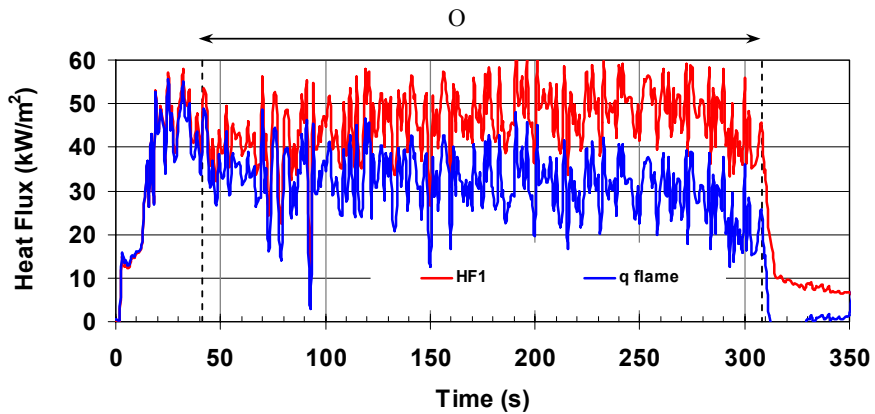


Figure 4.17 Measured Heat Flux (HF1) and Total Flame Heat Flux, $D_F = 9.5 \text{ cm}$,
 $A_0 = 42 \text{ cm}^2$, Regime 4: O = Oscillation

4.4.3 Heat Loss through Water and Pan

Considering the free burning, the net heat flux to fuel is given as:

$$\dot{q}_{fuel,net}'' = \dot{q}_f'' - \sigma(T_s^4 - T_\infty^4) - \dot{q}_{loss}'' \quad (4.35)$$

where $\sigma(T_s^4 - T_\infty^4)$ is heat flux lost by radiation due to heated fuel surface and $T_s = T_v$; \dot{q}_{loss}'' is total heat flux lost through pan and water

From fire dynamics principles, the steady burning rate is expressed by

$$\dot{m}_{F,\infty}'' = \frac{\dot{q}_{fuel,net}''}{L} \quad (4.36)$$

Substituting Eq (4.35) and (4.32) into (4.36) yields

$$\dot{m}_{F,\infty}'' = \frac{\dot{q}_m'' - \sigma(T_v^4 - T_\infty^4) - \dot{q}_{loss}''}{L} \quad (4.37)$$

From the expression above, the total heat loss through pan and water can be calculated for each pan size by substituting free burning rate, heat flux, from Table 3.2, and heat of vaporization $L = h_{fg} + c_p(T_v - T_\infty)$; $h_{fg} = 0.38 \text{ kJ/g}$, $c_p = 2.2 \text{ J/g-K}$. Results are shown in Figure 4.18. We shall see that calculated heat loss is quite high compared to the total flame heat flux. This is due to heat losses into the pan and to the water underneath heptane fuel.

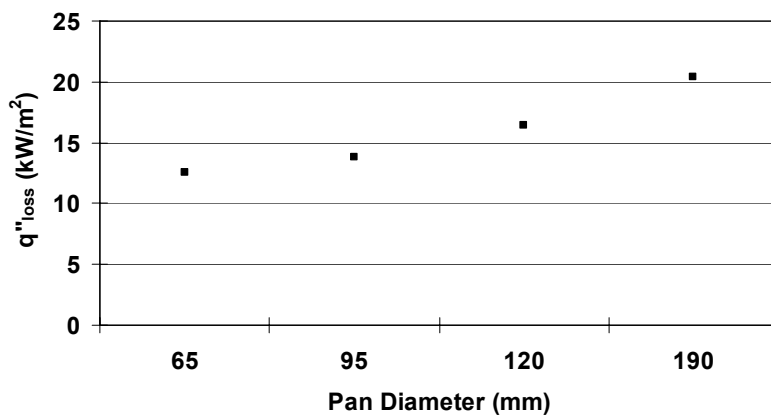


Figure 4.18 Total heat loss through pan and water

5. Conclusions

An investigation on wall-vent compartment fire behavior under low ventilation was experimentally performed. The results reveal an understanding of how fire behavior is affected by ventilation.

The fire behavior is grouped into 4 categories: (1) extinction due to filling, (2) extinction, (3) lower-vent burning, and (4) steady burning. These categories can be represented by regions of the ventilation parameter: $\left(\frac{A_0 \sqrt{H} \rho_\infty \sqrt{g}}{A_F} \right)$. The ventilation parameter represents the air to the fuel ratio under steady conditions.

Consistently selected data for each experiment are plotted as a function of the ventilation parameter in order to reveal their trends for each region. Burning rate per unit area is lower than the free burning rate in the region where extinction occurs, and highly increases when entering the steady burning region. This indicates the effect of fuel rich or lean conditions. At low ventilation, the burning rate is governed by oxygen supplied; at high ventilation, the burning rate is controlled by external heat from the enclosure.

Oxygen and temperature at extinction from experiment are in good agreement with extinction theory. Oscillation phenomenon can be considered as a form of extinction where the flame is suppressed due to reduced oxygen concentration when the flow is totally outward.

A mathematical model, based on a theory of extinction and the conservation of mass, energy and species, together with a simplified burning rate model, is able to simulate the oscillations in steady burning, and gives a fairly good agreement with experimental results.

Appendix A: Data Correction

A.1 Correction on mass loss rate

Since sudden pressure change in the compartment could lead to an error in fuel mass loss rate, a correction was made by using a force balance on the load cell with water seal as follows

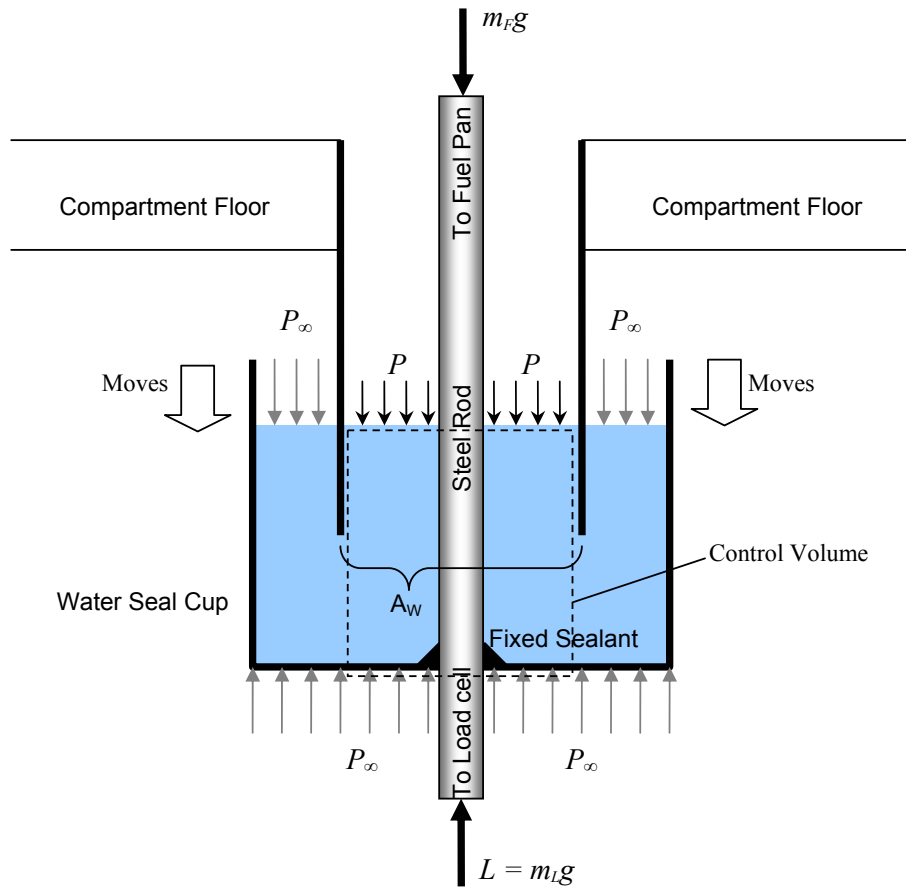


Figure A1 Force balance at water seal cup

From a force balance on the control volume in Figure A1

$$\sum F_y = L - m_F g + (P_\infty - P)A_w = 0$$

$$m_L g = m_F g - (P_\infty - P)A_w$$

$$\begin{aligned}
\frac{m_L}{A_F} &= \frac{m_F}{A_F} - \frac{(P_\infty - P)A_w}{gA_F} \\
m''_L &= m''_F - \frac{(P_\infty - P)}{g} \frac{A_w}{A_F} \\
\dot{m}''_L &= \dot{m}''_F - \frac{d(P_\infty - P)}{dt} \frac{A_w}{gA_F}
\end{aligned} \tag{A1}$$

Where \dot{m}''_L is recorded mass loss rate obtained by load cell measurement

\dot{m}''_F is actual fuel mass loss rate

A_w is exposed water surface area

A_F is fuel surface area or pan area

This correction in Eq (A1) was made to all mass loss rate results.

A.2 Correction on gas concentration measurements

Since the oxygen analyzer can be affected by humidity and carbon dioxide, in this experiment an ice box, Drierite®, and Ascarite® were used to trap these species. Hence a correction on gas concentration measured must be made to have it represent the concentration in the compartment.

Consider conservation of mass, where \dot{m}_1 is mass from the compartment, \dot{m}_2 is mass that goes to oxygen analyzer, \dot{m}_3 is the trapped mass flow rate

$$\dot{m}_1 = \dot{m}_2 + \dot{m}_3 \tag{A2}$$

$$\dot{m}_3 = \dot{m}_{CO_2} + \dot{m}_{CO} + \dot{m}_{H_2O}$$

$$\dot{m}_3 = Y_{CO_2} \dot{m}_1 + Y_{CO} \dot{m}_1 + Y_{H_2O} \dot{m}_1 \tag{A3}$$

Substituting (A3) into (A2) yields

$$\dot{m}_1 = \dot{m}_2 + (Y_{CO_2} \dot{m}_1 + Y_{CO} \dot{m}_1 + Y_{H_2O} \dot{m}_1) \quad (\text{A4})$$

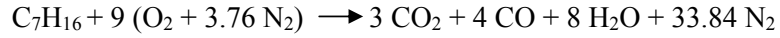
Conservation of oxygen

$$Y_{O_2} \dot{m}_1 = Y_{O_2, \text{measure}} \dot{m}_2 \quad (\text{A5})$$

Substituting into (A4) yields

$$\begin{aligned} Y_{O_2} \dot{m}_1 &= Y_{O_2, \text{measure}} \left(\dot{m}_1 - (Y_{CO_2} \dot{m}_1 + Y_{CO} \dot{m}_1 + Y_{H_2O} \dot{m}_1) \right) \\ Y_{O_2} &= Y_{O_2, \text{measure}} \left(1 - Y_{CO_2} - Y_{CO} - Y_{H_2O} \right) \end{aligned} \quad (\text{A6})$$

Approximate Y_{H_2O} by



We have $Y_{H_2O} = 0.108$

$$Y_{O_2} = Y_{O_2, \text{measure}} \left(1 - Y_{CO_2} - Y_{CO} - 0.108 \right) \quad (\text{A7})$$

The same process on carbon monoxide and carbon dioxide concentration data,

although only water was trapped. Then we have

$$Y_{CO_2} = Y_{CO_2, \text{measure}} (1 - 0.108) \quad (\text{A8})$$

$$Y_{CO} = Y_{CO, \text{measure}} (1 - 0.108) \quad (\text{A9})$$

All gas concentration data were corrected based on Eq (A7), (A8) and (A9)

Appendix B: Gas Temperature and Heat Flux Results

B.1 Gas Temperature

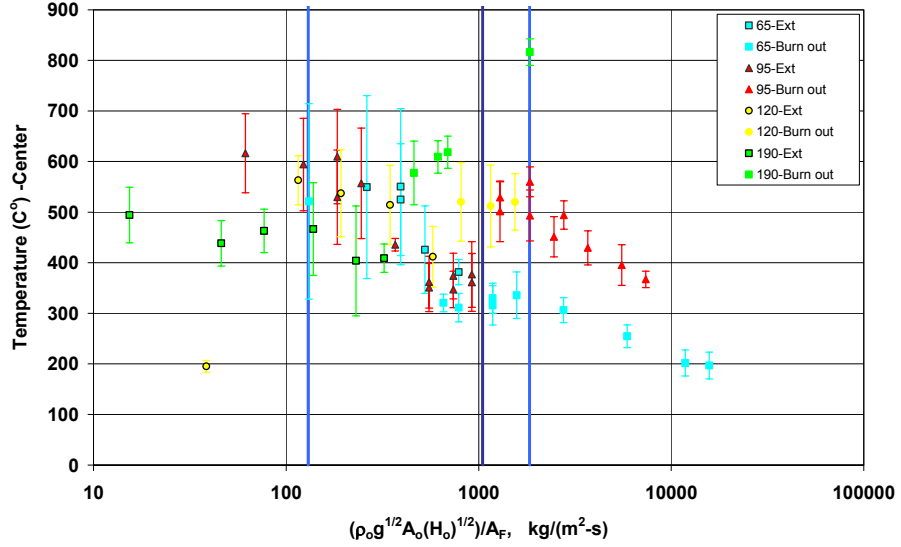


Figure B1 Gas Temperature from center thermocouple tree (TC17-TC19)

versus ventilation parameter

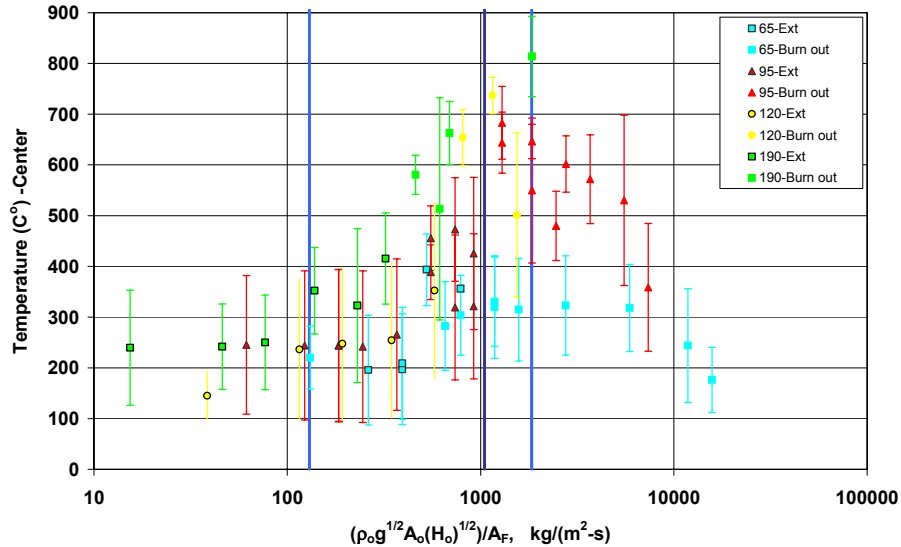


Figure B2 Gas Temperature from back thermocouple tree (TC13-TC16)

versus ventilation parameter

B.2 Heat Flux to Compartment

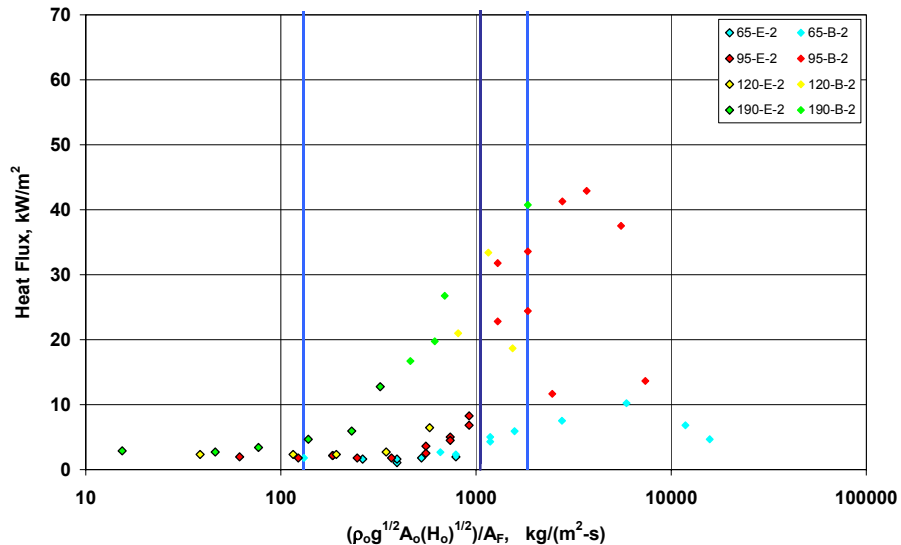


Figure B3 Heat flux to floor (HF2) versus ventilation parameter

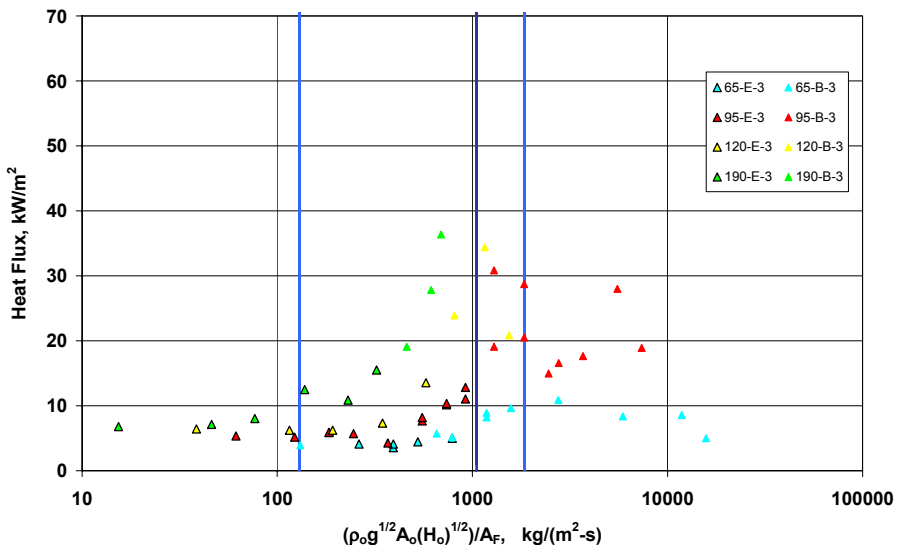


Figure B4 Heat flux to back wall (HF3) versus ventilation parameter

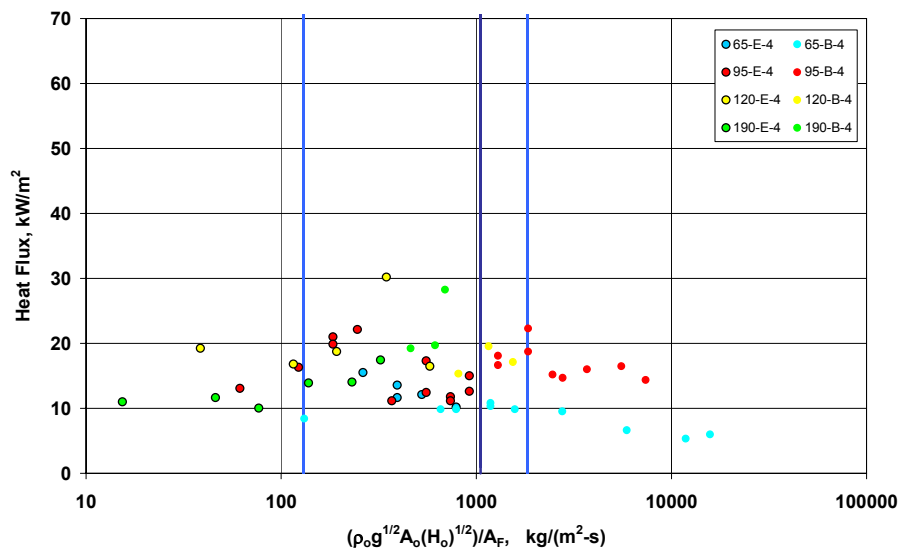


Figure B5 Heat flux to ceiling (HF4) versus ventilation parameter

Appendix C: Detail Drawing

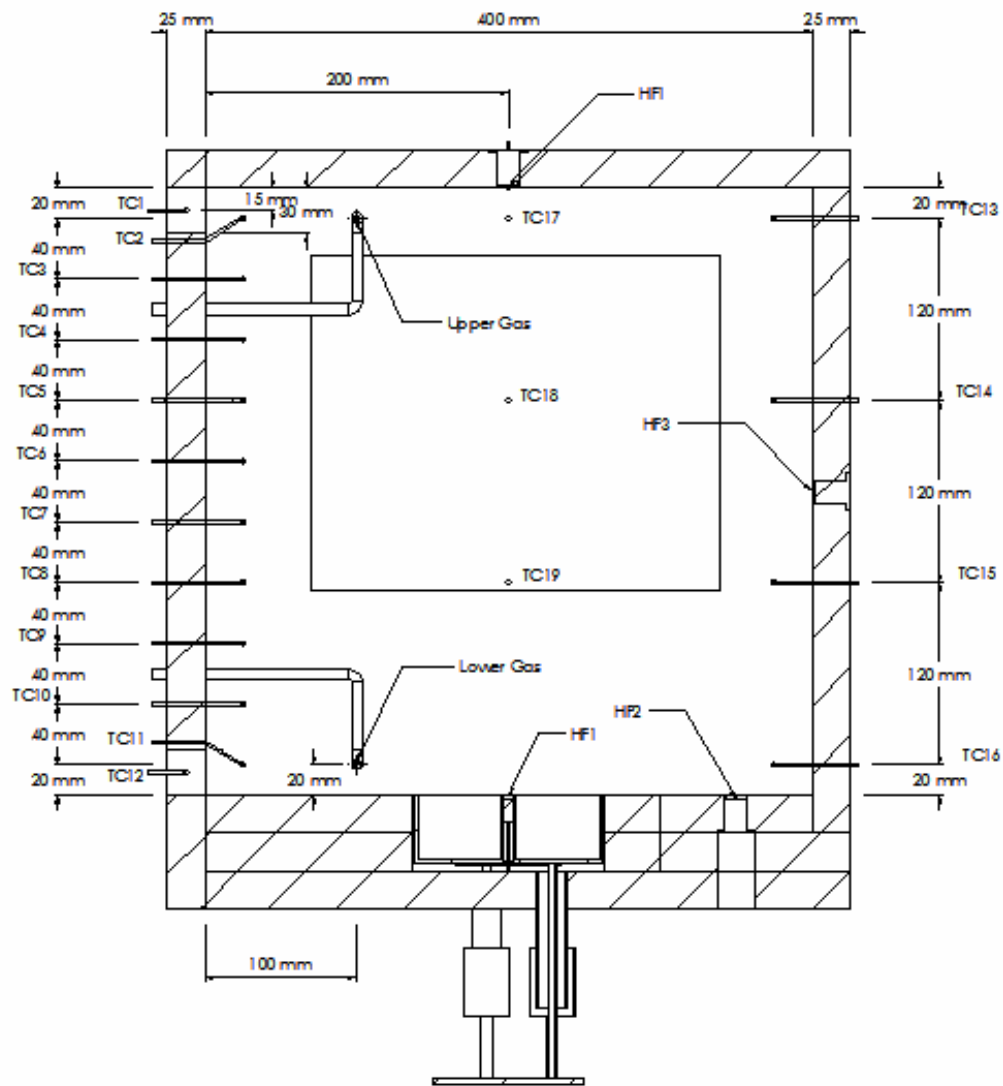


Figure C1 Section View showing experimental apparatus

Appendix D: Experimental and Predicted Results

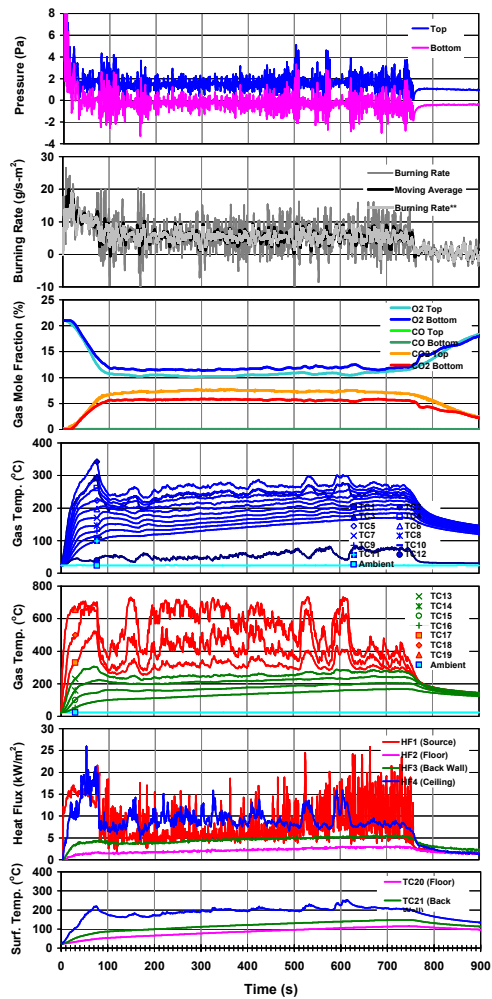
Note: Test title represents specific size of pan and vents, for example

Test 95-1×6 means 9.5 cm fuel pan with two 1 cm × 6 cm vent size

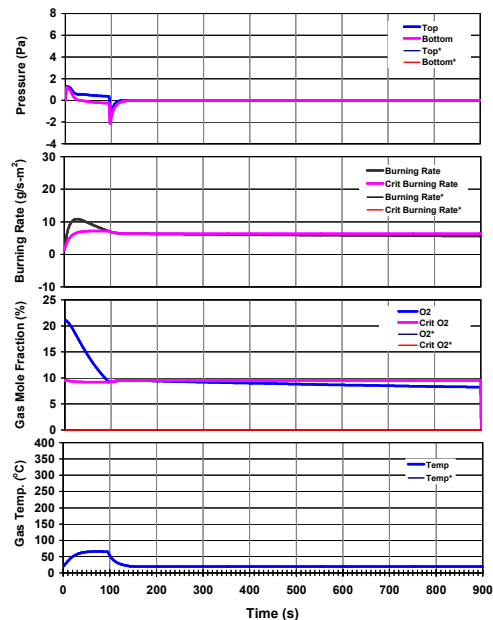
Test 65-1x1

Room Temp (°C) : 28.0 Initial Mass of Fuel (g) : 14.9
 Humidity (%) : 35.0 Final Mass of Fuel (g) : 0.0
 Fuel Pan Area (cm²) : 33.2 Mass Consumed (g) : 14.9
 Total Vent Area (cm²) : 2.0 Burn Time (s) : 755
 Category : 1

Experiment



Prediction



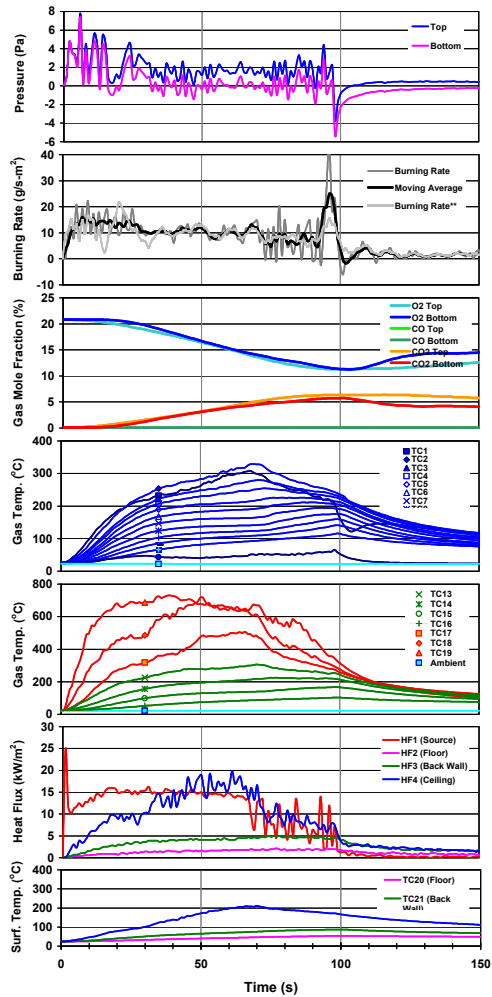
Ventilation Parameter ($\rho_0 g^{1/2} A_0 H^{1/2} / A_F$): 131 g/m²·s

Vertical Plume: 4 s
 Laminar Flame: 54 s
 Blue-Base Laminar Flame: 59 s
 Shrinking Flame: 63 s
 Laminar Flame: 141 s
 Shrinking Flame: 162 s
 Exhausted Fuel: 757 s

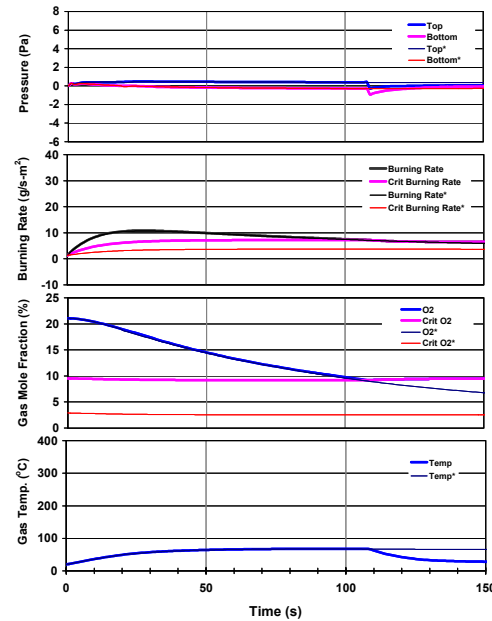
Test 65-1x2

Room Temp (°C) : 22.6 Initial Mass of Fuel (g) : 19.0
 Humidity (%) : 56.0 Final Mass of Fuel (g) : 13.2
 Fuel Pan Area (cm²) : 33.2 Mass Consumed (g) : 5.8
 Total Vent Area (cm²) : 4.0 Burn Time (s) : 98
 Category : 2

Experiment



Prediction



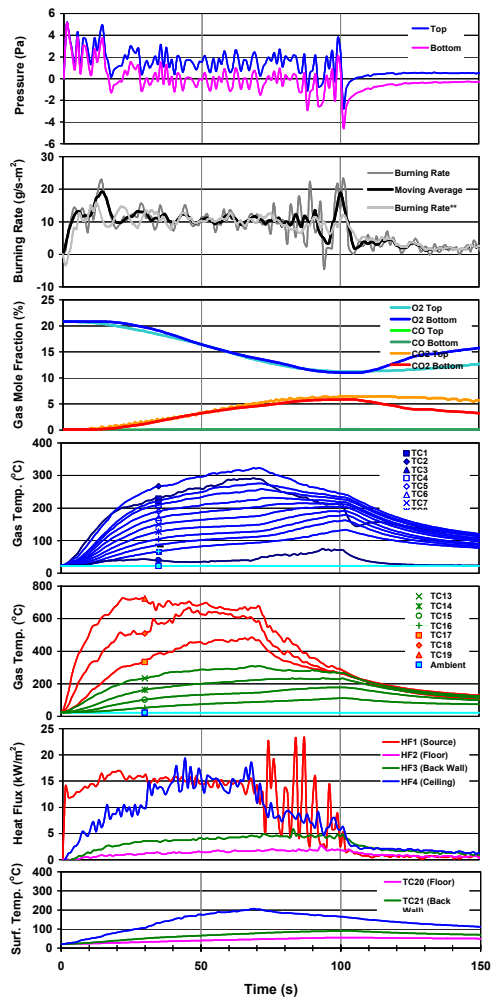
Ventilation Parameter ($\rho_0 g^{1/2} A_0 H^{1/2} / A_F$): 262 g/m²·s

Vertical Plume: 11 s
 Flickering Tip: 30 s
 Blue Base Flame: 54 s
 Shrinking Flame: 66 s
 Small Puffing and Oscillating: 73 s
 Ghosting Flame: 93 s
 Extinction: 97 s

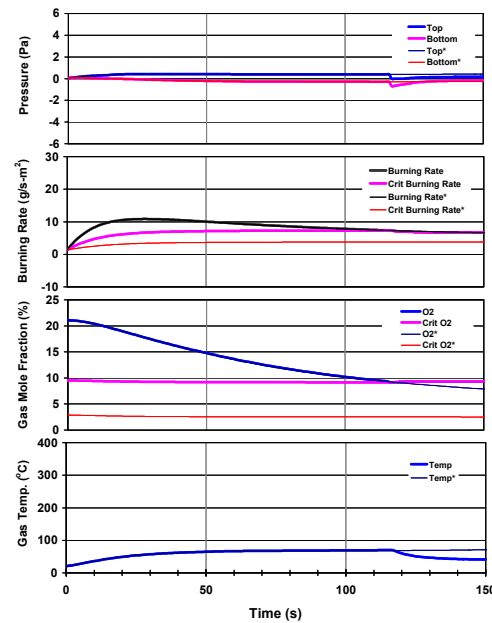
Test 65-1x3

Room Temp (°C) : 22.6 Initial Mass of Fuel (g) : 16.1
 Humidity (%) : 56.0 Final Mass of Fuel (g) : 8.8
 Fuel Pan Area (cm²) : 33.2 Mass Consumed (g) : 7.3
 Total Vent Area (cm²) : 6.0 Burn Time (s) : 101
 Category : 2

Experiment



Prediction



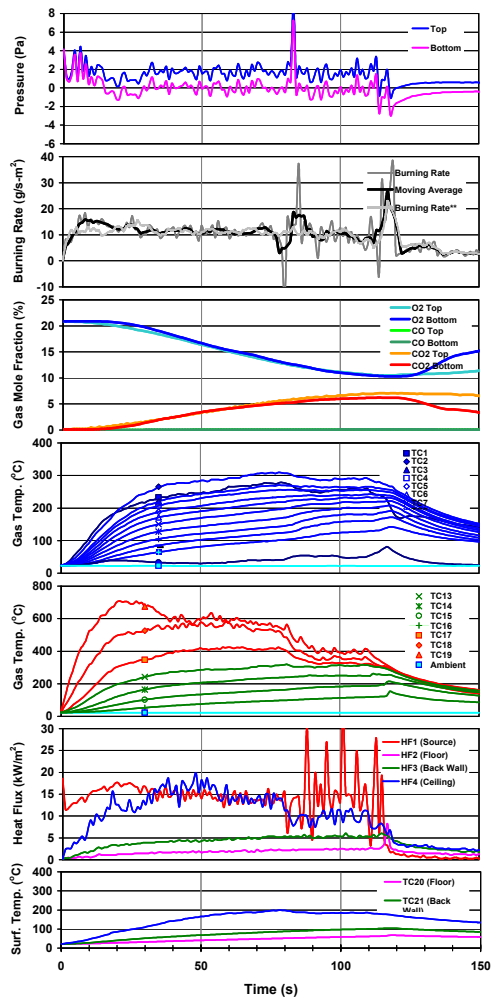
Ventilation Parameter ($\rho_0 \delta^{1/2} A_0 H^{1/2} / A_F$): 393 g/m²·s

Vertical Plume: 20 s
 Flickering Tip: 32 s
 Blue Base Flame: 60 s
 Shrinking Flame: 69 s
 Oscillating: 71 s
 Ghosting Flame: 92 s
 Extinction: 100 s

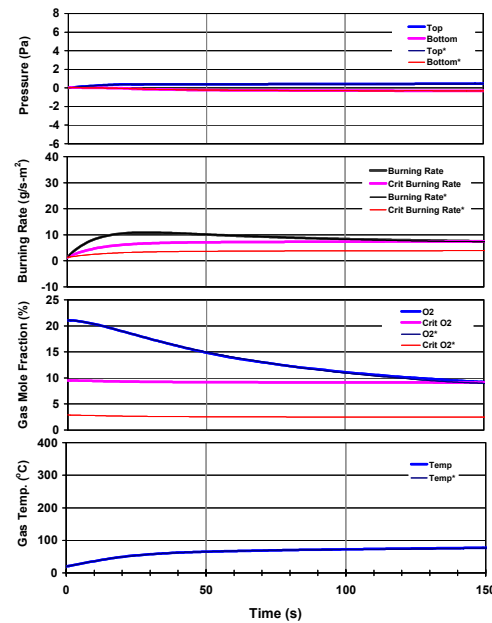
Test 65-1x4

Room Temp (°C) : 22.6 Initial Mass of Fuel (g) : 15.8
 Humidity (%) : 56.0 Final Mass of Fuel (g) : 7.1
 Fuel Pan Area (cm²) : 33.2 Mass Consumed (g) : 8.7
 Total Vent Area (cm²) : 8.0 Burn Time (s) : 118
 Category : 2

Experiment



Prediction



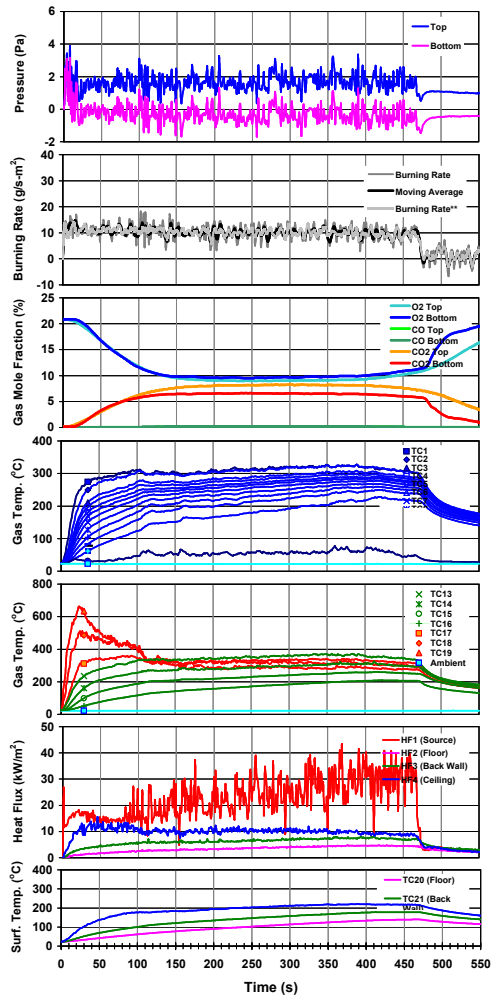
Ventilation Parameter ($\rho_0 \delta^{1/2} A_0 H^{1/2} / A_f$): 525 g/m²·s

Vertical Plume: 30 s
 Wind-Blown Flame: 67 s
 Oscillating: 83 s
 Ghosting Flame: 115 s
 Extinction: 119 s

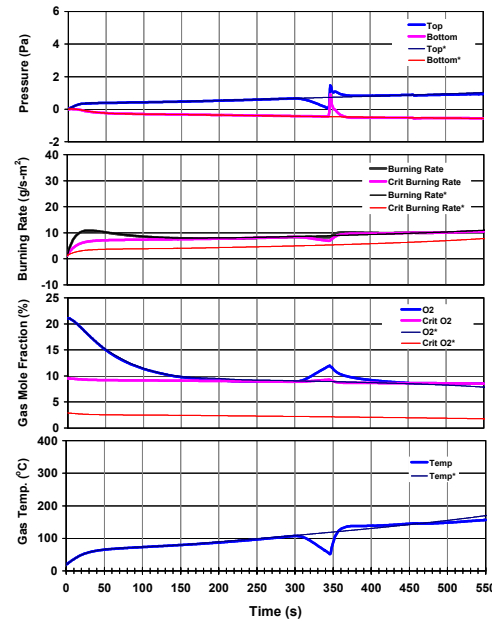
Test 65-1x5

Room Temp (°C) : 22.6 Initial Mass of Fuel (g) : 17.1
 Humidity (%) : 56.0 Final Mass of Fuel (g) : 0.0
 Fuel Pan Area (cm²) : 33.2 Mass Consumed (g) : 17.1
 Total Vent Area (cm²) : 10.0 Burn Time (s) : 473
 Category : 4

Experiment



Prediction

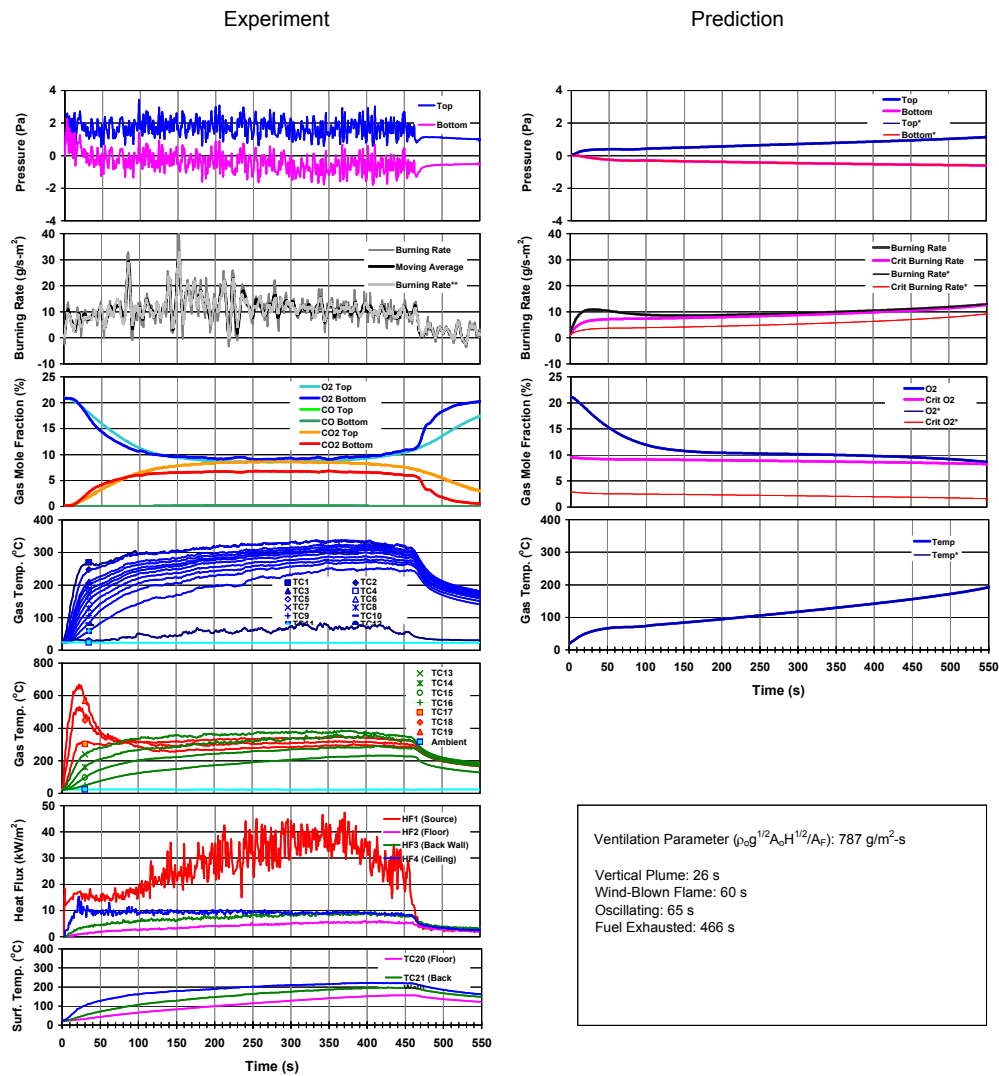


Ventilation Parameter ($\rho_0 g^{1/2} A_0 H^{1/2} / A_f$): 656 g/m²·s

Vertical Plume: 30 s
 Wind-Blown Flame: 60 s
 Oscillating: 74 s
 Fuel Exhausted: 473 s

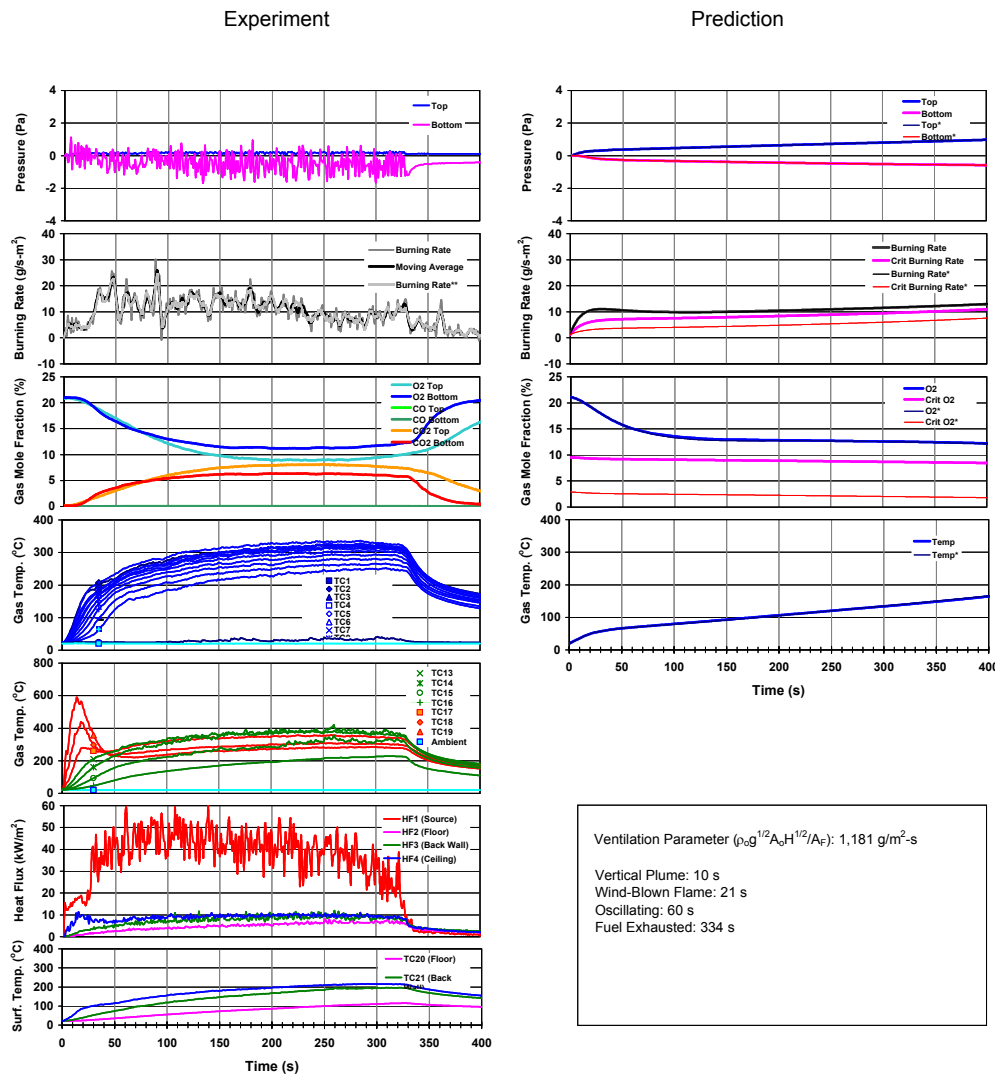
Test 65-1x6

Room Temp (°C) : 22.9 Initial Mass of Fuel (g) : 19.3
 Humidity (%) : 30.0 Final Mass of Fuel (g) : 0.0
 Fuel Pan Area (cm²) : 33.2 Mass Consumed (g) : 19.3
 Total Vent Area (cm²) : 12.0 Burn Time (s) : 468
 Category : 4



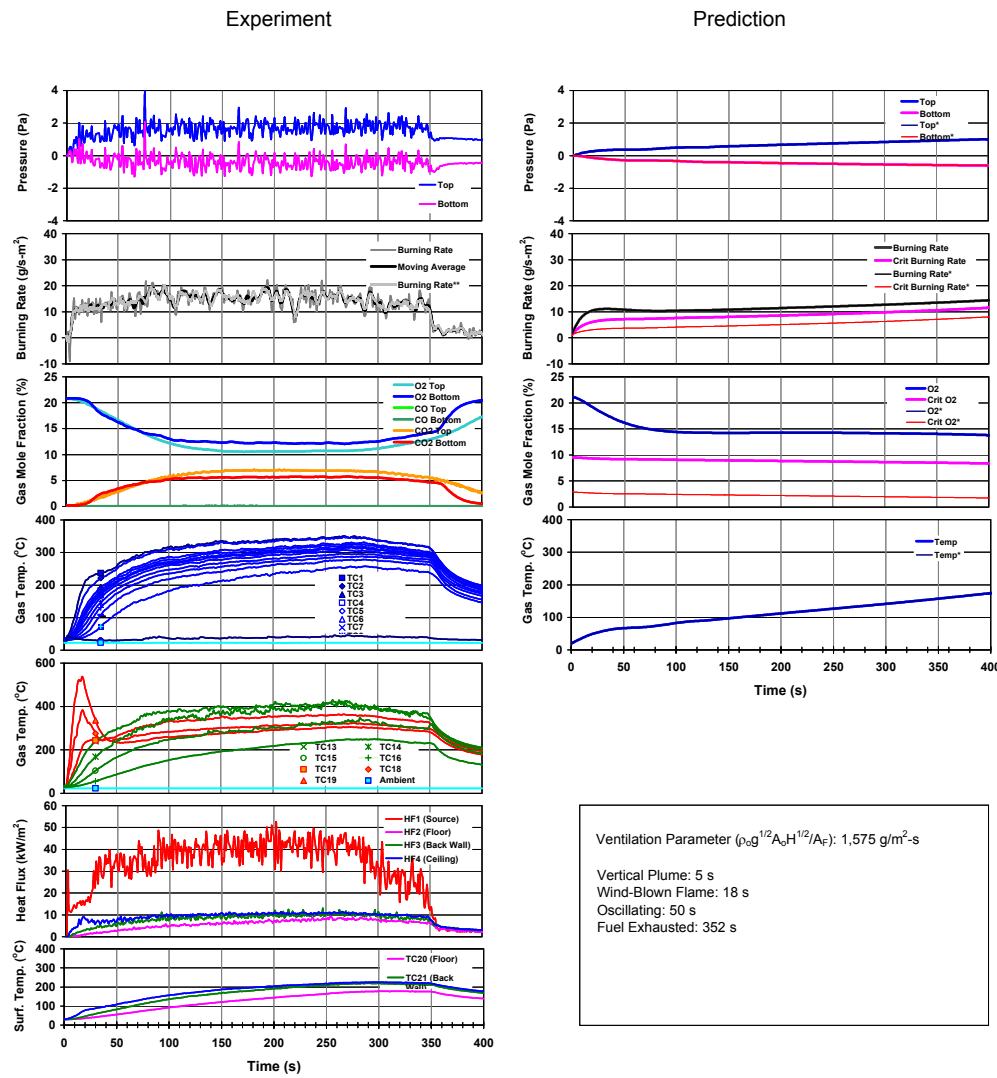
Test 65-1x9

Room Temp (°C) : 20.2 Initial Mass of Fuel (g) : 14.9
 Humidity (%) : 72.0 Final Mass of Fuel (g) : 0.0
 Fuel Pan Area (cm²) : 33.2 Mass Consumed (g) : 14.9
 Total Vent Area (cm²) : 18.0 Burn Time (s) : 334
 Category : 4



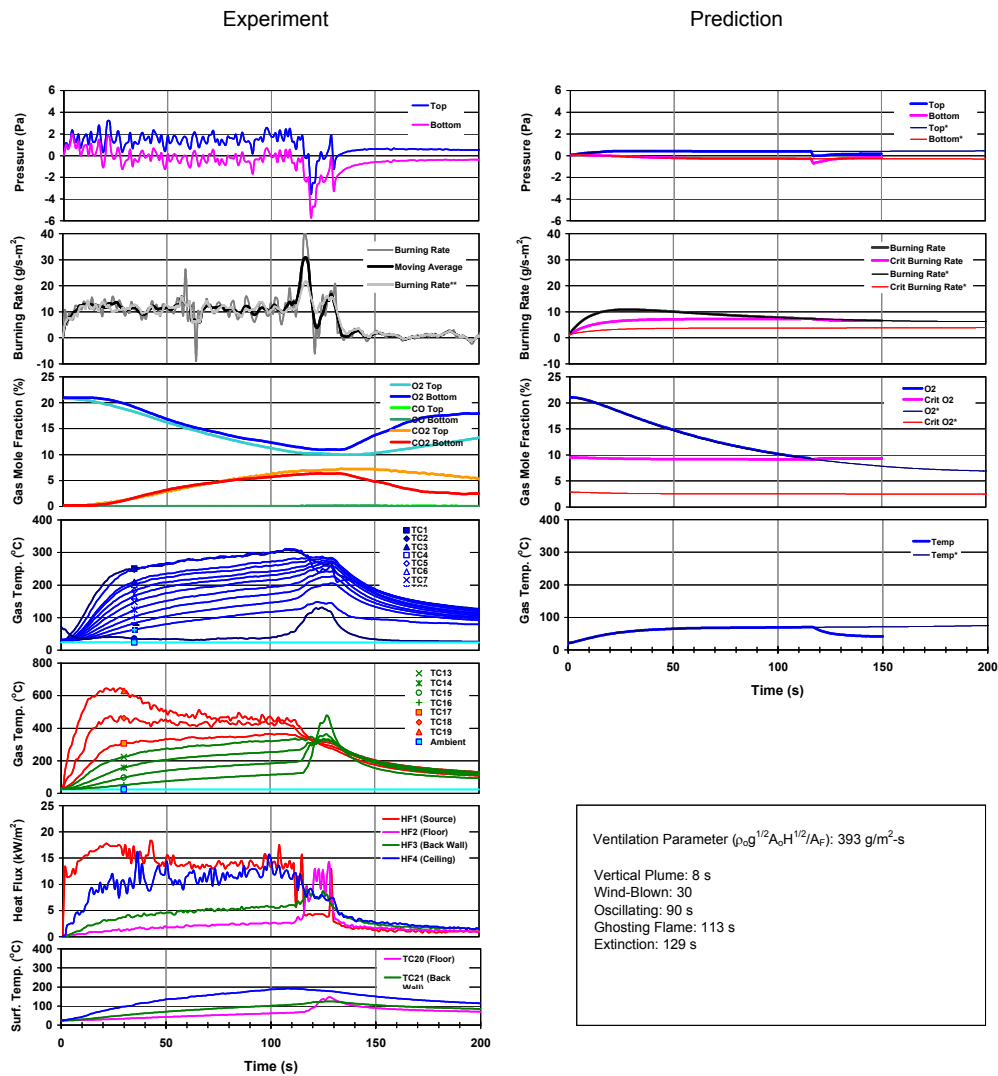
Test 65-1x12

Room Temp (°C) : 22.9
 Humidity (%) : 30.0
 Fuel Pan Area (cm²) : 33.2
 Total Vent Area (cm²) : 24.0
 Initial Mass of Fuel (g) : 17.7
 Final Mass of Fuel (g) : 0.0
 Mass Consumed (g) : 17.7
 Burn Time (s) : 350
 Category : 4



Test 65-3x1

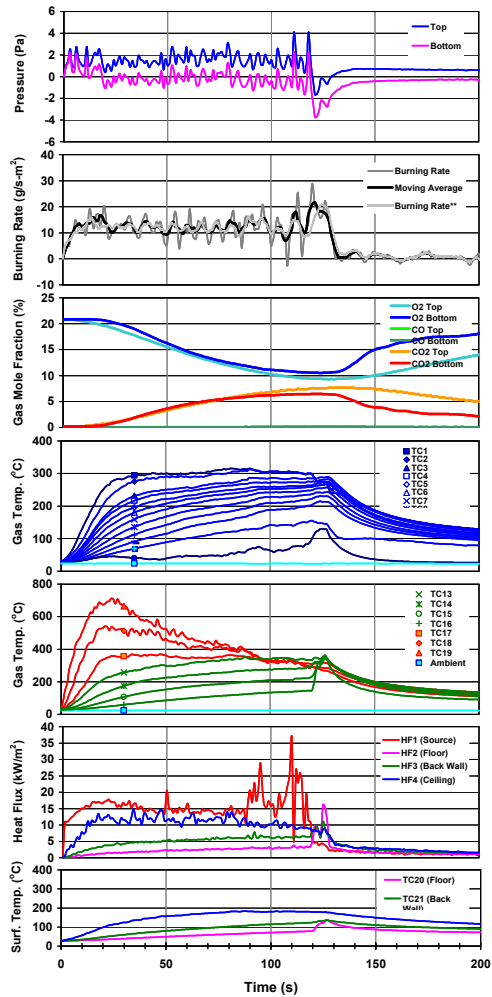
Room Temp (°C) : 28.0 Initial Mass of Fuel (g) : 19.1
 Humidity (%) : 35.0 Final Mass of Fuel (g) : 11.7
 Fuel Pan Area (cm²) : 33.2 Mass Consumed (g) : 7.4
 Total Vent Area (cm²) : 6.0 Burn Time (s) : 130
 Category : 2



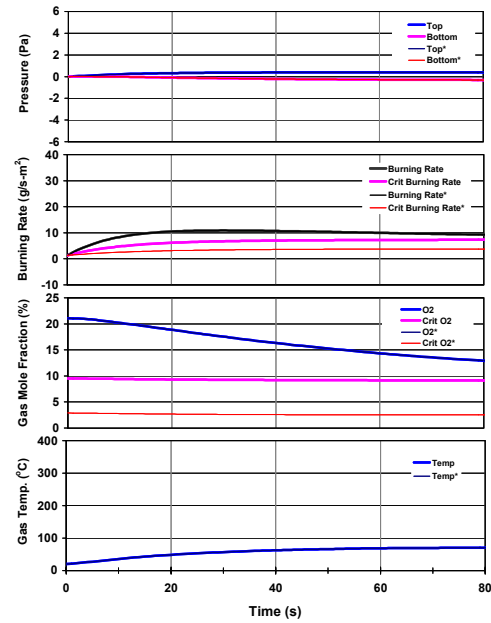
Test 65-3x2

Room Temp (°C) : 28.0 Initial Mass of Fuel (g) : 16.6
 Humidity (%) : 35.0 Final Mass of Fuel (g) : 4.9
 Fuel Pan Area (cm²) : 33.2 Mass Consumed (g) : 11.7
 Total Vent Area (cm²) : 12.0 Burn Time (s) : 129
Category : 2

Experiment



Prediction



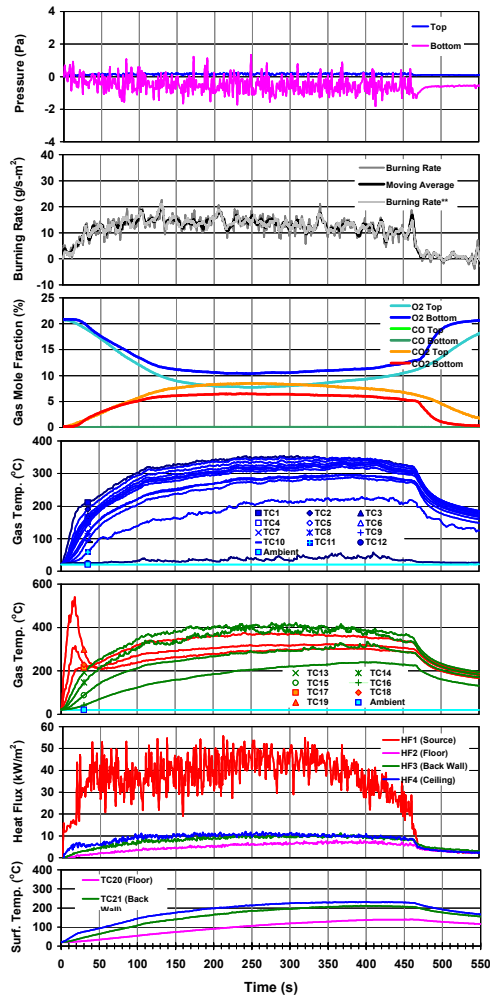
Ventilation Parameter ($\rho_0 \beta^{1/2} A_0 H^{1/2} / A_F$): 787 g/m²·s

Vertical Plume: 6 s
 Wind-Blown: 31
 Oscillating: 78 s
 Ghosting Flame: 119 s
 Extinction: 127 s

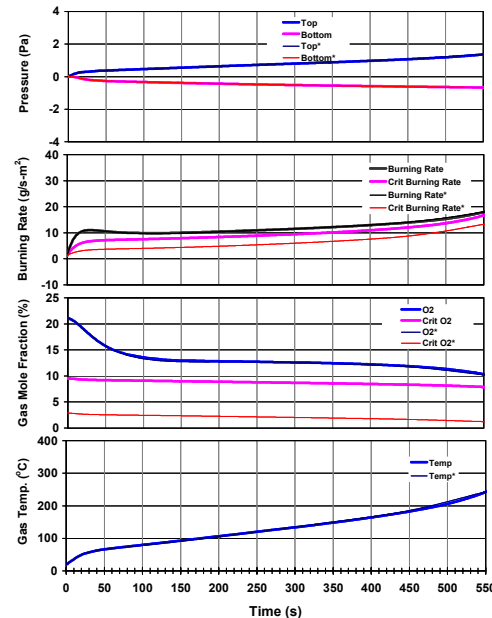
Test 65-3x3

Room Temp (°C) : 28.0 Initial Mass of Fuel (g) : 19.9
 Humidity (%) : 35.0 Final Mass of Fuel (g) : 19.9
 Fuel Pan Area (cm²) : 33.2 Mass Consumed (g) : 0.0
 Total Vent Area (cm²) : 18.0 Burn Time (s) : 470
 Category : 4

Experiment



Prediction

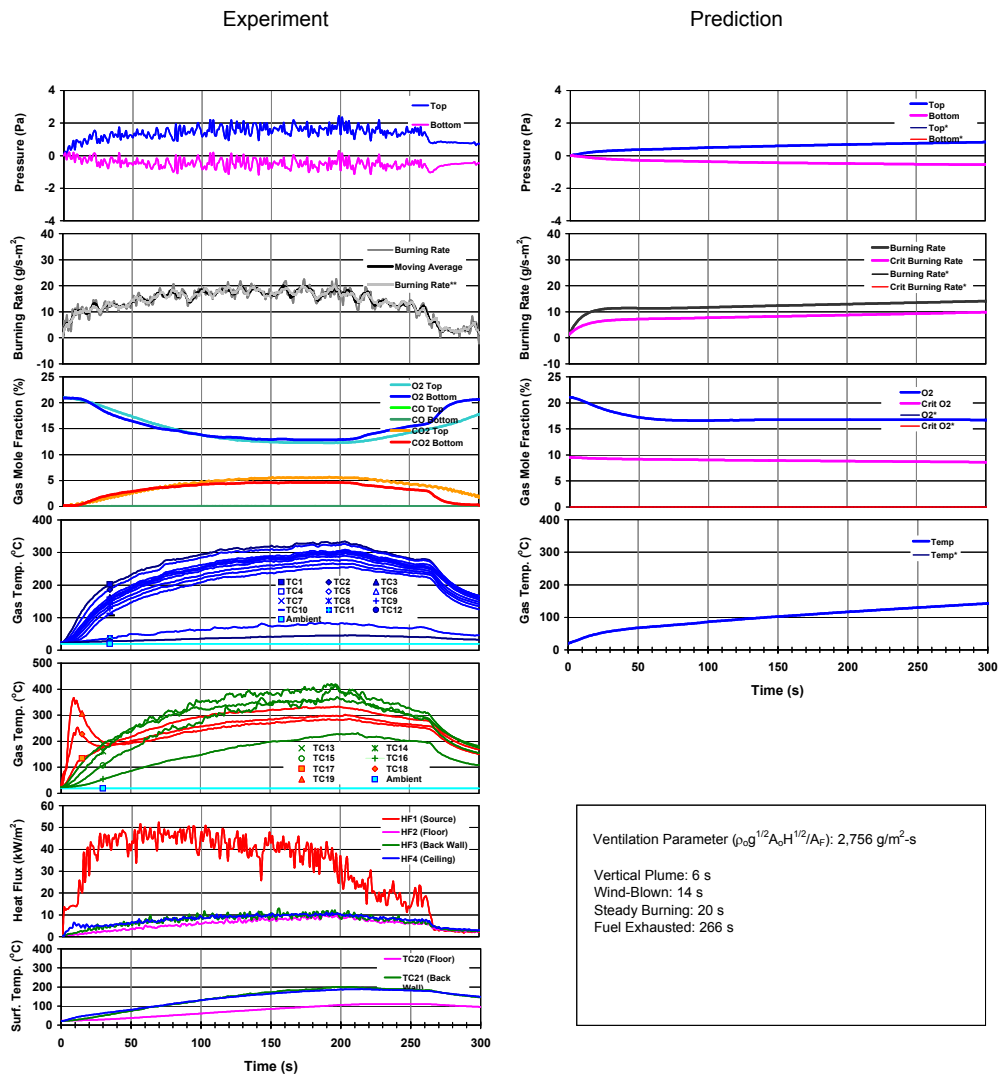


Ventilation Parameter ($\rho_0 g^{1/2} A_0 H^{1/2} / A_F$): 1,181 g/m²·s

Vertical Plume: 15 s
 Wind-Blown: 22 s
 Leaning Backward & Puffing: 40 s
 Oscillating: 100 s
 Fuel Exhausted: 467 s

Test 65-3x7

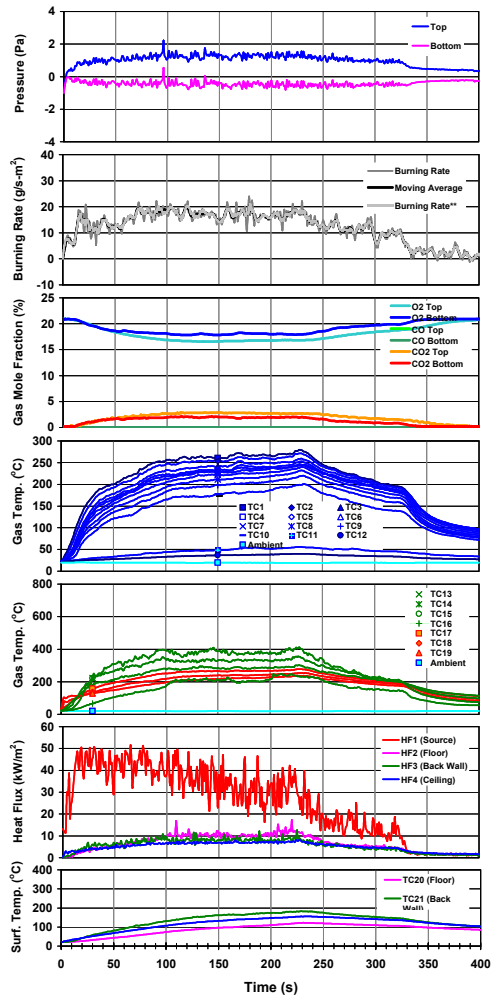
Room Temp (°C) : 20.0 Initial Mass of Fuel (g) : 13.8
 Humidity (%) : 58.0 Final Mass of Fuel (g) : 0.0
 Fuel Pan Area (cm²) : 33.2 Mass Consumed (g) : 13.8
 Total Vent Area (cm²) : 42.0 Burn Time (s) : 266
 Category : 4



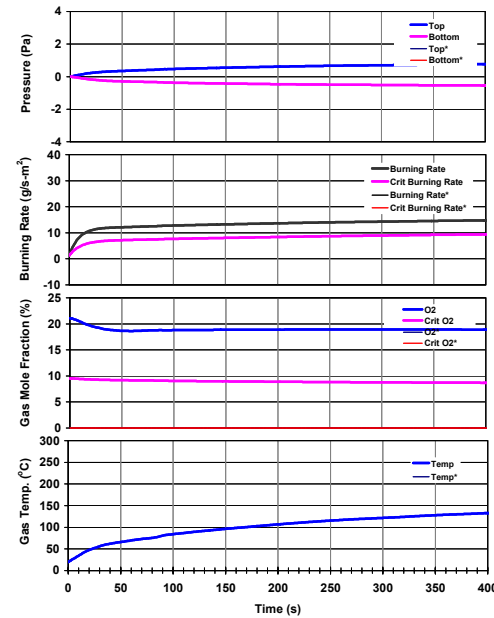
Test 65-3x15

Room Temp (°C) : 20.6 Initial Mass of Fuel (g) : 16.5
 Humidity (%) : 65.0 Final Mass of Fuel (g) : 0.0
 Fuel Pan Area (cm²) : 33.2 Mass Consumed (g) : 16.5
 Total Vent Area (cm²) : 90.0 Burn Time (s) : 330
Category : 4

Experiment



Prediction



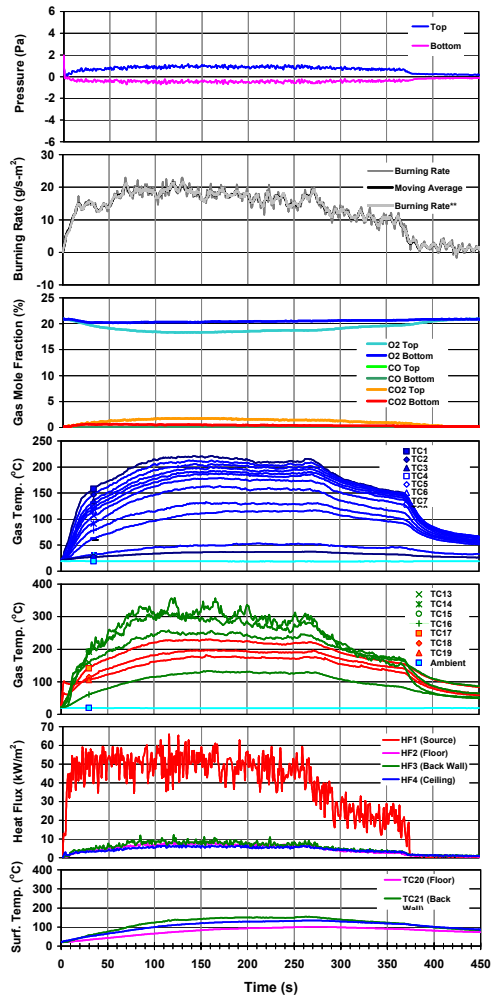
Ventilation Parameter ($\rho_0 g^{1/2} A_0 H^{1/2} / A_F$): 2,756 g/m²·s

Vertical Plume: 2 s
 Wind-Blown: 5 s
 Steady Burning: 15 s
 Fuel Exhausted: 330 s

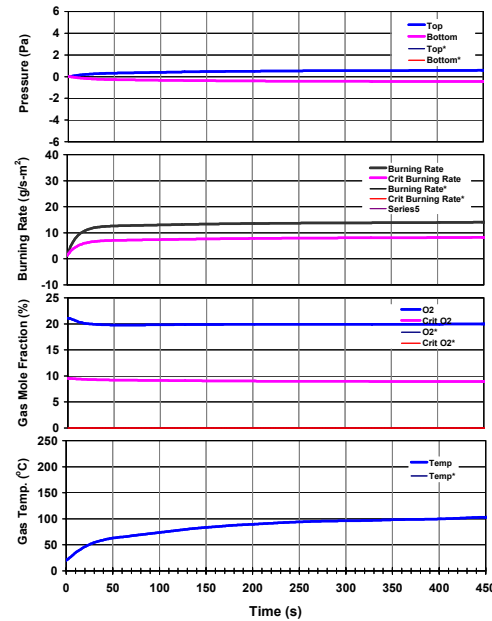
Test 65-3x30

Room Temp (°C) : 20.9 Initial Mass of Fuel (g) : 19.2
 Humidity (%) : 45.0 Final Mass of Fuel (g) : 0.0
 Fuel Pan Area (cm²) : 33.2 Mass Consumed (g) : 19.2
 Total Vent Area (cm²) : 180.0 Burn Time (s) : 375
 Category : 4

Experiment



Prediction



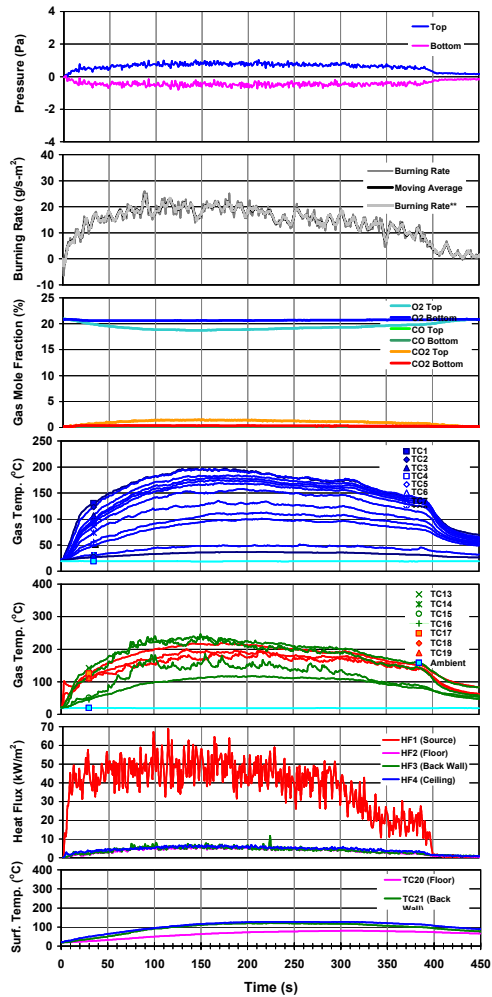
Ventilation Parameter ($\rho_0 \beta^{1/2} A_0 H^{1/2} / A_F$): 11,815 g/m²·s

Vertical Plume: 2 s
 Wind-Blown: 4 s
 Steady Burning: 10 s
 Fuel Exhausted: 375 s

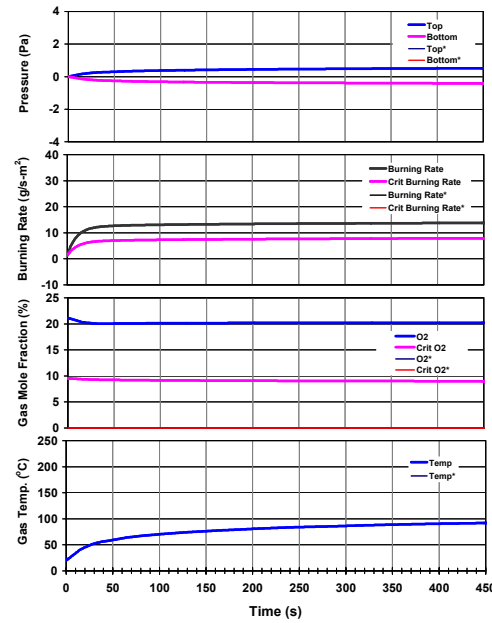
Test 65-3x40

Room Temp (°C) : 20.5
 Humidity (%) : 45.0
 Fuel Pan Area (cm²) : 33.2
 Total Vent Area (cm²) : 240.0
 Initial Mass of Fuel (g) : 20.6
 Final Mass of Fuel (g) : 0.0
 Mass Consumed (g) : 20.6
 Burn Time (s) : 397
 Category : 4

Experiment



Prediction

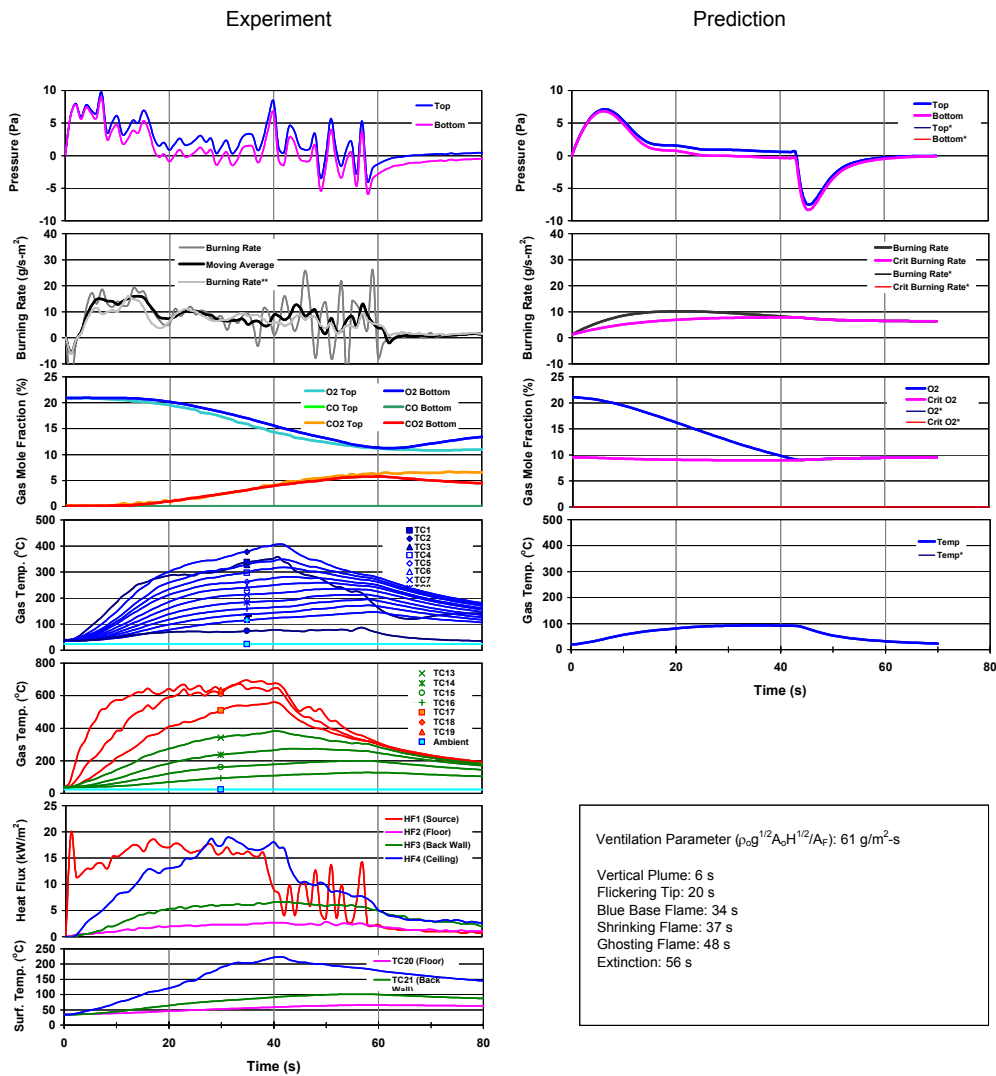


Ventilation Parameter ($\rho_0 g^{1/2} A_0 H^{1/2} / A_F$): 15.753 g/m²·s

Vertical Plume: 2 s
 Wind-Blown: 4 s
 Steady Burning: 10 s
 Fuel Exhausted: 397 s

Test 95-1x1

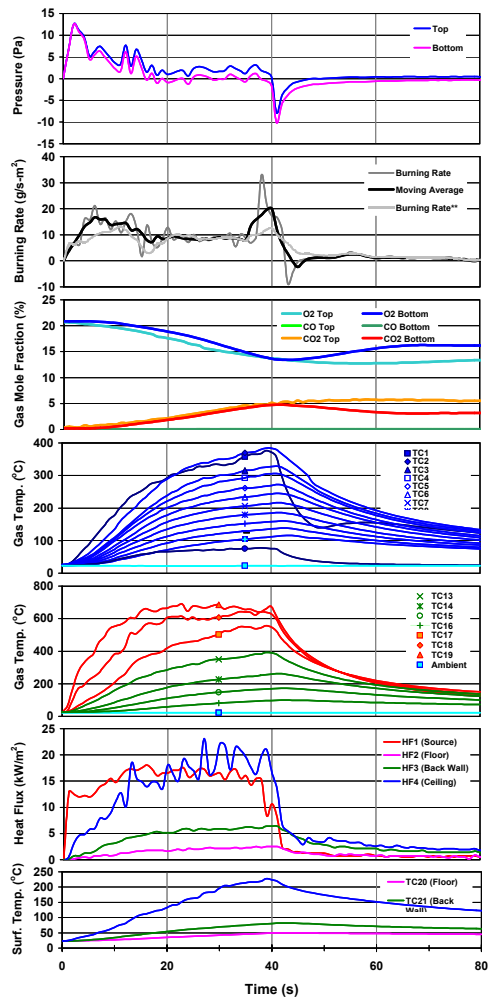
Room Temp (°C) : 23.8 Initial Mass of Fuel (g) : 39.2
 Humidity (%) : 35.0 Final Mass of Fuel (g) : 33.0
 Fuel Pan Area (cm²) : 70.9 Mass Consumed (g) : 6.2
 Total Vent Area (cm²) : 2.0 Burn Time (s) : 59
 Category : 1



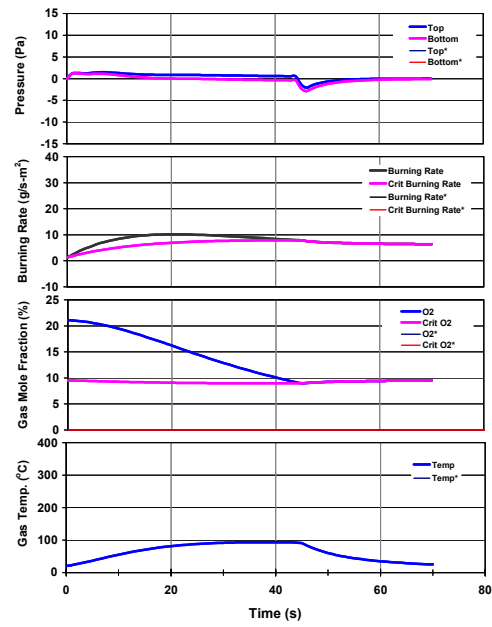
Test 95-1x2

Room Temp (°C) : 23.9 Initial Mass of Fuel (g) : 36.4
 Humidity (%) : 54.0 Final Mass of Fuel (g) : 30.0
 Fuel Pan Area (cm²) : 70.9 Mass Consumed (g) : 6.4
 Total Vent Area (cm²) : 4.0 Burn Time (s) : 42
 Category : 1

Experiment



Prediction



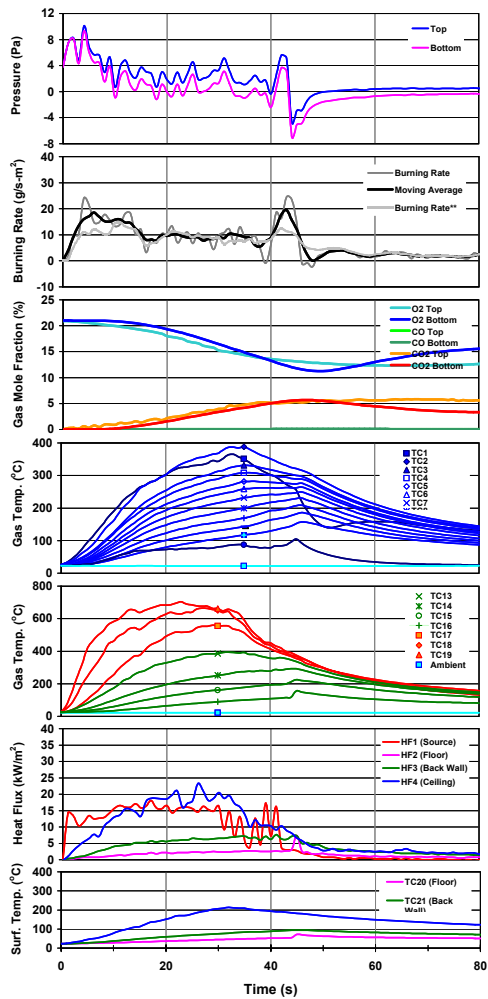
Ventilation Parameter ($\rho_0 g^{1/2} A_0 H^{1/2} / A_f$): 122 g/m²·s

Vertical Plume with Flickering Tip: 20 s
 Blue Base Flame: 30 s
 Shrinking Flame: 37 s
 Extinction: 41 s

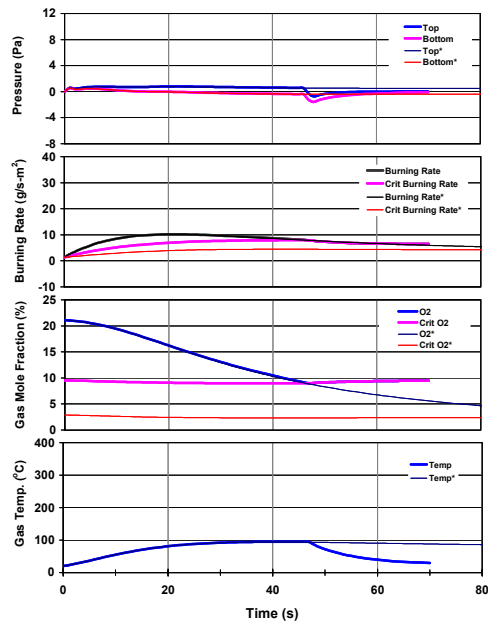
Test 95-1x3

Room Temp (°C) : 23.9 Initial Mass of Fuel (g) : 46.6
 Humidity (%) : 54.0 Final Mass of Fuel (g) : 38.7
 Fuel Pan Area (cm²) : 70.9 Mass Consumed (g) : 7.9
 Total Vent Area (cm²) : 6.0 Burn Time (s) : 46
 Category : 2

Experiment



Prediction



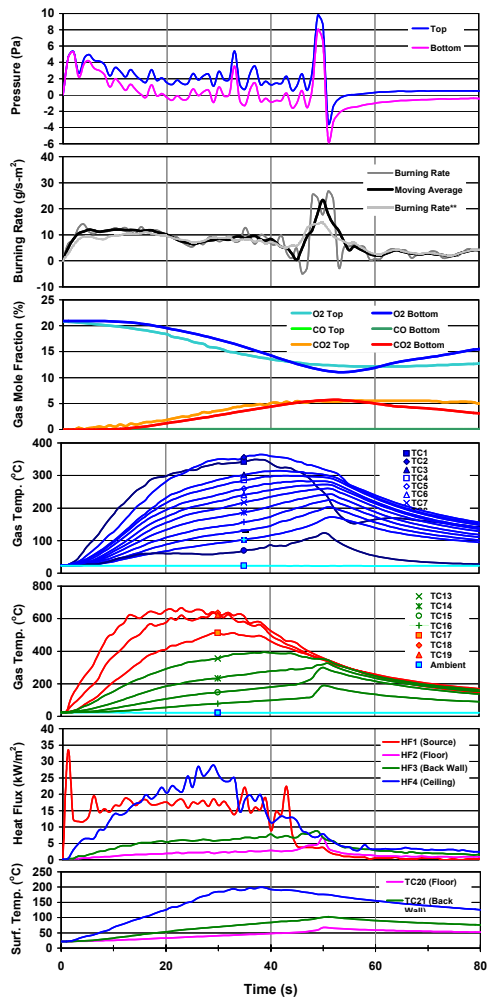
Ventilation Parameter ($\rho_0 g^{1/2} A_0 H^{1/2} / A_F$): 184 g/m²·s

Vertical Plume with Flickering Tip: 13 s
 Blue Base Flame: 20 s
 Puffing and Oscillating: 37 s
 Ghosting Flame: 42 s
 Extinction: 45 s

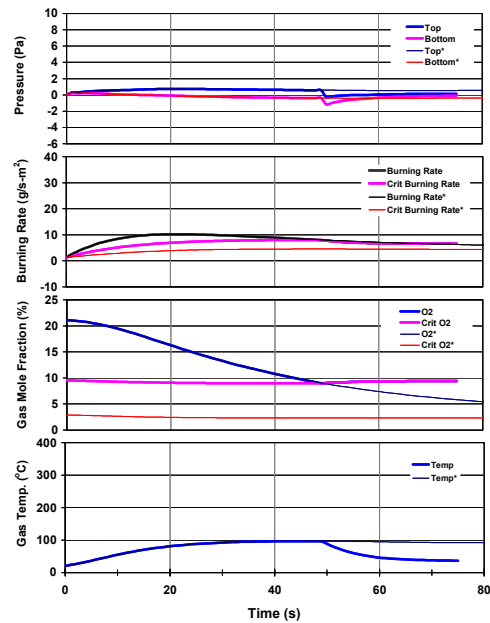
Test 95-1x4

Room Temp (°C) : 23.9 Initial Mass of Fuel (g) : 43.7
 Humidity (%) : 54.0 Final Mass of Fuel (g) : 35.4
 Fuel Pan Area (cm²) : 70.9 Mass Consumed (g) : 8.3
 Total Vent Area (cm²) : 8.0 Burn Time (s) : 51
 Category : 2

Experiment



Prediction

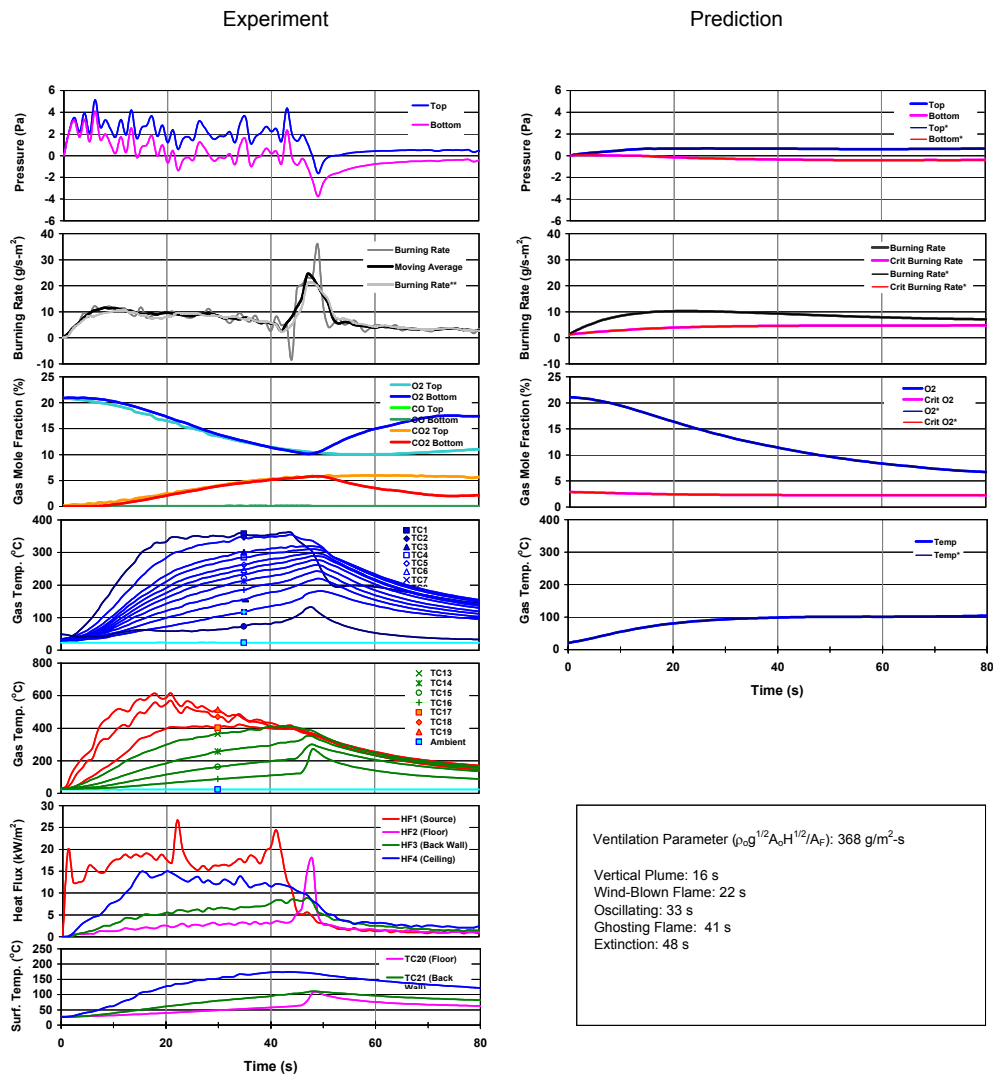


Ventilation Parameter ($\rho_0 g^{1/2} A_0 H^{1/2} / A_F$): 245 g/m²·s

Vertical Plume with Flickering Tip: 25 s
 Blue Base Flame: 32 s
 Puffing and Oscillating: 37 s
 Ghosting Flame: 44 s
 Extinction: 50 s

Test 95-1x6

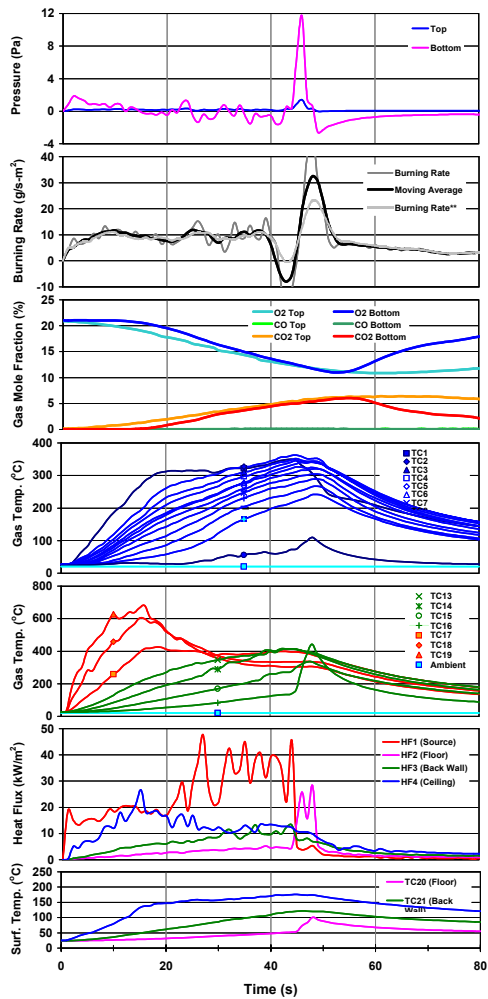
Room Temp (°C) : 22.6 Initial Mass of Fuel (g) : 43.4
 Humidity (%) : 30.0 Final Mass of Fuel (g) : 32.7
 Fuel Pan Area (cm²) : 70.9 Mass Consumed (g) : 10.7
 Total Vent Area (cm²) : 12.0 Burn Time (s) : 48
 Category : 2



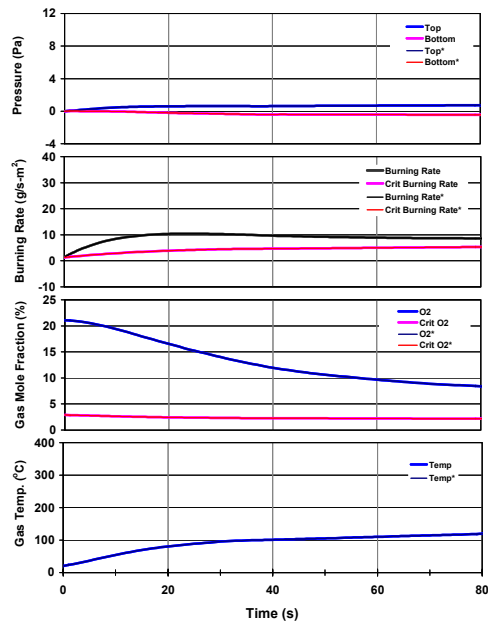
Test 95-1x9

Room Temp (°C) : 22.0 Initial Mass of Fuel (g) : 31.0
 Humidity (%) : 71.0 Final Mass of Fuel (g) : 19.7
 Fuel Pan Area (cm²) : 70.9 Mass Consumed (g) : 11.3
 Total Vent Area (cm²) : 18.0 Burn Time (s) : 49
 Category : 2

Experiment



Prediction



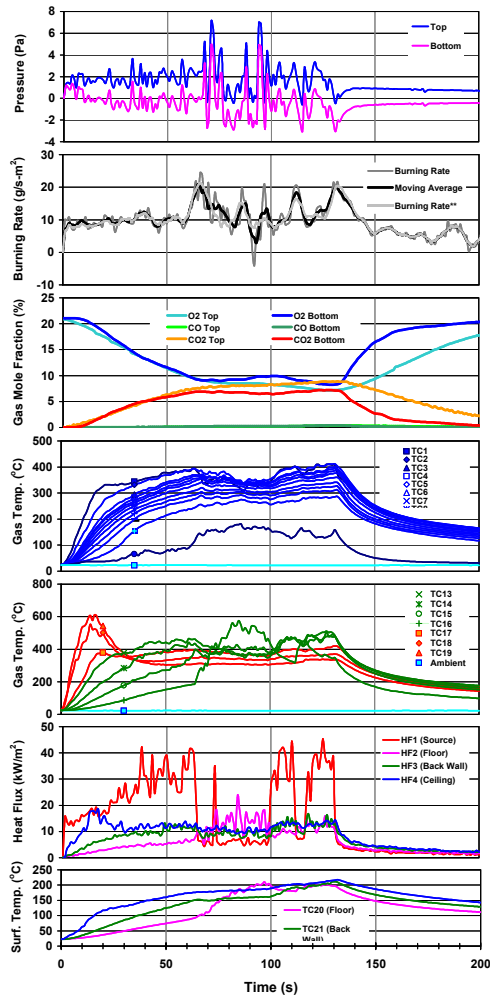
Ventilation Parameter ($\rho_0 g^{1/2} A_0 H^{1/2} / A_F$): 553 g/m²·s

Vertical Plume: 6 s
 Wind-Blown Flame: 15 s
 Oscillating: 30 s
 Ghosting Flame: 44 s
 Extinction: 48 s

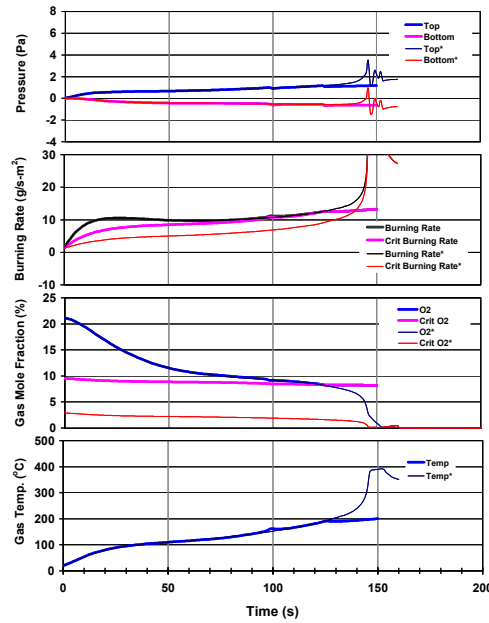
Test 95-1x12

Room Temp (°C) : 23.0 Initial Mass of Fuel (g) : 48.8
 Humidity (%) : 30.0 Final Mass of Fuel (g) : 25.6
 Fuel Pan Area (cm²) : 70.9 Mass Consumed (g) : 23.2
 Total Vent Area (cm²) : 24.0 Burn Time (s) : 134
 Category : 2

Experiment



Prediction

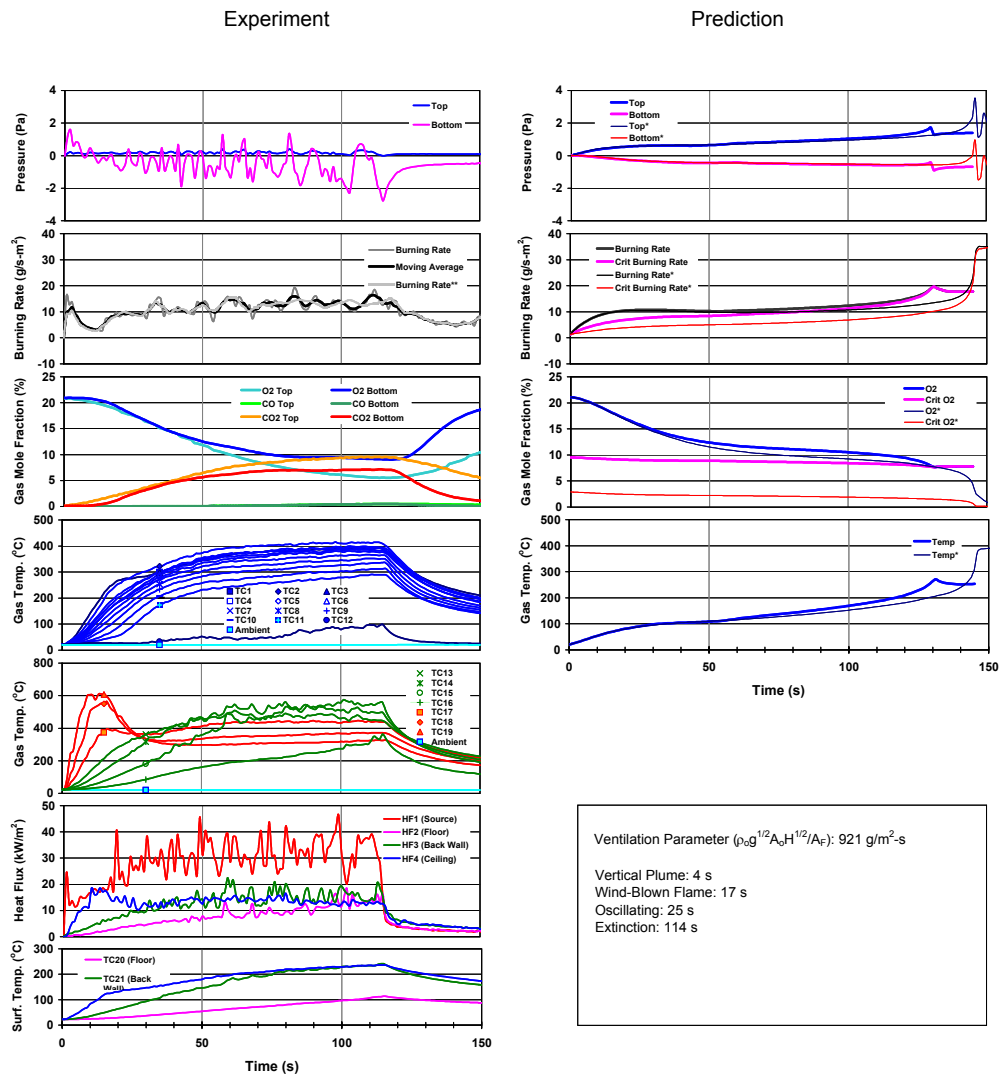


Ventilation Parameter ($\rho_{\text{air}}^{1/2} A_0 H^{1/2} / A_F$): 737 g/m²·s

Vertical Plume: 10 s
 Wind-Blown Flame: 20 s
 Oscillating: 30 s
 Ghosting Flame: 64 s
 Oscillating: 100 s
 Ghosting Flame: 110 s
 Oscillating: 116 s
 Ghosting Flame: 130 s
 Extinction: 133 s

Test 95-1x15

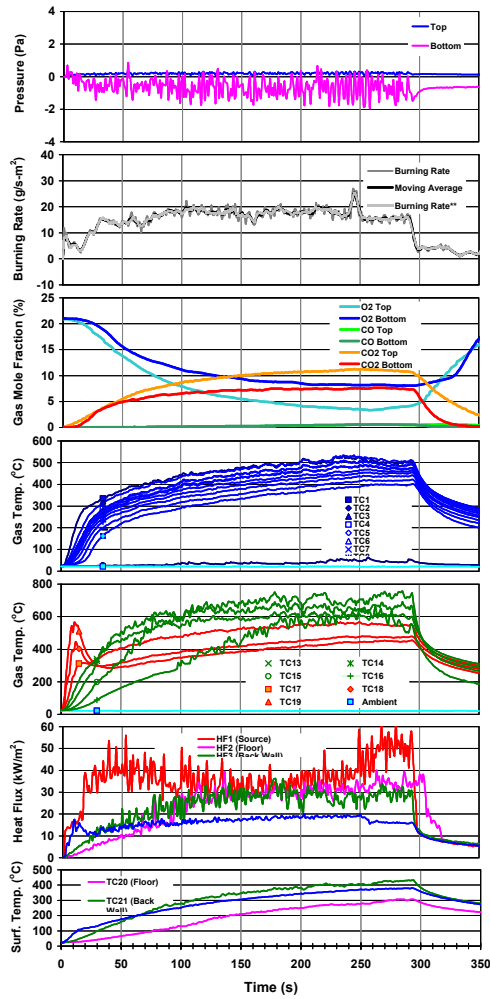
Room Temp (°C) : 22.0 Initial Mass of Fuel (g) : 47.0
 Humidity (%) : 71.0 Final Mass of Fuel (g) : 28.5
 Fuel Pan Area (cm²) : 70.9 Mass Consumed (g) : 18.5
 Total Vent Area (cm²) : 30.0 Burn Time (s) : 115
 Category : 2



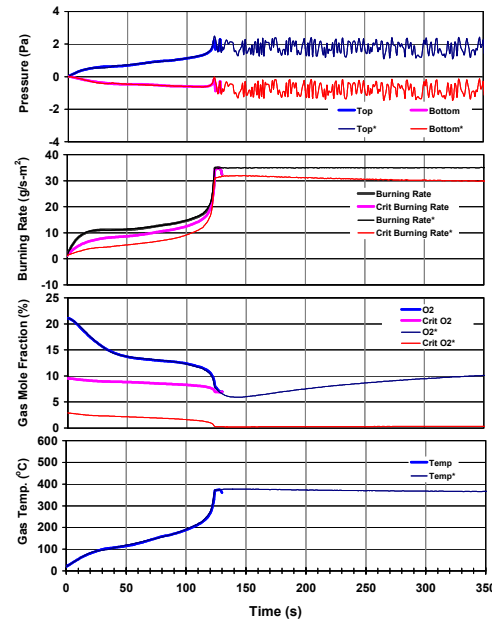
Test 95-1x21

Room Temp (°C) : 21.6 Initial Mass of Fuel (g) : 40.1
 Humidity (%) : 71.0 Final Mass of Fuel (g) : 0.0
 Fuel Pan Area (cm²) : 70.9 Mass Consumed (g) : 40.1
 Total Vent Area (cm²) : 42.0 Burn Time (s) : 299
 Category : 4

Experiment



Prediction



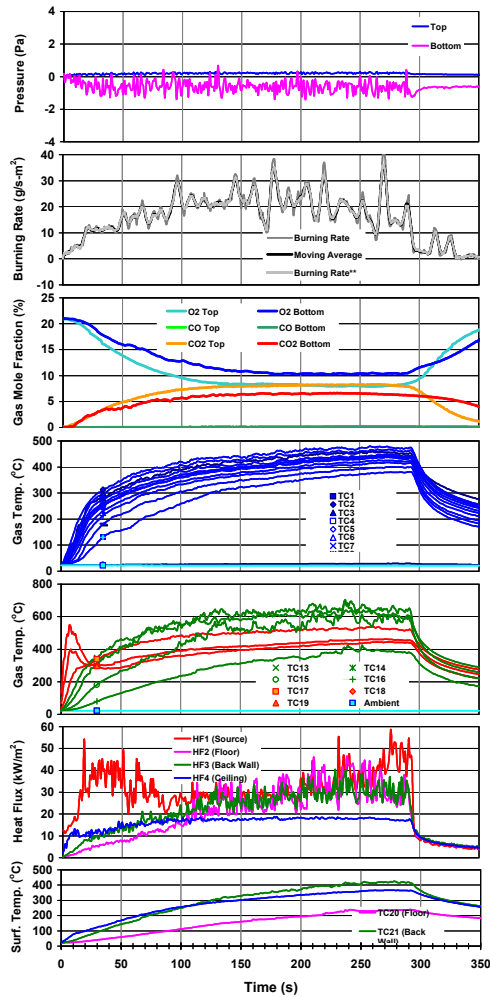
Ventilation Parameter ($\rho_0 g^{1/2} A_0 H^{1/2} / A_F$): 1,290 g/m²·s

Vertical Plume: 4 s
 Wind-Blown Flame: 10 s
 Leaning Backward with Puffing Flame: 20 s
 Oscillating: 60 s
 Fuel Exhausted: 298 s

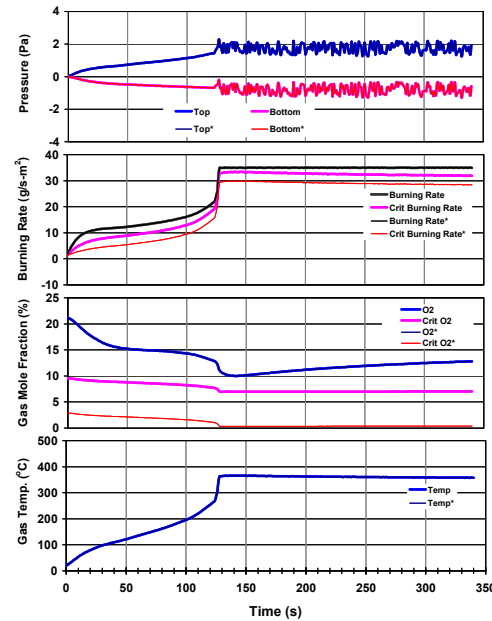
Test 95-1x30

Room Temp (°C) : 23.1
 Humidity (%) : 40.0
 Fuel Pan Area (cm²) : 70.9
 Total Vent Area (cm²) : 60.0
 Initial Mass of Fuel (g) : 44.7
 Final Mass of Fuel (g) : 0.0
 Mass Consumed (g) : 44.7
 Burn Time (s) : 297
 Category : 4

Experiment



Prediction

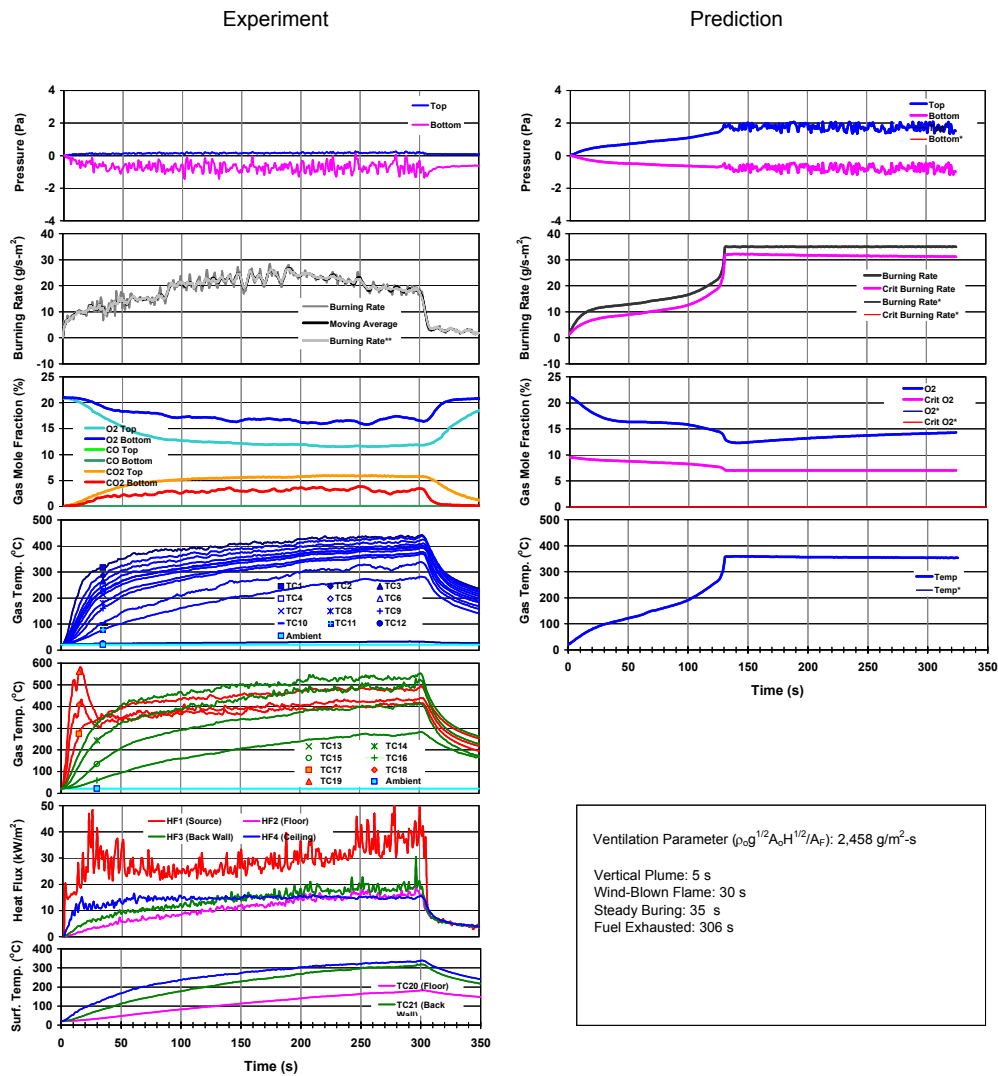


Ventilation Parameter ($\rho_0 g^{1/2} A_0 H^{1/2} / A_F$): 1,843 g/m²·s

Vertical Plume: 3 s
 Wind-Blown Flame: 12 s
 Leaning Backward: 30 s
 Leaning Backward Flame with Puffing: 137 s
 Fuel Exhausted: 297 s

Test 95-1x40

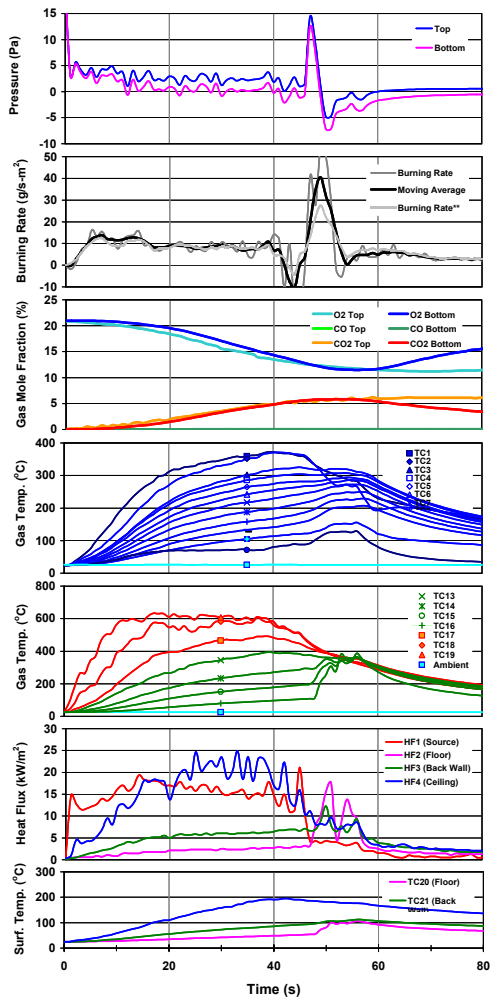
Room Temp (°C) : 23.6 Initial Mass of Fuel (g) : 44.9
 Humidity (%) : 50.0 Final Mass of Fuel (g) : 0.0
 Fuel Pan Area (cm²) : 70.9 Mass Consumed (g) : 44.9
 Total Vent Area (cm²) : 80.0 Burn Time (s) : 306
 Category : 4



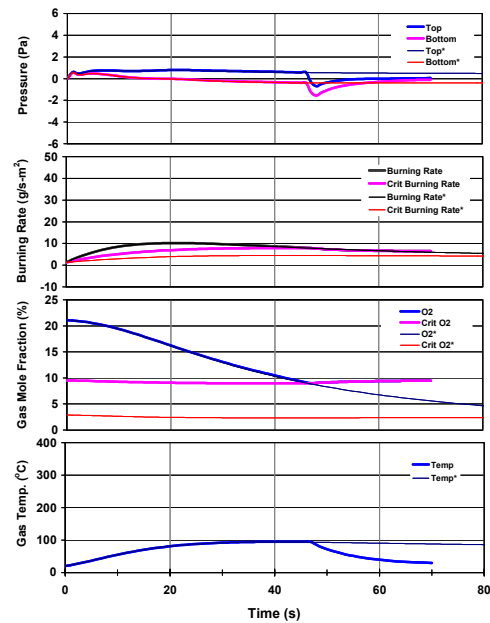
Test 95-3x1

Room Temp (°C) : 26.5 Initial Mass of Fuel (g) : 46.8
 Humidity (%) : 35.0 Final Mass of Fuel (g) : 39.3
 Fuel Pan Area (cm²) : 70.9 Mass Consumed (g) : 7.5
 Total Vent Area (cm²) : 6.0 Burn Time (s) : 57
 Category : 2

Experiment



Prediction



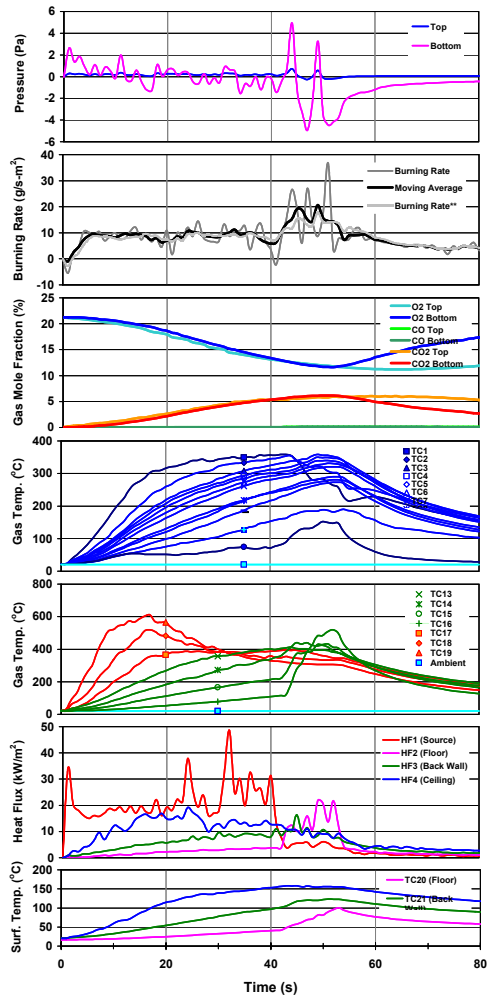
Ventilation Parameter ($\rho_0 g^{1/2} A_0 H^{1/2} / A_F$): 184 g/m²·s

Vertical Plume: 3 s
 Wind-Blown Flame: 13 s
 Blue Base Flame: 32 s
 Oscillation: 36 s
 Ghosting Flame: 40 s
 Extinction: 52 s

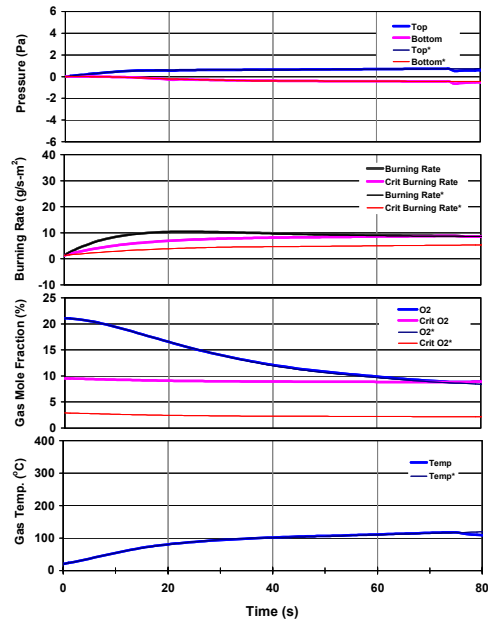
Test 95-3x3

Room Temp (°C) : 23.3
 Humidity (%) : 40.0
 Fuel Pan Area (cm²) : 70.9
 Total Vent Area (cm²) : 18.0
 Initial Mass of Fuel (g) : 47.9
 Final Mass of Fuel (g) : 24.4
 Mass Consumed (g) : 23.5
 Burn Time (s) : 53
 Category : 2

Experiment



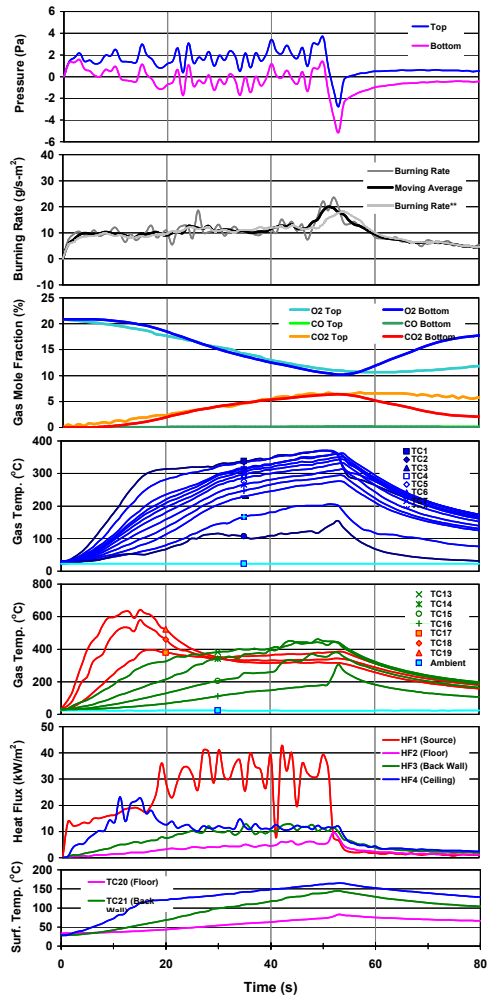
Prediction



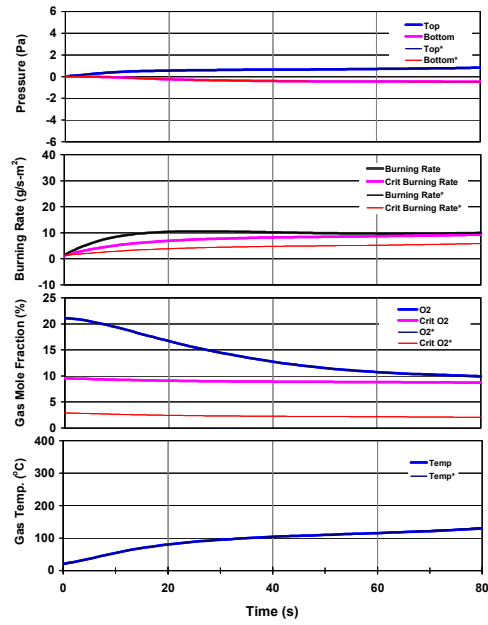
Test 95-3x4

Room Temp (°C) : 22.7 Initial Mass of Fuel (g) : 47.6
 Humidity (%) : 35.0 Final Mass of Fuel (g) : 31.3
 Fuel Pan Area (cm²) : 70.9 Mass Consumed (g) : 16.3
 Total Vent Area (cm²) : 24.0 Burn Time (s) : 53
 Category : 2

Experiment



Prediction



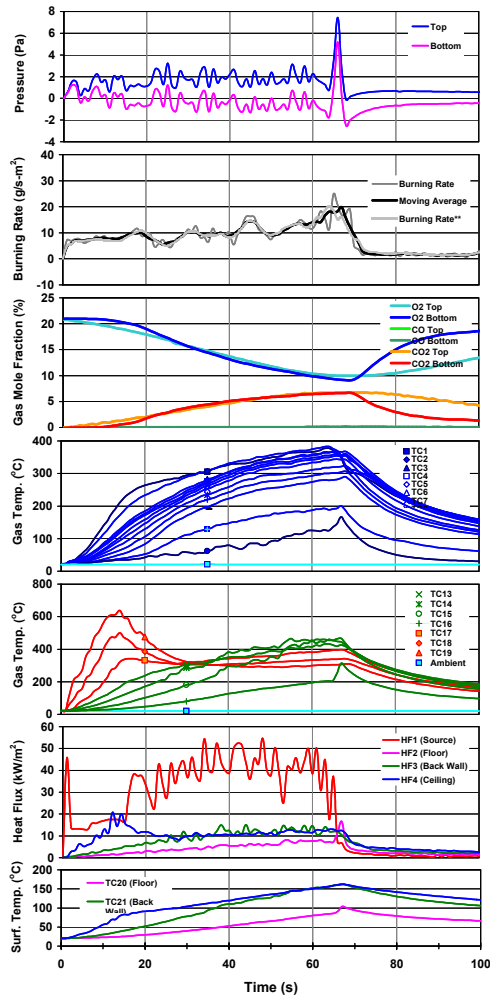
Ventilation Parameter ($\rho_0 g^{1/2} A_0 H^{1/2} / A_F$): 737 g/m²-s

Oscillation: 40 s
 Ghosting Flame: 51 s
 Extinction: 52 s

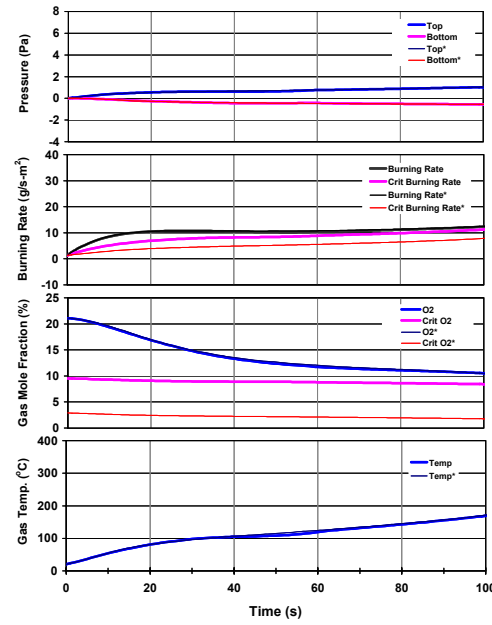
Test 95-3x5

Room Temp (°C) : 21.9 Initial Mass of Fuel (g) : 38.1
 Humidity (%) : 50.0 Final Mass of Fuel (g) : 26.4
 Fuel Pan Area (cm²) : 70.9 Mass Consumed (g) : 11.7
 Total Vent Area (cm²) : 30.0 Burn Time (s) : 126
 Category : 2

Experiment



Prediction

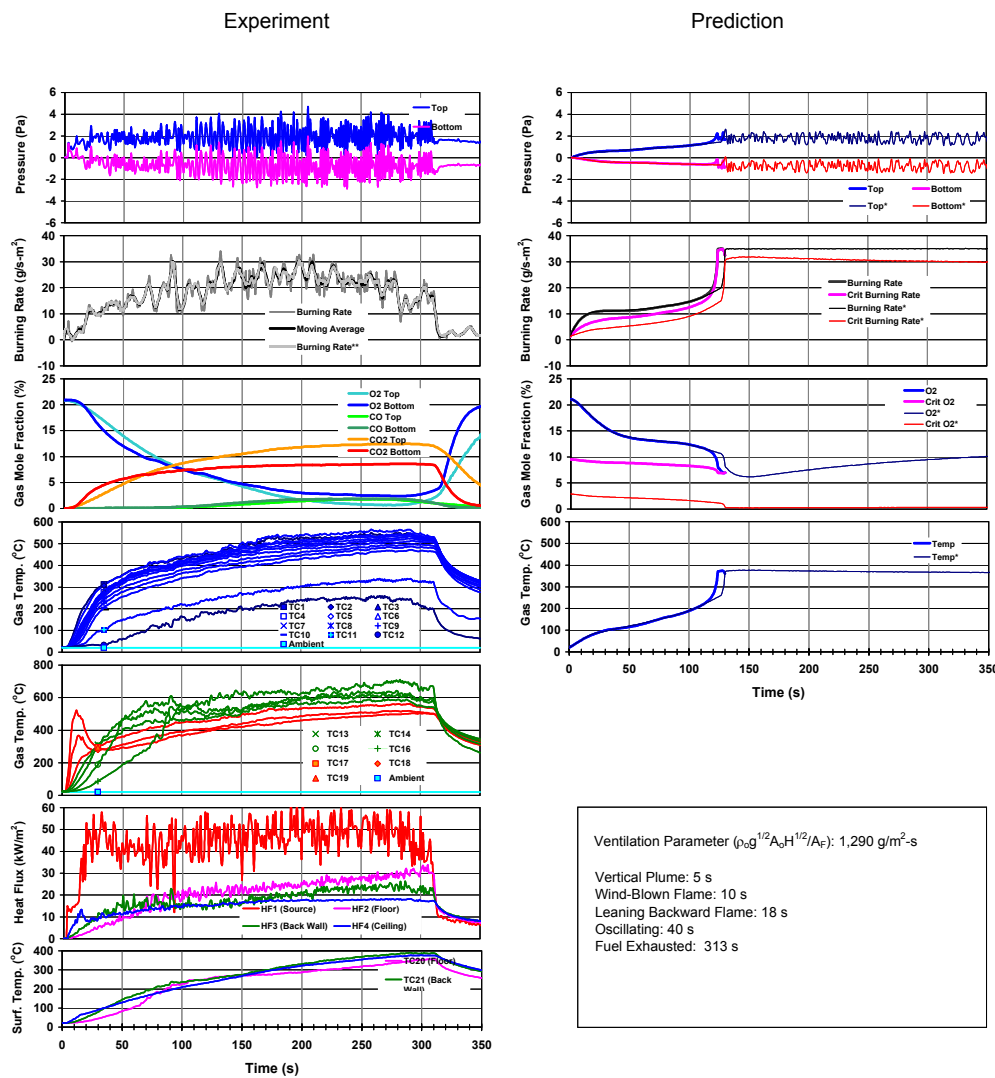


Ventilation Parameter ($\rho_0 g^{1/2} A_0 H^{1/2} / A_f$): 921 g/m²·s

Vertical Plume: 5 s
 Wind-Blown Flame: 14 s
 Oscillation: 25 s
 Ghosting Flame: 64 s
 Extinction: 66 s

Test 95-3x7

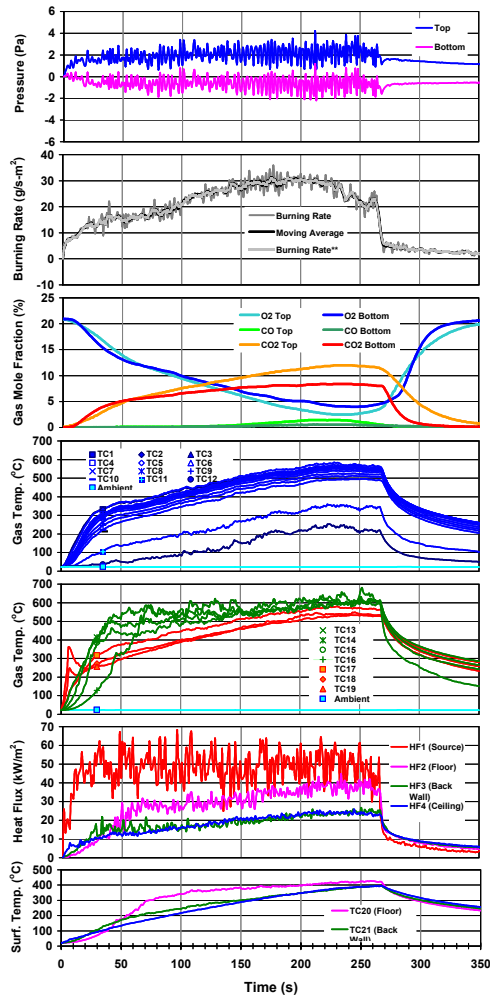
Room Temp (°C) : 20.6 Initial Mass of Fuel (g) : 46.7
 Humidity (%) : 50.0 Final Mass of Fuel (g) : 0.0
 Fuel Pan Area (cm²) : 70.9 Mass Consumed (g) : 46.7
 Total Vent Area (cm²) : 42.0 Burn Time (s) : 313
 Category : 4



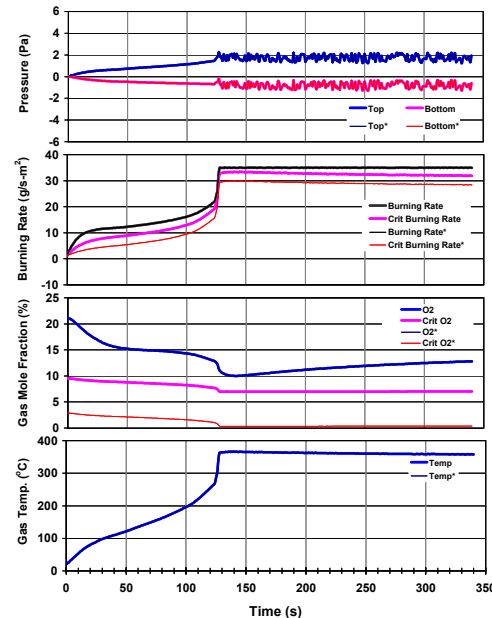
Test 95-3x10

Room Temp (°C) : 22.7 Initial Mass of Fuel (g) : 45.6
 Humidity (%) : 40.0 Final Mass of Fuel (g) : 0.0
 Fuel Pan Area (cm²) : 70.9 Mass Consumed (g) : 45.6
 Total Vent Area (cm²) : 60.0 Burn Time (s) : 271
 Category : 4

Experiment



Prediction



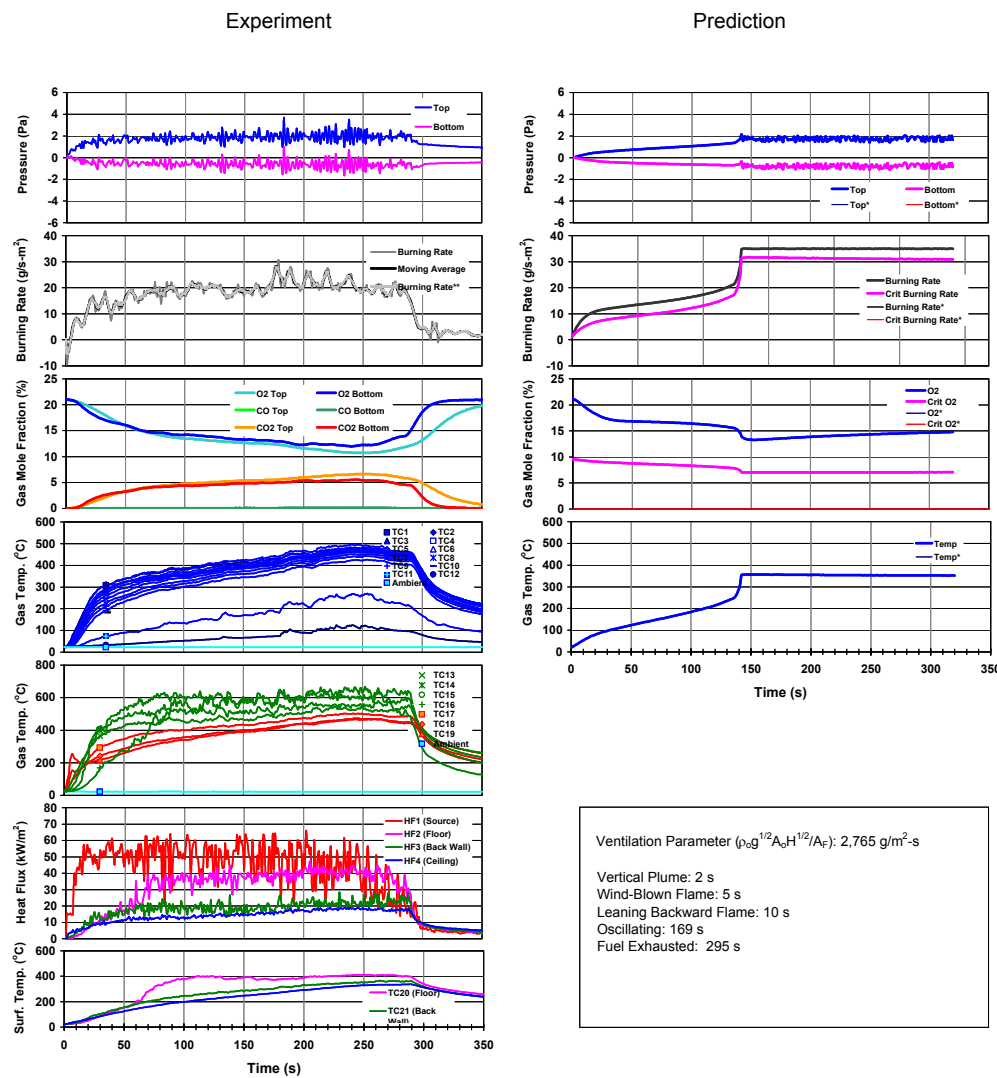
Ventilation Parameter ($\rho_0 g^{1/2} A_0 H^{1/2} / A_F$): 1,843 g/m²·s

Vertical Plume: 3 s
 Leaning Backward Flame: 10 s
 Oscillating: 108 s
 Fuel Exhausted: 271 s

Test 95-3x15

Room Temp (°C) : 22.9
 Humidity (%) : 35.0
 Fuel Pan Area (cm²) : 70.9
 Total Vent Area (cm²) : 30.0

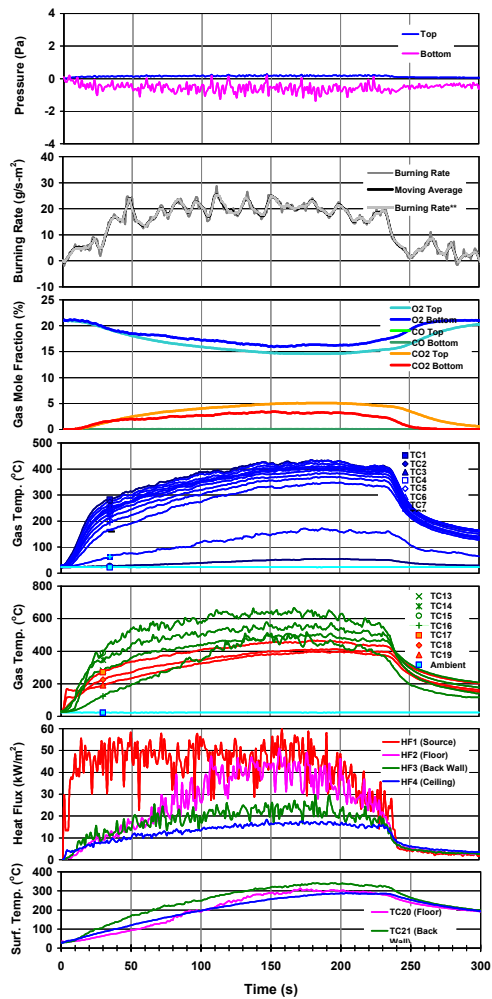
Initial Mass of Fuel (g) : 45.0
 Final Mass of Fuel (g) : 0.0
 Mass Consumed (g) : 45.0
 Burn Time (s) : 295
 Category : 4



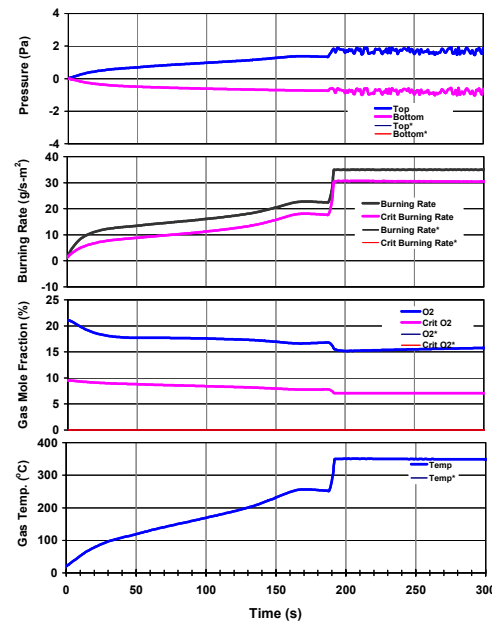
Test 95-3x20

Room Temp (°C) : 17.6 Initial Mass of Fuel (g) : 32.8
 Humidity (%) : 40.0 Final Mass of Fuel (g) : 0.0
 Fuel Pan Area (cm²) : 70.9 Mass Consumed (g) : 32.8
 Total Vent Area (cm²) : 120.0 Burn Time (s) : 237
 Category : 4

Experiment



Prediction

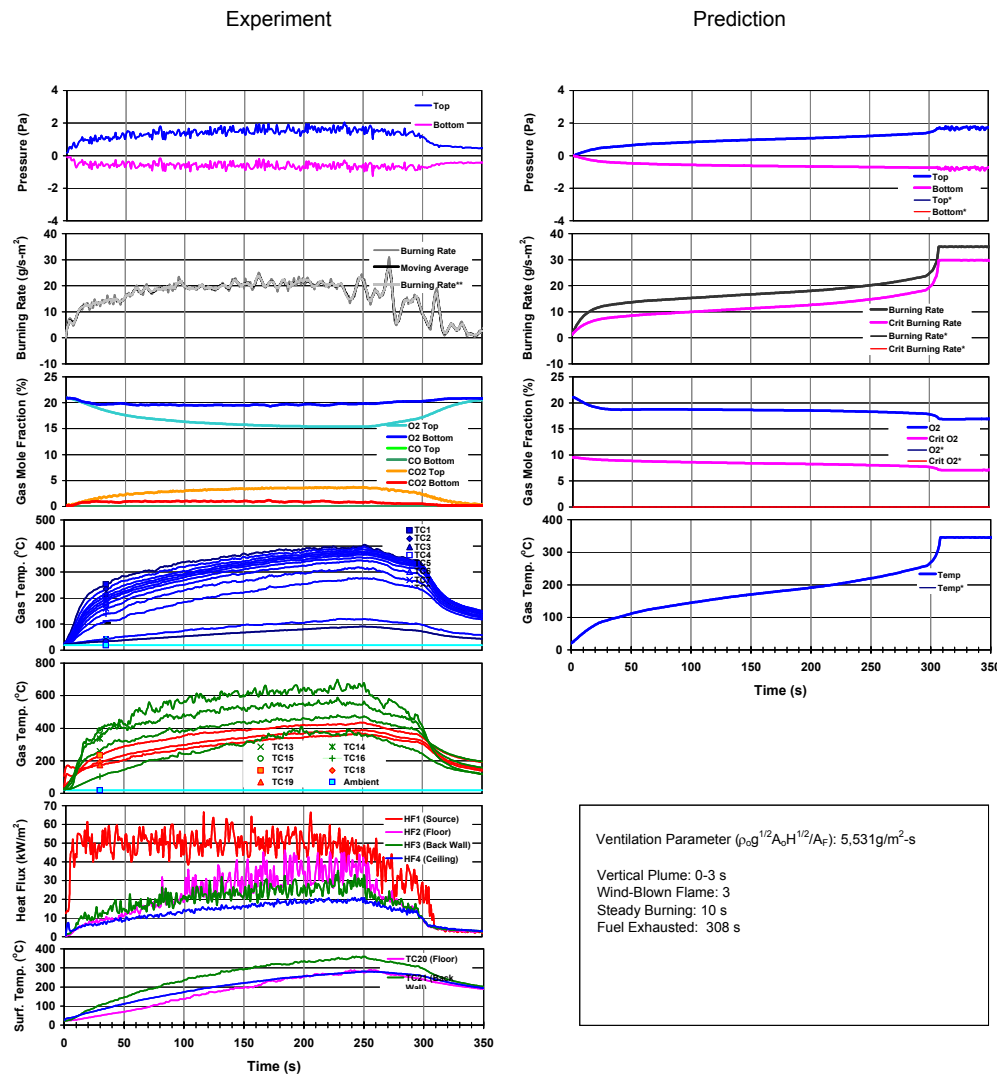


Ventilation Parameter ($\rho_0 g^{1/2} A_0 H^{1/2} / A_F$): 3,687 g/m²·s

Vertical Plume: 3 s
 Leaning Backward Flame: 10 s
 Steady Burning: 50 s
 Fuel Exhausted: 237 s

Test 95-3x30

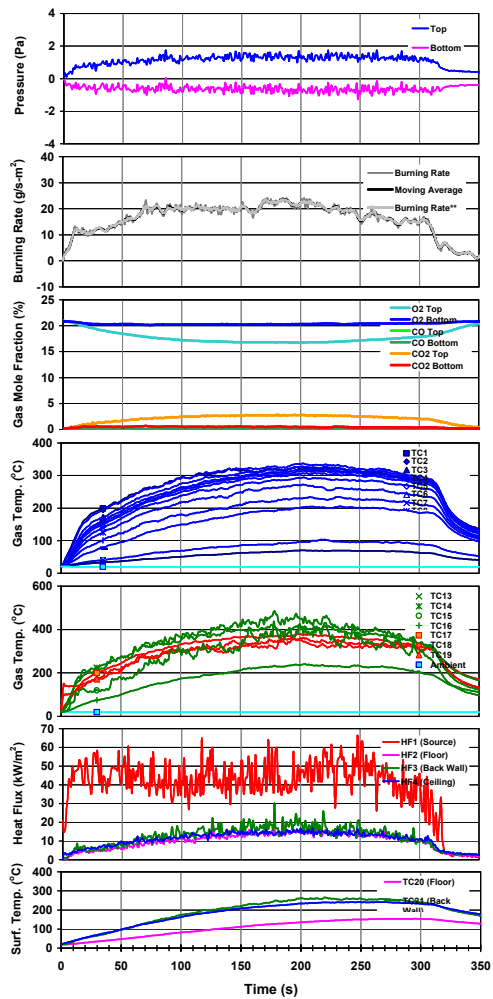
Room Temp (°C) : 20.8 Initial Mass of Fuel (g) : 44.5
 Humidity (%) : 40.0 Final Mass of Fuel (g) : 0.0
 Fuel Pan Area (cm²) : 70.9 Mass Consumed (g) : 44.5
 Total Vent Area (cm²) : 180.0 Burn Time (s) : 308
 Category : 4



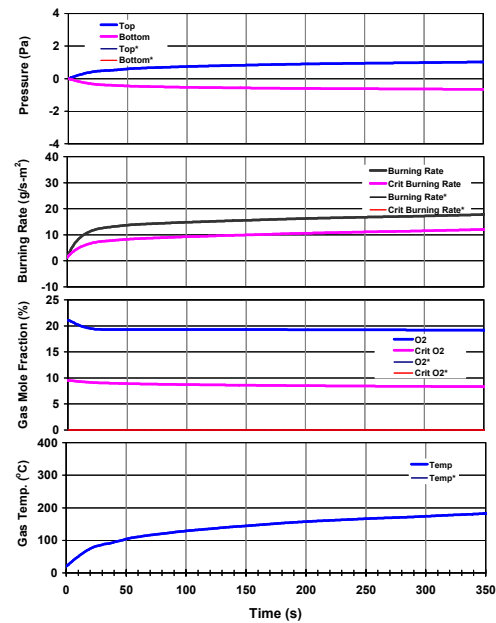
Test 95-3x40

Room Temp (°C) : 20.7 Initial Mass of Fuel (g) : 45.0
 Humidity (%) : 45.0 Final Mass of Fuel (g) : 0.0
 Fuel Pan Area (cm²) : 70.9 Mass Consumed (g) : 45.0
 Total Vent Area (cm²) : 240.0 Burn Time (s) : 322
 Category : 4

Experiment



Prediction



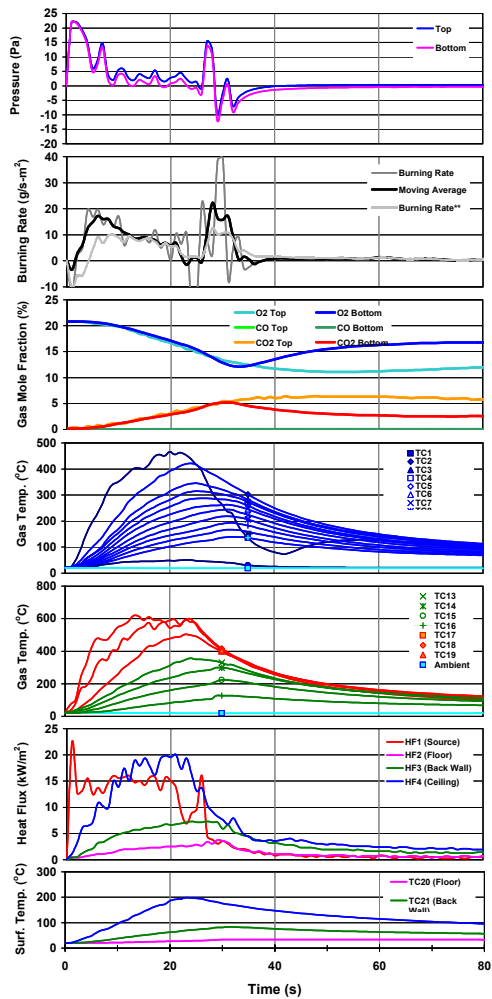
Ventilation Parameter ($\rho_0 g^{1/2} A_0 H^{1/2} / A_F$): 7,374 g/m²·s

Vertical Plume: 0-3 s
 Wind-Blown Flame: 3
 Steady Burning: 10 s
 Fuel Exhausted: 322 s

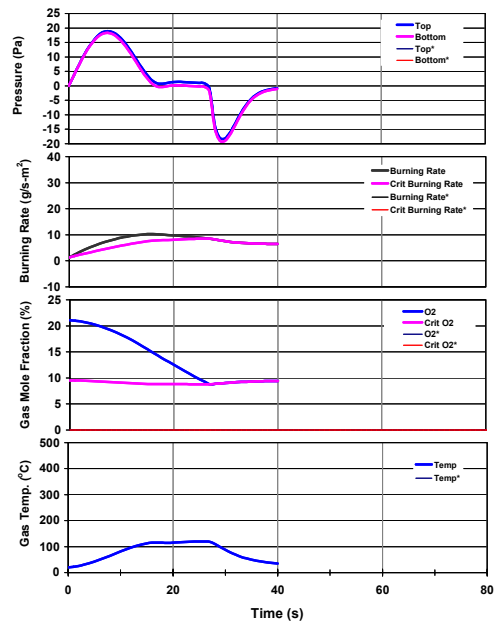
Test 120-1x1

Room Temp (°C) : 20.6 Initial Mass of Fuel (g) : 33.3
 Humidity (%) : 58.0 Final Mass of Fuel (g) : 24.4
 Fuel Pan Area (cm²) : 113.1 Mass Consumed (g) : 8.9
 Total Vent Area (cm²) : 2.0 Burn Time (s) : 33
 Category : 1

Experiment



Prediction



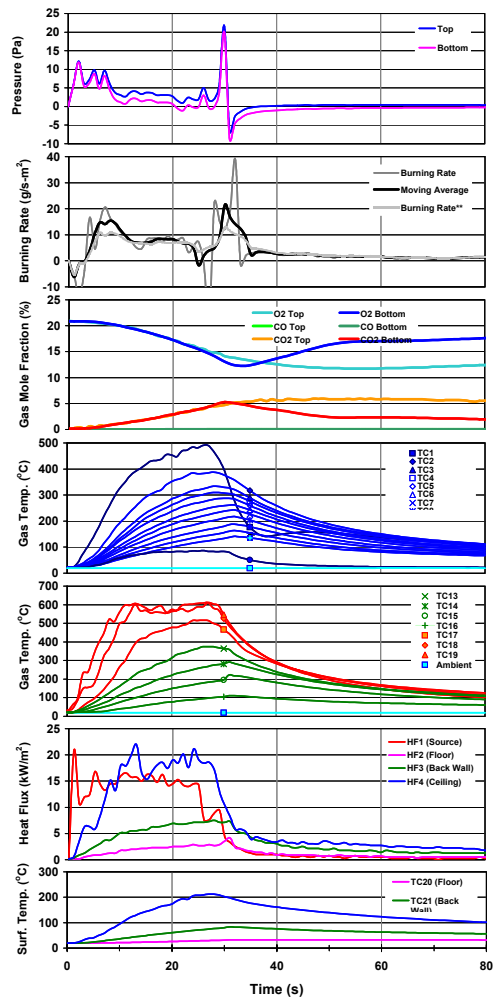
Ventilation Parameter ($\rho_0 \beta^{1/2} A_0 H^{1/2} / A_F$): 38 g/m²·s

Vertical Plume: 7 s
 Blue Base Flame: 15 s
 Shrinking Flame: 20 s
 Ghosting Flame: 27 s
 Extinction: 31 s

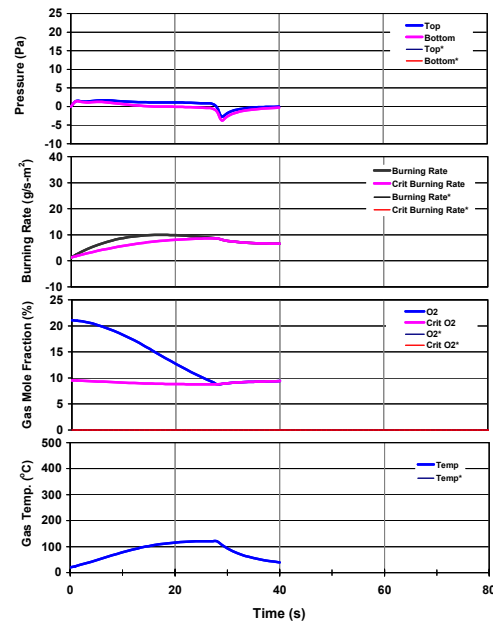
Test 120-1x3

Room Temp (°C) : 20.6 Initial Mass of Fuel (g) : 42.3
 Humidity (%) : 58.0 Final Mass of Fuel (g) : 33.9
 Fuel Pan Area (cm²) : 113.1 Mass Consumed (g) : 8.4
 Total Vent Area (cm²) : 6.0 Burn Time (s) : 31
 Category : 1

Experiment



Prediction



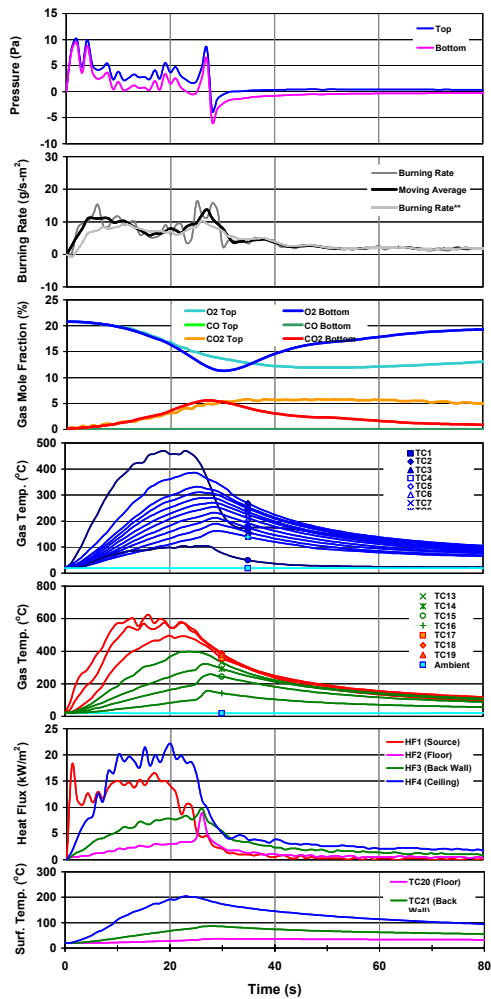
Ventilation Parameter ($\rho_0 g^{1/2} A_0 H^{1/2} / A_F$): 115 g/m²·s

Vertical Plume: 5 s
 Blue Base Flame: 18 s
 Shrinking Flame: 22 s
 Ghosting Flame: 28 s
 Extinction: 30 s

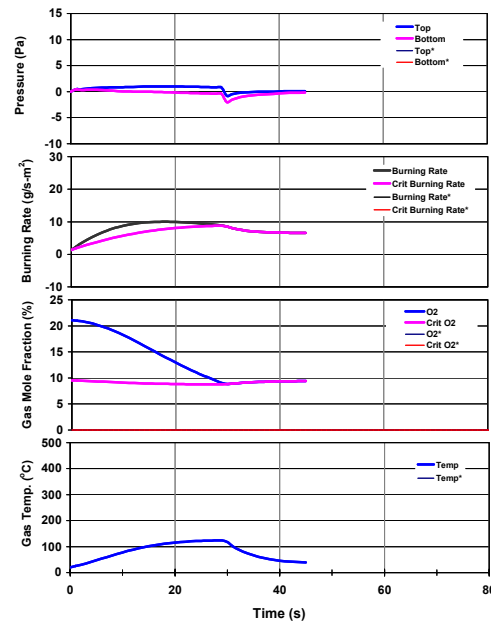
Test 120-1x5

Room Temp (°C) : 20.6
 Humidity (%) : 58.0
 Fuel Pan Area (cm²) : 113.1
 Total Vent Area (cm²) : 10.0
 Initial Mass of Fuel (g) : 38.6
 Final Mass of Fuel (g) : 26.6
 Mass Consumed (g) : 12.0
 Burn Time (s) : 28
 Category : 2

Experiment



Prediction



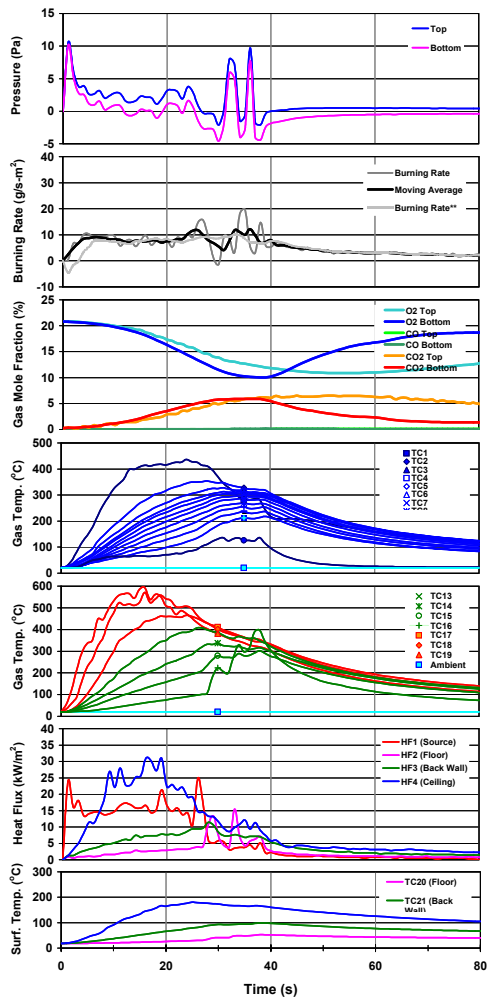
Ventilation Parameter ($\rho_0 g^{1/2} A_0 H^{1/2} / A_F$): 192 g/m²·s

Vertical Plume: 6 s
 Wind Blown Flame: 18 s
 Shrinking Flame: 20 s
 Ghosting Flame: 24 s
 Extinction: 28 s

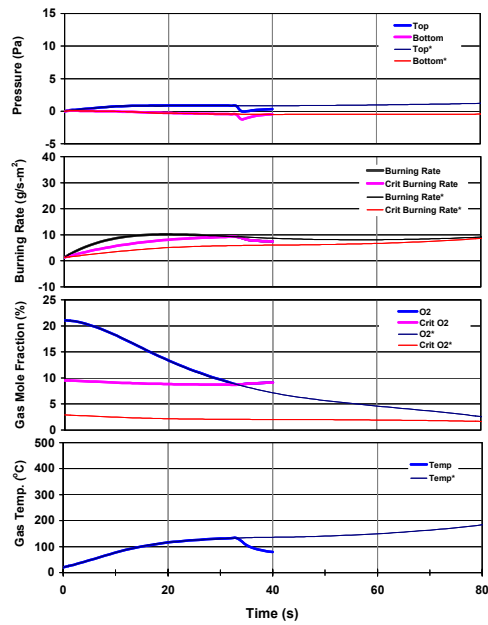
Test 120-1x9

Room Temp (°C) : 20.6 Initial Mass of Fuel (g) : 61.5
 Humidity (%) : 58.0 Final Mass of Fuel (g) : 48.8
 Fuel Pan Area (cm²) : 113.1 Mass Consumed (g) : 12.7
 Total Vent Area (cm²) : 18.0 Burn Time (s) : 39
 Category : 2

Experiment



Prediction



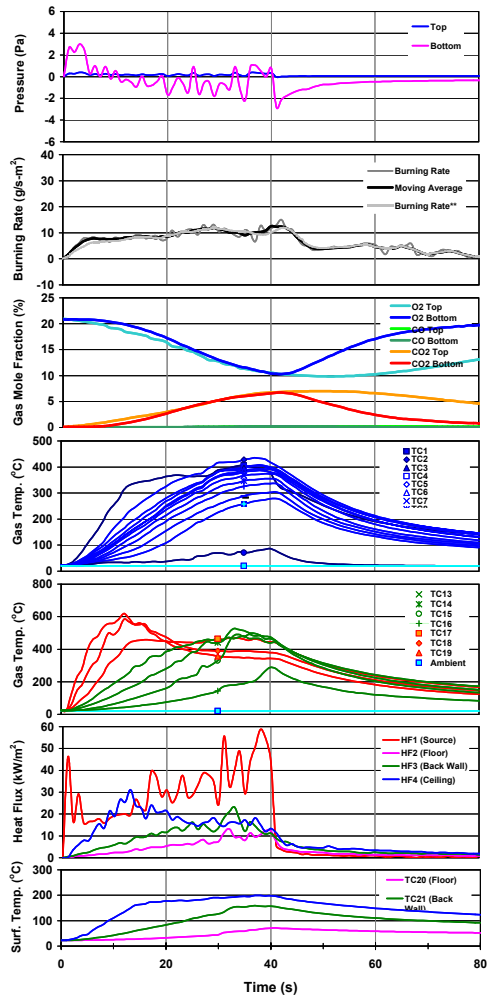
Ventilation Parameter ($\rho_0 g^{1/2} A_0 H^{1/2} / A_F$): 346 g/m²·s

Vertical Plume: 3 s
 Wind Blown Flame: 13 s
 Oscillating: 22 s
 Ghosting Flame: 27 s
 Extinction: 37 s

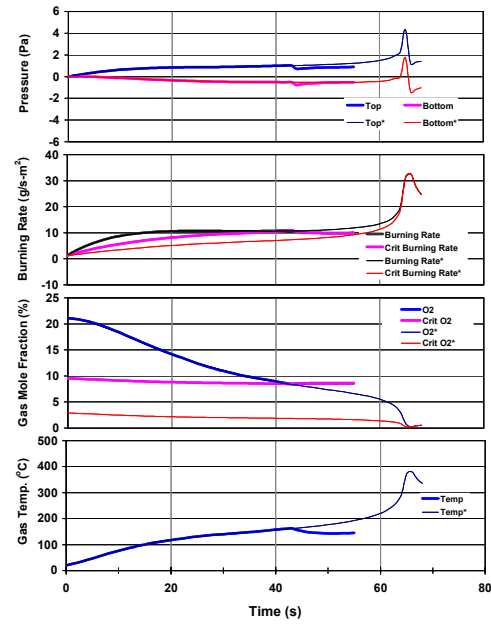
Test 120-1x15

Room Temp (°C) : 22.9 Initial Mass of Fuel (g) : 40.7
 Humidity (%) : 72.0 Final Mass of Fuel (g) : 13.0
 Fuel Pan Area (cm²) : 113.1 Mass Consumed (g) : 27.7
 Total Vent Area (cm²) : 30.0 Burn Time (s) : 41
 Category : 2

Experiment



Prediction



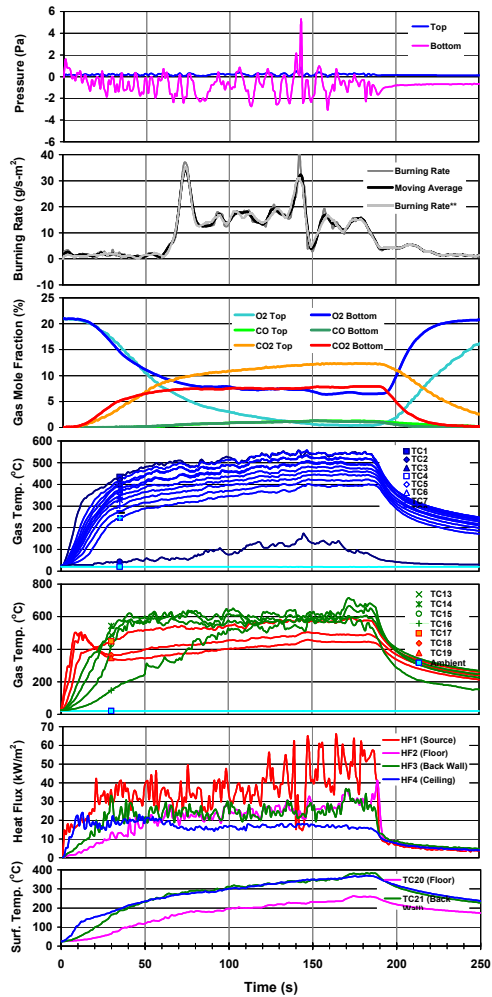
Ventilation Parameter ($\rho_0 g^{1/2} A_0 H^{1/2} / A_F$): 577 g/m²·s

Vertical Plume: 6 s
 Wind Blown Flame: 10 s
 Oscillating: 18 s
 Ghosting Flame: 20 s
 Oscillating: 28 s
 Extinction: 41 s

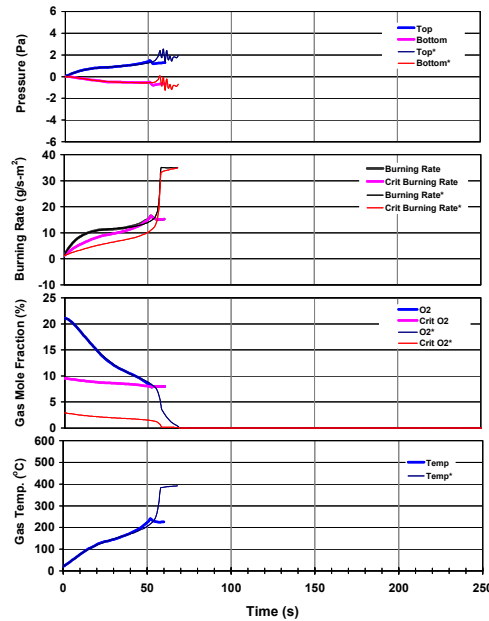
Test 120-1x21

Room Temp (°C) : 20.3 Initial Mass of Fuel (g) : 31.2
 Humidity (%) : 72.0 Final Mass of Fuel (g) : 0.0
 Fuel Pan Area (cm²) : 113.1 Mass Consumed (g) : 31.2
 Total Vent Area (cm²) : 42.0 Burn Time (s) : 191
 Category : 1

Experiment



Prediction



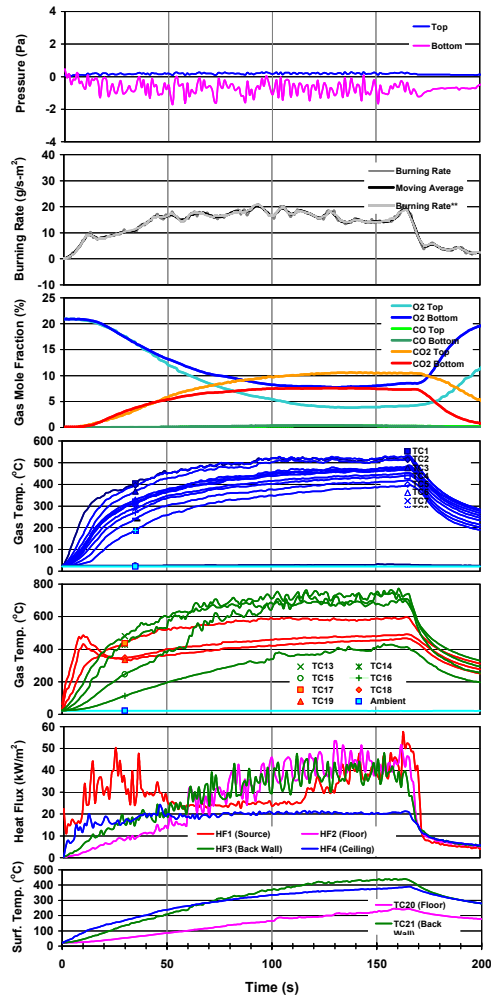
Ventilation Parameter ($\rho_0 g^{1/2} A_0 H^{1/2} / A_F$): 808 g/m²·s

Vertical Plume: 4 s
 Wind Blown Flame: 10 s
 Leaning Backward Flame: 20 s
 Oscillating: 60 s
 Fuel Exhausted: 191 s

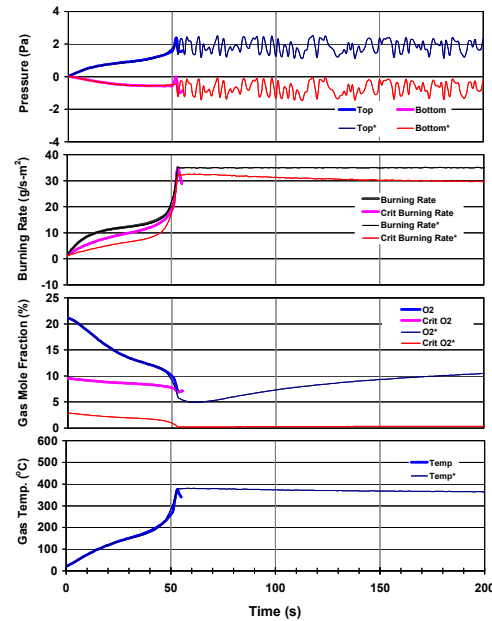
Test 120-1x30

Room Temp (°C) : 22.0 Initial Mass of Fuel (g) : 32.5
 Humidity (%) : 72.0 Final Mass of Fuel (g) : 0.0
 Fuel Pan Area (cm²) : 113.1 Mass Consumed (g) : 32.5
 Total Vent Area (cm²) : 60.0 Burn Time (s) : 172
 Category : 4

Experiment



Prediction



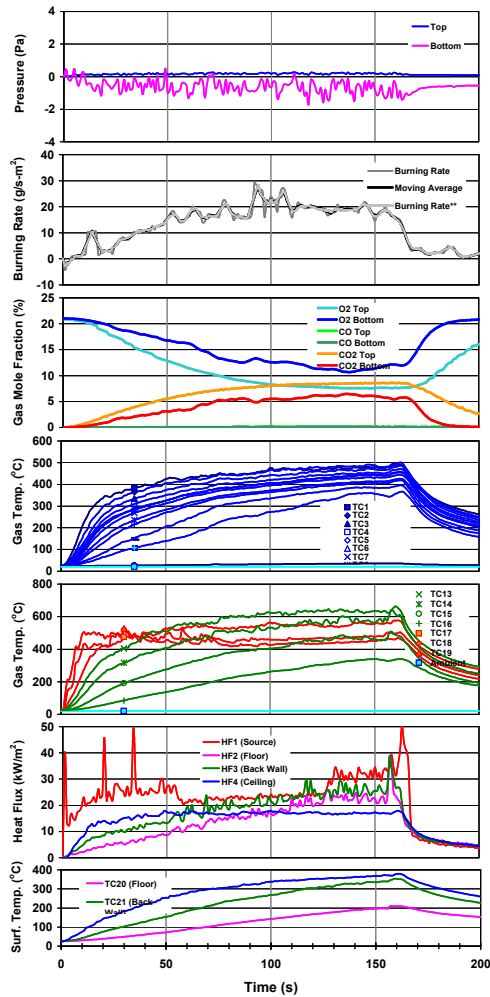
Ventilation Parameter ($\rho_0 g^{1/2} A_0 H^{1/2} / A_F$): 1155 g/m²-s

Vertical Plume: 3 s
 Wind Blown Flame: 12 s
 Leaning Backward and Puffing: 30 s
 Some Oscillating Occurred: 130 s
 Fuel Exhausted: 172 s

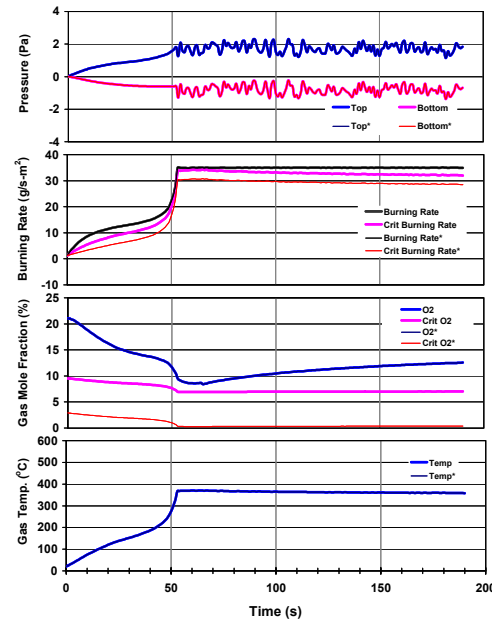
Test 120-1x40

Room Temp (°C) : 23.7 Initial Mass of Fuel (g) : 30.8
 Humidity (%) : 72.0 Final Mass of Fuel (g) : 0.0
 Fuel Pan Area (cm²) : 113.1 Mass Consumed (g) : 30.8
 Total Vent Area (cm²) : 80.0 Burn Time (s) : 166
Category : 4

Experiment



Prediction



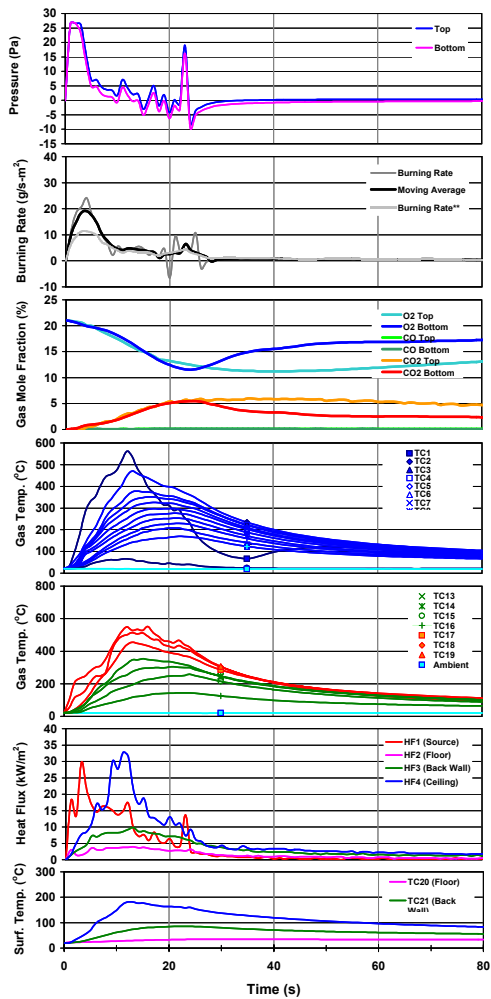
Ventilation Parameter ($\rho_0 g^{1/2} A_0 H^{1/2} / A_F$): 1540 g/m²·s

Vertical Plume: 6 s
 Wind Blown Flame: 20 s
 Leaning Backward and Puffing: 60 s
 Some Oscillating Occurred: 120 s
 Fuel Exhausted: 166 s

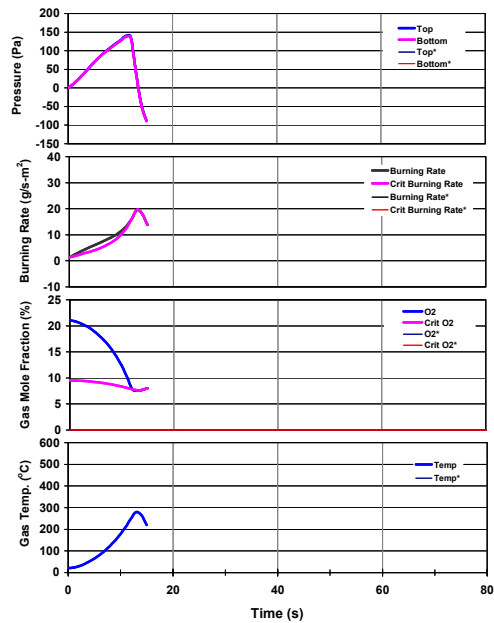
Test 190-1x1

Room Temp (°C) : 20.4 Initial Mass of Fuel (g) : 106.5
 Humidity (%) : 56.0 Final Mass of Fuel (g) : 36.9
 Fuel Pan Area (cm²) : 283.6 Mass Consumed (g) : 69.6
 Total Vent Area (cm²) : 2.0 Burn Time (s) : 23
 Category : 1

Experiment



Prediction



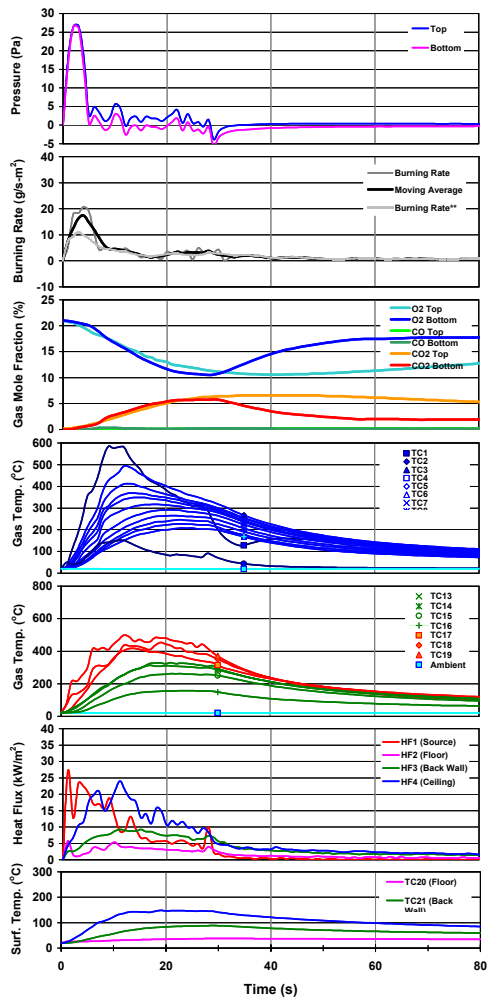
Ventilation Parameter ($\rho_0 g^{1/2} A_0 H^{1/2} / A_f$): 15 g/m²·s

Vertical Plume: 3 s
 Blue Base Flame: 9 s
 Shrinking Flame: 11 s
 Extinction: 23 s

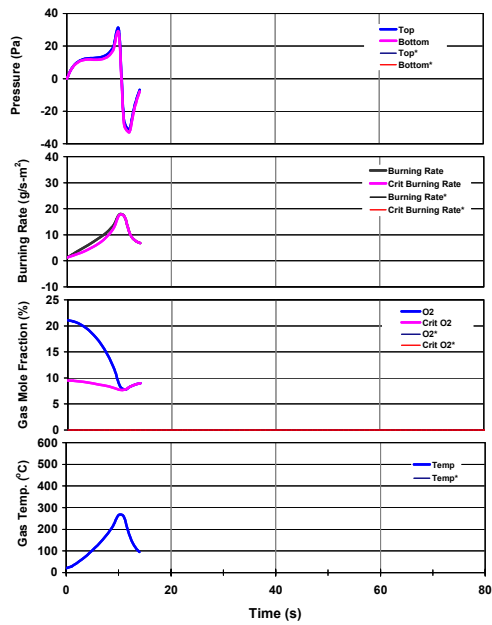
Test 190-1x3

Room Temp (°C) : 21.3 Initial Mass of Fuel (g) : 115.9
 Humidity (%) : 56.0 Final Mass of Fuel (g) : 99.6
 Fuel Pan Area (cm²) : 283.6 Mass Consumed (g) : 16.3
 Total Vent Area (cm²) : 6.0 Burn Time (s) : 29
 Category : 1

Experiment



Prediction



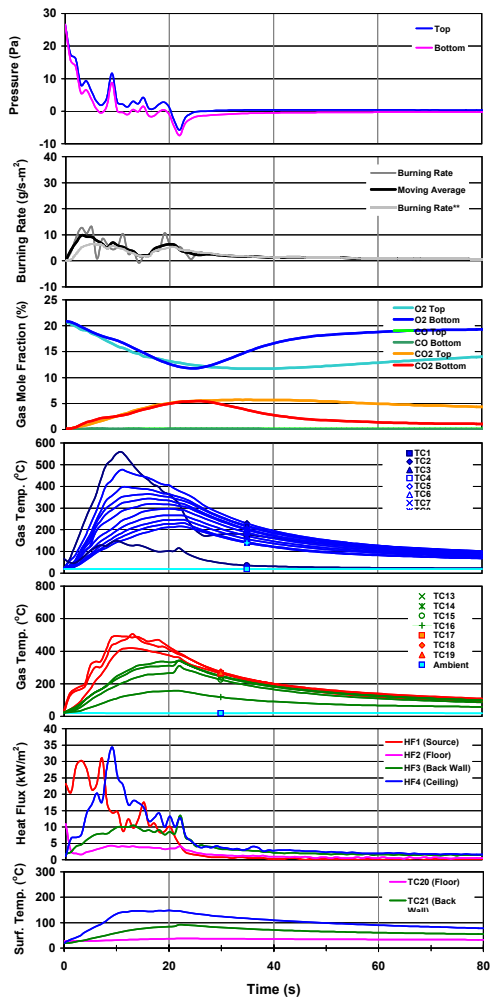
Ventilation Parameter ($\rho_0 g^{1/2} A_0 H^{1/2} / A_f$): 46 g/m²-s

Vertical Plume: 3 s
 Blue Base Flame: 9 s
 Shrinking Flame: 11 s
 Oscillating: 13 s
 Extinction: 27 s

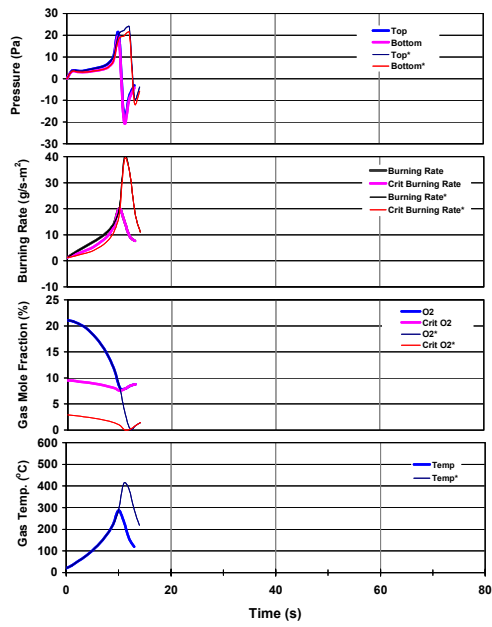
Test 190-1x5

Room Temp (°C) : 20.1 Initial Mass of Fuel (g) : 76.5
 Humidity (%) : 56.0 Final Mass of Fuel (g) : 62.8
 Fuel Pan Area (cm²) : 283.6 Mass Consumed (g) : 13.7
 Total Vent Area (cm²) : 10.0 Burn Time (s) : 25
Category : 2

Experiment



Prediction



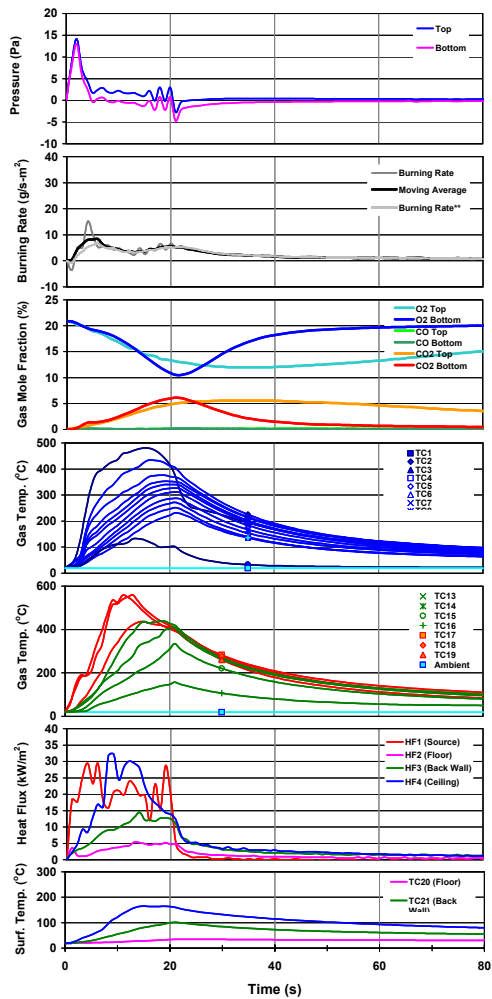
Ventilation Parameter ($\rho_0 \beta^{1/2} A_0 H^{1/2} / A_F$): 76 g/m²·s

Vertical Plume: 7 s
 Wind Blown Flame: 9 s
 Oscillating: 11 s
 Ghosting Flame: 21 s
 Extinction: 23 s

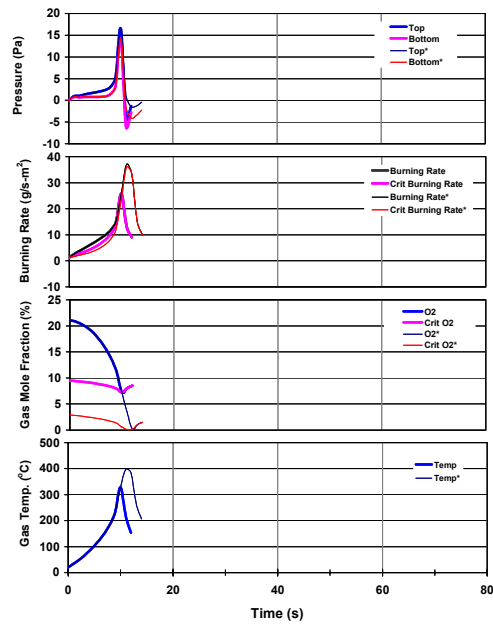
Test 190-1x9

Room Temp (°C) : 20.1 Initial Mass of Fuel (g) : 112.4
 Humidity (%) : 56.0 Final Mass of Fuel (g) : 92.8
 Fuel Pan Area (cm²) : 283.6 Mass Consumed (g) : 19.6
 Total Vent Area (cm²) : 18.0 Burn Time (s) : 17
 Category : 2

Experiment



Prediction



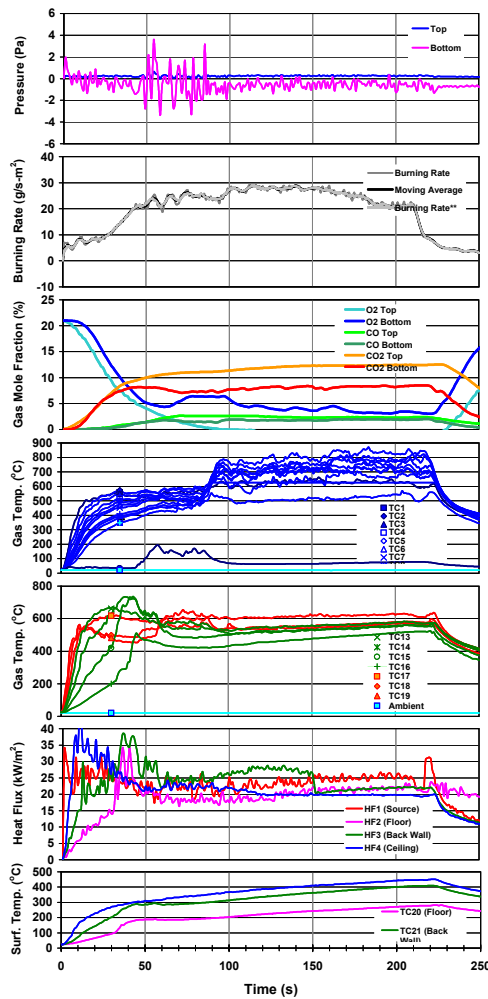
Ventilation Parameter ($\rho_0 g^{1/2} A_0 H^{1/2} / A_F$): 138 g/m²·s

Vertical Plume: 4 s
 Wind Blown Flame: 9 s
 Blue Base Flame: 11 s
 Oscillating Flame: 13 s
 Extinction: 20 s

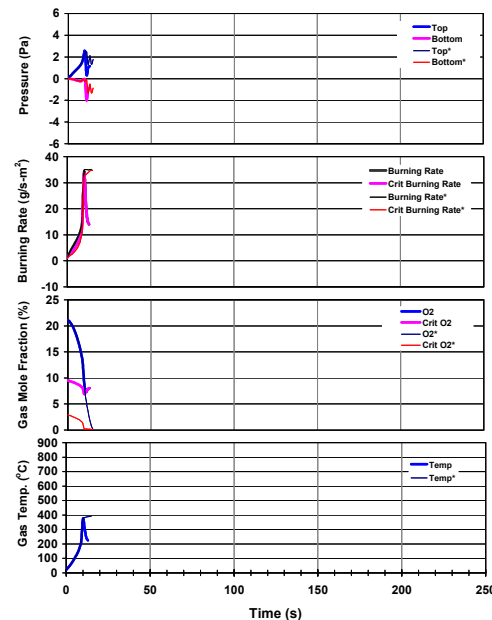
Test 190-1x40

Room Temp (°C) : 23.7 Initial Mass of Fuel (g) : 141.0
 Humidity (%) : 50.0 Final Mass of Fuel (g) : 0.0
 Fuel Pan Area (cm²) : 283.6 Mass Consumed (g) : 141.0
 Total Vent Area (cm²) : 80.0 Burn Time (s) : 230
 Category : 3

Experiment



Prediction



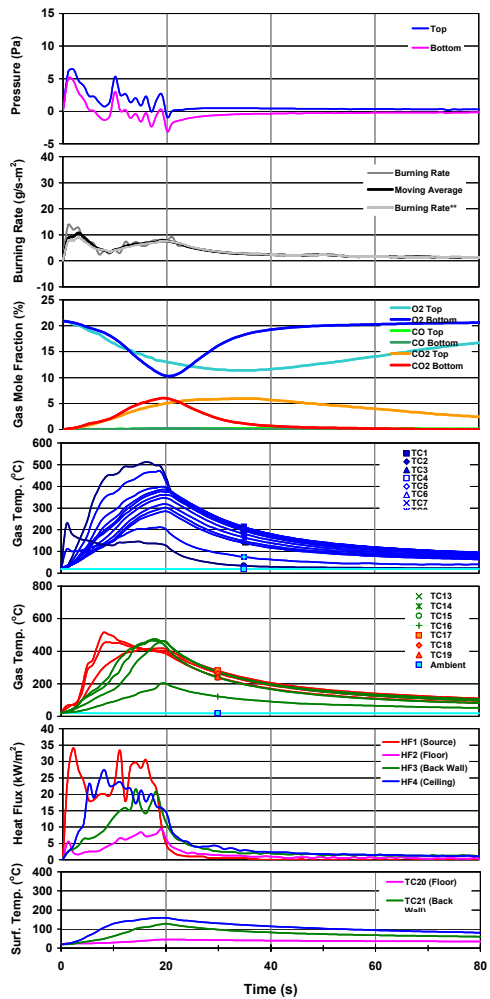
Ventilation Parameter ($\rho_0 g^{1/2} A_0 H^{1/2} / A_F$): 614 g/m²·s

Vertical Plume: 0-7 s
 Wind Blown Flame: 16 s
 Leaning Backward Flame with Puffing: 18 s
 Oscillating Flame: 46 s
 Moving to Vent with Oscillating: 58 s
 Burning at Vent: 82 s

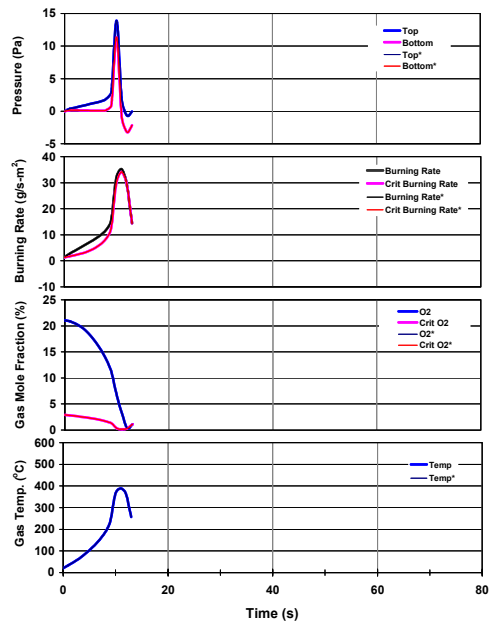
Test 190-3x5

Room Temp (°C) : 20.8 Initial Mass of Fuel (g) : 126.9
 Humidity (%) : 58.0 Final Mass of Fuel (g) : 90.3
 Fuel Pan Area (cm²) : 283.6 Mass Consumed (g) : 36.6
 Total Vent Area (cm²) : 30.0 Burn Time (s) : 15
 Category : 2

Experiment



Prediction



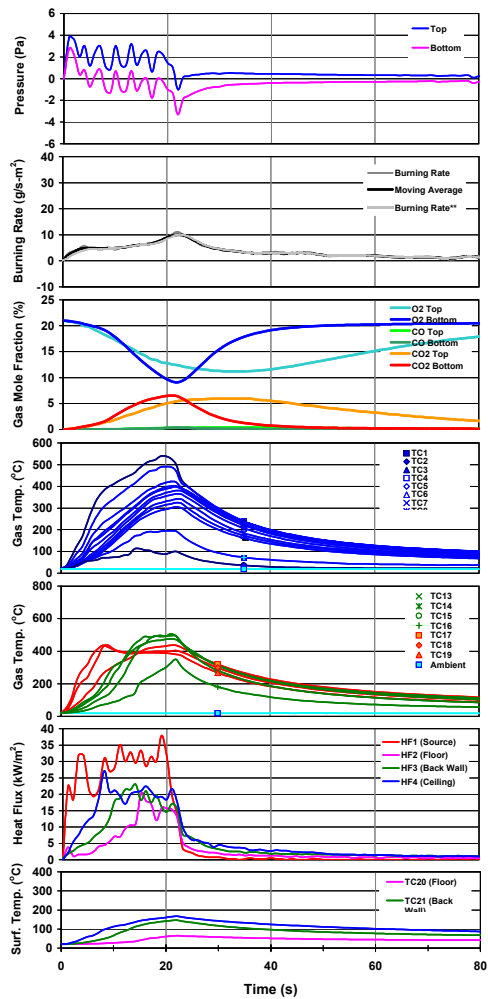
Ventilation Parameter ($\rho_0 g^{1/2} A_0 H^{1/2} / A_F$): 230 g/m²-s

Vertical Plume: 8 s
 Oscillating: 10 s
 Extinction: 19 s

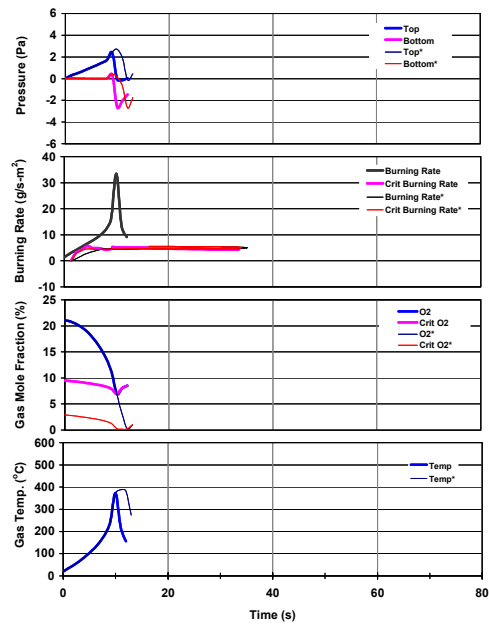
Test 190-3x7

Room Temp (°C) : 19.1 Initial Mass of Fuel (g) : 103.3
 Humidity (%) : 58.0 Final Mass of Fuel (g) : 72.4
 Fuel Pan Area (cm²) : 283.6 Mass Consumed (g) : 30.9
 Total Vent Area (cm²) : 42.0 Burn Time (s) : 23
Category : 2

Experiment



Prediction



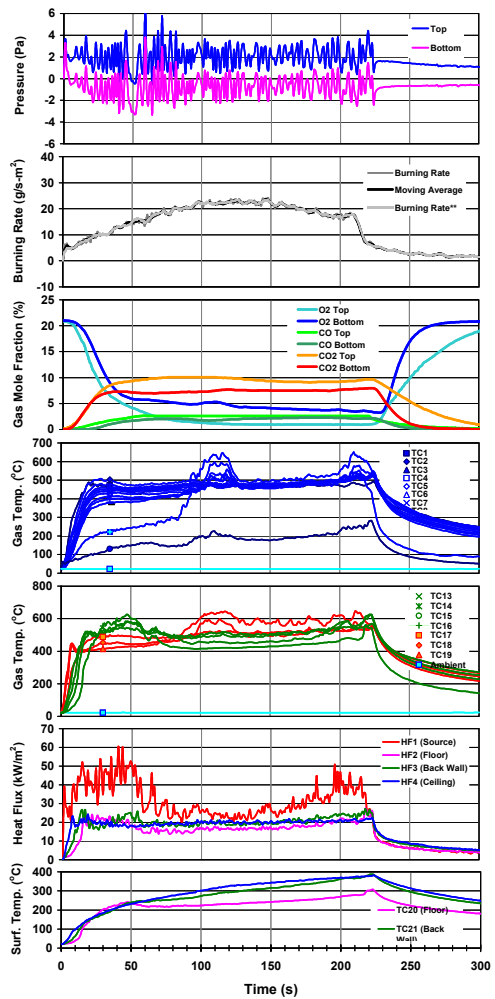
Ventilation Parameter ($\rho_0 g^{1/2} A_0 H^{1/2} / A_F$): 322 g/m²·s

Vertical Plume: 3 s
Oscillating: 7 s
Extinction: 21 s

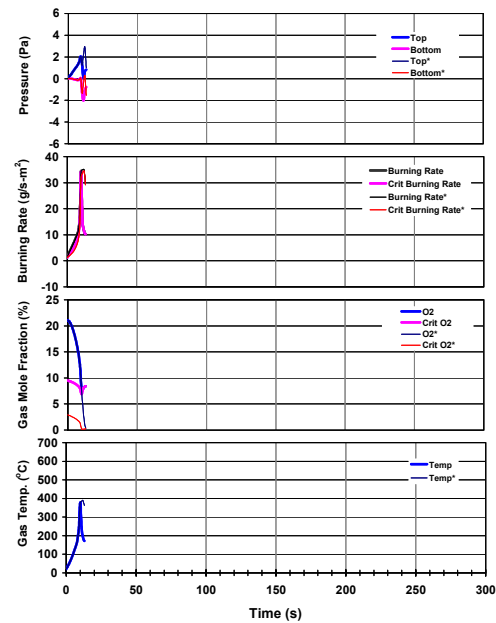
Test 190-3x10

Room Temp (°C) : 23.4
 Humidity (%) : 38.0
 Fuel Pan Area (cm²) : 283.6
 Total Vent Area (cm²) : 60.0
 Initial Mass of Fuel (g) : 109.6
 Final Mass of Fuel (g) : 0.0
 Mass Consumed (g) : 109.6
 Burn Time (s) : 228
 Category : 3

Experiment



Prediction



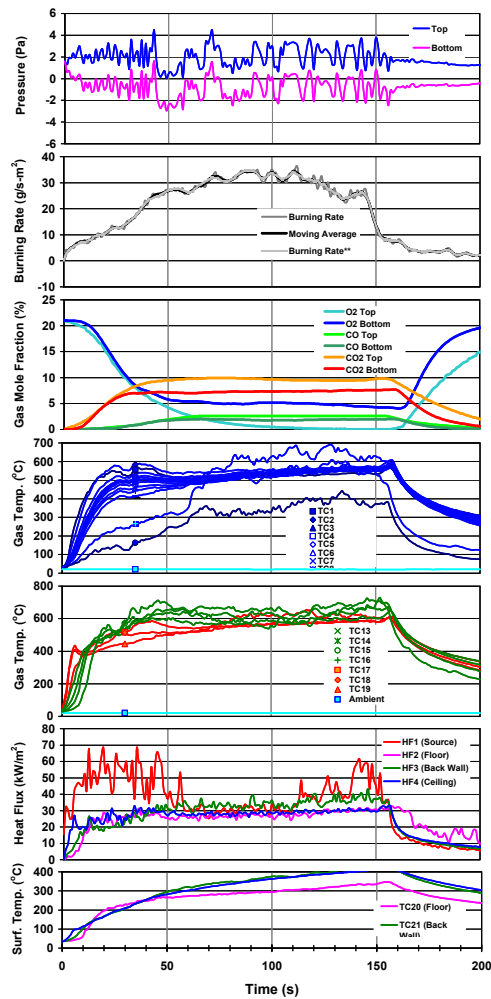
Ventilation Parameter ($\rho_0 g^{1/2} A_0 H^{1/2} / A_F$): 460 g/m²·s

Vertical Plume: 3 s
 Oscillating: 10 s
 Moving to Vent with Oscillating: 52 s
 Burning at Vent with Oscillating: 59 s
 Fuel Exhausted: 228 s

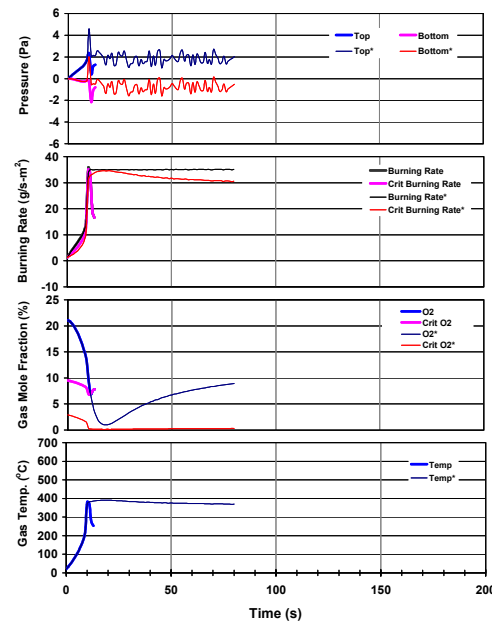
Test 190-3x15

Room Temp (°C) : 22.9
 Humidity (%) : 38.0
 Fuel Pan Area (cm²) : 283.6
 Total Vent Area (cm²) : 90.0
 Initial Mass of Fuel (g) : 109.0
 Final Mass of Fuel (g) : 0.0
 Mass Consumed (g) : 109.0
 Burn Time (s) : 161
 Category : 3

Experiment



Prediction



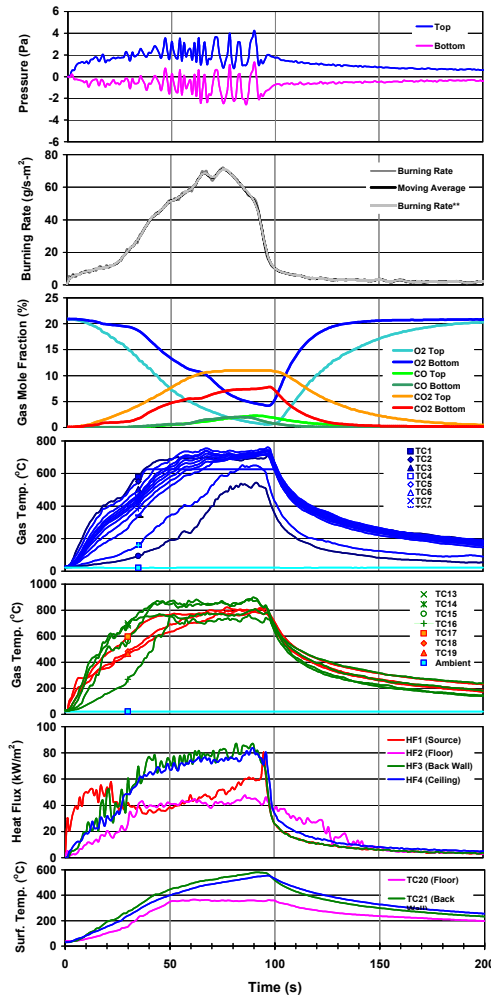
Ventilation Parameter ($\rho_0 g^{1/2} A_0 H^{1/2} / A_F$): 691 g/m²-s

Vertical Plume: 2 s
 Wind Blown Flame: 4 s
 Oscillating: 6 s
 Moving to Lower Vent with Oscillating: 43 s
 Burning at Lower Vent with Oscillating: 54 s
 Fuel Exhausted: 161 s

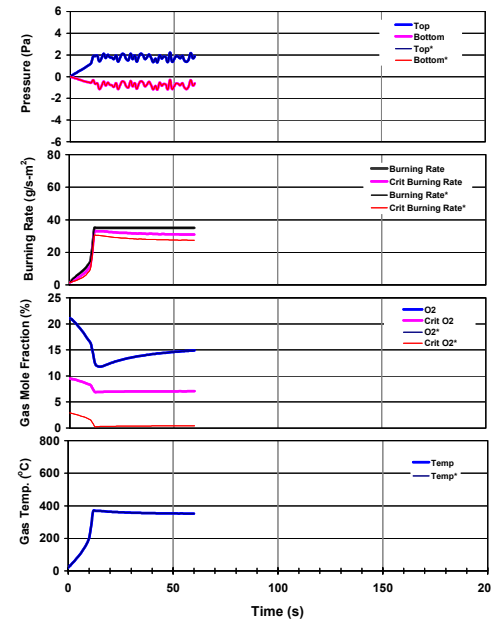
Test 190-3x40

Room Temp (°C) : 21.6 Initial Mass of Fuel (g) : 116.4
 Humidity (%) : 38.0 Final Mass of Fuel (g) : 0.0
 Fuel Pan Area (cm²) : 283.6 Mass Consumed (g) : 116.4
 Total Vent Area (cm²) : 240.0 Burn Time (s) : 130
 Category : 3

Experiment



Prediction



Ventilation Parameter ($\rho_0 g^{1/2} A_0 H^{1/2} / A_F$): 1843 g/m²·s

Vertical Plume: 0-3 s
 Wind Blown Flame: 3 s
 Steady Burning(Leaning Backward): 9 s
 Oscillating: 40 s
 Burning at Lower Vent with Oscillating: 50 s
 Fuel Exhausted: 130 s

REFERENCE

1. Ringwelski, B. A., "Low Ventilation Small-Scale Compartment Fire Phenomena: Ceiling Vents", MS Thesis, Dept. of Fire protection Engineering, University of Maryland, College Park, MD, (2001).
2. Wakatsuki, K., "Low Ventilation Small-Scale Compartment Fire Phenomena: Ceiling Vents", MS Thesis, Dept. of Fire Prot. Engineering, Univ. of Maryland, College Park, MD, 2001.
3. Takeda, H. and Akita, K., "Critical Phenomenon in Compartment Fires with Liquid Fuels", Proc. Combust. Inst., 18, 1980, pp. 519-527.
4. Tewarson, A., "Some Observations on Experimental Fires in Enclosures, Part II - Ethyl Alcohol and Paraffin Oil", Combustion and Flame 19, 1972, pp. 363-371.
5. Kim, I.K., Ohtani, H., and Uehara, Y., "Experimental Study on Oscillating Behaviour in a Small-Scale Compartment Fire", Short Communication, Fire Safety Journal, 20, 1993, pp. 377-384.
6. Rangwala A.S., "Mathematical Modeling of Low Ventilation Compartment Fires", M.S. Thesis, University of Maryland, College Park, MD (2002).
7. Quintiere, J. G., "Fire Behaviour in Building Compartments", Proc. Combust. Inst., 29, 2002, pp. 181-193.
8. Quintiere, J.G. and Rangwala A.S., "A Theory for Flame Extinction Base on Flame Temperature", Fire and Materials 2003 8th International Conference, San Francisco, January 27-28 (2003).
9. Wakatsuki, K., Ringwelski B. and Quintiere J.G., "Fire Behavior in a Poorly Ventilated Compartment", Department of Fire Protection Engineering, University of Maryland, College Park, MD.
10. Bullen, M. L, and Thomas, P. H., "Compartment Fires with Non-Cellulosic Fuels", Proc. Combust. Inst., 17, 1978, pp. 1139-1148.
11. Bertin, G., Most, J., and Coutin, M., "Wall Fire Behavior in an Under-ventilated Room", Fire Safety Journal 37, Elsevier Science Ltd. (2002).
12. Kerrison, L., Galea, E.R. and Patel, M.K., "A Two-dimensional Numerical Investigation of the Oscillatory Flow Behavior in Rectangular Fire Compartments with a Single Horizontal Ceiling Vent", Fire Safety Journal 30, Elsevier Science Ltd., London (1998).

13. Quintiere, J.G., McCaffrey, B.J. and Braven, K.D., "Experiment and Theoretical Analysis of Quasi-steady Small-scale Enclosure Fires", National Bureau of Standards, Gaithersburg, MD.
14. Naruse, T., Rangwala, A.S., Ringwelski, B.A., Utiskul, Y., Wakatsuki, K. and Quintiere, J.G., "Compartment Fire Behavior under Limited Ventilation", Department of Fire Protection Engineering, University of Maryland, College Park, MD.
15. Karlsson, B. and Quintiere, J.G., " Enclosure Fire Dynamics", CRS Press, Florida (1999)
16. Lyon, R.E. and Abramowitz, A., "Effect of Instrument Response Time on Heat Release Rate Measurements", Fire and Materials Vol. 19 (1995).
17. "Thermal Radiation Heat Transfer", Engineering Treatment of Gas Radiation in Enclosures.
18. Rhodes, B.T., Quintiere, J.G., "Burning Rate and Flame Heat Flux for PMMA in a Cone Calorimeter, Fire Safety Journal, 26, 1996, pp. 221-239.
19. Takeda, H., "Oscillatory Phenomenon and Inverse Temperature Profile Appearing in Compartment Fires" Combustion and Flame, 61, 1985, pp.103-105.
20. Tewarson, A., "Some Observations on Experimental Fires in Enclosures, Part I – Cellulosic Materials", Combustion and Flame 19, 1972, pp. 101–111.
21. Emmons, H.W., "Some Observations on Pool Burning", International Symposium on The Use of Models in Fire Research, 1959, pp. 50-67.